

**DEVELOPMENT OF 3D PRINTING FOR TISSUE  
ENGINEERING OF EAR PINNA**

A THESIS SUBMITTED  
TO



**D.Y. PATIL EDUCATION SOCIETY (DEEMED TO BE UNIVERSITY),  
KOLHAPUR**  
(Declared u/s 3 of the UGC Act 1956)

FOR THE DEGREE  
OF  
**DOCTOR OF PHILOSOPHY**  
IN  
**STEM CELL AND REGENERATIVE MEDICINE**

BY  
**NILESH CHATUR BHAMARE**

**M.Sc.**

UNDER THE GUIDENCE  
OF

**DR. MEGHNAD G. JOSHI**

**M.Sc., Ph.D.**

Associate Professor,  
Department of Stem Cells and Regenerative Medicine  
Centre For Interdisciplinary Research  
D.Y. Patil Education Society,  
(Deemed to be University), Kolhapur  
(M. S.) India.

**2021**

## **DECLARATION**

I hereby declare that the work presented in this thesis entitled “**Development of 3D Printing for Tissue Engineering of Ear Pinna**” is entirely original and was carried out by me independently in the D. Y. Patil Education Society (Deemed to be University), Kolhapur under the guidance of Dr. Meghnad G Joshi, Associate Professor, Department of Stem Cells and Regenerative Medicine, D.Y. Patil University, Kolhapur (M. S.) India. I further declare that present work has not form the basis for the award of any degree, diploma, fellowship or similar title of any University or institutions. The extend information derived from the existing literature has been indicated in the body of the thesis at appropriate places giving the references.

Place: Kolhapur

Date:

**(Nilesh Chatur Bhamare)**

## **CERTIFICATE**

This is to certify that the work incorporated in the thesis “**Development of 3D Printing for Tissue Engineering of Ear Pinna**” submitted herewith for the degree of Doctor of Philosophy in Stem Cell and Regenerative Medicine of D. Y. Patil Education Society (Deemed to be University), Kolhapur by Nilesh Chatur Bhamare was carried out under my supervision. This thesis or any part of it was part of any not submitted for any degree or diploma or any academic elsewhere.

Place: Kolhapur

Date:

**Dr. Meghnad G. Joshi**

Associate Professor,

Department of Stem Cells and Regenerative Medicine,

Centre For Interdisciplinary Research,

D.Y. Patil University, Kolhapur

(M. S.) India.

## **ACKNOWLEDGEMENT**

This has been a fantastic experience of high and low from start to end. Many great people have helped me throughout this work both in academic and personal terms and I would like to thank them all here. First of all, I would like to express my deepest gratitude towards my guide Dr. Meghnad Joshi who has supported me for my Ph.D. work unconditionally with invaluable guidance, constant encouragement, inspiring and thought-provoking discussions. I am heartily indebted to my guide for accepting and training me in my journey to achieve a respectable degree in Stem Cell and Regenerative Medicine. I greatly appreciate the freedom my mentor gave me and the opportunity to pursue my research in my own way. My guide has been an inextinguishable fire of inspiration to me. He will forever remain a constant source of inspiration in my journey of life. I take the liberty to dedicate this section of my thesis and thank him from the bottom of my heart for all that he has given to me. I will cherish all the moments of enlightenment he had shared with me. Undoubtedly, a free thinker and believer, I will always remember him for his attitude of pushing all limits for his dear students.

I would like to acknowledge to Prof. (Dr.) C. D. Lokhande, Research Director, CIR, D.Y. Patil Education Society (Deemed to be University), Kolhapur at the completion of my Ph.D. thesis for the continuous support of my Ph.D. study and related research for his motivation and immense knowledge. I found a very thirsty researcher in him while approaching regarding any research related query his guidance helped me in all the time of research and writing of this thesis. I feel very fortunate to be part of CDL group.

I would like to acknowledge to Prof. (Dr.) Shimpa Sharma Pro-Vice-Chancellor, D Y Patil Medical College, D. Y.Patil Education Society (Deemed to be University), Kolhapur for helping me with her immense knowledge and encouragement during my research work.

I would like to acknowledge to Dr. Mohan Karuppayil (Head of Department- Stem Cell and Regenerative Medicine) CIR, D Y Patil Education Society (Deemed to be University), Kolhapur) for guidance me with his enormous knowledge, support and encouragement during my research work.

I would like to acknowledge to Dr V. V. Bhosale, Registrar, D Y Patil Medical College, D. Y.Patil Education Society (Deemed to be University), Kolhapur for providing me moral support and encouragement during my research work.

I would like to acknowledge to Hon'ble Prof. Rakesh Kumar Mudgal, Vice-Chancellor ,D Y Patil Medical Collage, D. Y. Patil Education Society (Deemed to be University), Kolhapur. I would like to acknowledge to Dr. R. K. Sharma, Dean, D Y Patil Medical Collage, D. Y. Patil Education Society (Deemed to be University), Kolhapur.

This work would not have been possible without the support and motivation of many people namely, Dr. S. H. Pawar, Ex. Vice Chancellor, Dr. Arvind Gulbake, Dr. Indumathi Somasundaram , Dr. Shivaji Kashte, Dr Arpita Tiwari, Dr Ashwini Jadhav (Department of Stem Cell and Regenerative Medicine, CIR, D Y Patil Education Society (Deemed to be University), Kolhapur), Dr. Jayawant Gunjkar, Dr. Umakant Patil, Dr. Vishwajit Khot (Department of Medical Physics, CIR, D Y Patil Education Society (Deemed to be University), Kolhapur), Dr. Deepak Sawant (Department of Microbiology, CIR, D Y Patil Education Society (Deemed to be University), Kolhapur), Dr. Raghvindra Bohara, Dr Patkar V R (Pharmacology department, DYP university, Kolhapur), Dr. Dhavalshankh A G (Pharmacology department, DYP university, Kolhapur), Mr. Pandit patil (Sanitary inspector, DYP hospital, Kolhapur), Dr. Mansingh Nimbalkar (Botany department, Shivaji university, Kolhapur), Mr. Lipare S V (Civil engineering department, KIT's college of Engineering, Kolhapur ), Mr. Raju. shetty (Patho-Histology department, DYP university, Kolhapur), for their support and guidance. Mr. S.P. Kole, Finance Adviser, D.Y. Patil Education Society (Deemed to be University), Kolhapur and other faculty and staff members who have helped me directly or indirectly during my research work.

I wish to express my appreciation towards my colleague Dr. Kishor Tardalkar for cooperation, scientific discussion and encouragement that he provided to me during the course of research work. The benevolent moral support in ups and downs throughout my Ph.D period. I also have a thank to my laboratory colleagues Dr. Jeevita Kshirsagar, Dr. ravi Kshirsagar, Saurabh Pise, Mrs. Priyanka Hilage, Mrs. Apoorva Kodolika, Mrs. Akshita Sharma (Department of Stem Cell and Regenerative Medicine, CIR, D Y Patil Education Society (Deemed to be University) ,Kolhapur), Mr. Shashikant Desai (Stem Plus Biotech), Ms. Trupti Ghogare, Ms. Sheetal Kale (Department of Physics, D Y Patil Education Society (Deemed to be University) ,Kolhapur) all have enlarged their support in a very exceptional way and benefited plenty from them across their academic and personal interactions, their suggestions at different places of my research work. I thank to Raviraj Karale (Rio 3D printers-karad) for providing me 3D printer assembly for my research work. I thank to Mr.

Parijat Bhave (FAN services) for providing me tensometer facilities for my research work. I also thank to Stem Plus Biotech and Stem Plus Cryopreservation, Sangli, for providing laboratory training during my research work. I am happy to mention Ms. Pratima Parulekar and Ms. Archana Khadilkar (KIT's College of Engineering (Autonomous), Kolhapur) for enormous help in data arrangement, thesis writing and editing.

I would like to tender my deepest gratitude to Mrs. Namrata Shinde, Mr. Ramdas Ghugare, Mr. Krishna, Mr. Ajinkya Barale and Uttam Kaka. Special thanks to my other co-workers in D.Y. Patil Education Society (Deemed to be University), Kolhapur; who are too numerous to name here, I thank all of them for their help, time and inputs. I am lucky to have had the opportunity to meet all of you. I would like to convey my heartfelt admiration to all my teachers from my school days to post graduation level.

The laboratory facility at the stage of before and after Ph.D. work some special thanks are reserved to my parents mother (Mrs. Meena Chatur Bhamare), father (Mr. Chatur Sitaram Bhamare), friends and relatives. My hardworking parents have sacrificed their lives for my education with unconditional love and care and I would not have made it this far without them. I sincerely apologize for any omissions and sincerely thanks, all concerned.

Place: Kolhapur

Date:

-Nilesh C. Bhamare

## LIST OF PUBLICATIONS

### Research Articles Accepted/Submitted at International Journals

1. Bohara R, Bhamare N, Kshersagar J, Tardalkar K, Desai S, Despande M, Joshi M\*  
Platelet Rich Plasma: A Potential Treatment Option in Hyper Pigmentation of Skin.  
Clin Surg. 2018, 3, 1-5
2. Nilesh C. Bhamare, Kishor R. Tardalkar, Jeevitaa Kshersagar, Shashikant R.  
Desai, Tejas B. Marsale, Mansingraj S. Nimbalkar, Shimpa Sharma, Meghnad G.  
Joshi\*. Tissue engineered human ear pinna derived from decellularized goat ear  
cartilage: clinically useful and biocompatible auricle construct. Cell Tissue  
Bank (2021). <https://doi.org/10.1007/s10561-021-09911-1>.
3. Nilesh Bhamare, Kishor Tardalkar, Pratima Parulekar, Archana Khadilkar, and  
Meghnad Joshi\*. 3D Printing of Human Ear Pinna using Cartilage Specific ink. -  
Biofabrication- Under Review.
4. Nilesh Bhamare, Kishor Tardalkar, Pratima Parulekar, Archana Khadilkar and  
Meghnad Joshi\*. Tissue Engineered Human Ear Pinna – Review – International  
Journal of Oral and Maxillofacial Surgery – Under Review

## LIST OF PATENTS

1. "Method of constructing tissue engineered human ear pinna prosthesis" (Application Filing Receipt (AFR) for application no. 201921004685, year- 2019).
2. "Synthesis process of composite artificial skin bioink for 3d bioprinting and wound healing application" (AFR application no. 201921004686, year -2019).
3. "Synthesis method of bioink for 3d printing of cartilage" (AFR application no. 202121004796, year- 2021).

## PAPERS PRESENTED AT NATIONAL/INTERNATIONAL CONFERENCES

### **Conferences:**

1. 2<sup>nd</sup> national conference on Regenerative Medicine and Stem Cell research. Multidisciplinary unit dhanlakshmi shrinivasan medical college and hospital, Perambalur, Tamilnadu held on 6-7, April 2018.
2. 5<sup>th</sup> International conference: Angiogenesis research targeted anti-angiogenic therapy. Center of Interdisciplinary Research, D. Y. Patil Education Society (Deemed to be University), Kolhapur held on October-26-27, 2018.
3. International conference on cancer biology: Basic science to translational research (CBTR 2020). Center of Interdisciplinary Research, D. Y. Patil Education Society (Deemed to be University) Kolhapur held on January 17-18, 2020.
4. Virtual International Conference on “Stem cells and regenerative medicine–academic and industrial outlooks” Center of Interdisciplinary Research, D. Y. Patil Education Society (Deemed to be University), Kolhapur held on 19-20 March 2021.

### **Workshops:**

Good laboratory practices. Center of Interdisciplinary Research, D. Y. Patil Education Society (Deemed to be university), Kolhapur held on February 6, 2021.

### **Paper Presentation (Oral):**

1. 3<sup>rd</sup> International conference on stem cell and regenerative medicine. Dr. D. Y. Patil Vidyapith, Pimpri-Pune held on March-29-31, 2019.
2. Virtual International Conference on “Stem cells and regenerative medicine–academic and industrial outlooks” Center of Interdisciplinary Research, D. Y. Patil Education Society (Deemed to be University), Kolhapur held on 19-20 March 2021.

### **Poster Presentations:**

1. International conference on nanotechnology addressing the convergence of the material science, biotechnology and medical science. Center of Interdisciplinary Research, D. Y. Patil Education Society (Deemed to be University), Kolhapur held on November 9-11, 2017.
2. 3<sup>rd</sup> International conference on Stem Cell and Regenerative Medicine. Dr. D. Y. Patil vidyapith, Pimpri-Pune held on March-29-31, 2019.



# D. Y. PATIL MEDICAL COLLEGE, KOLHAPUR

Constituent College of D.Y.Patil Education Society Deemed University, Kolhapur  
NAAC Accredited 'A' Grade

**Dr. Rakesh Kumar Sharma**  
Dean & Professor (Obst. & Gyn.)

**Padmshree Dr. D. Y. Patil**  
Founder President

**Dr. Sanjay D. Patil**  
President

Outward No. DMCK/155/2018.

Date :  
**14 MAY 2018**

## INSTITUTIONAL ETHICS COMMITTEE, D. Y. PATIL MEDICAL COLLEGE, KOLHAPUR.

This is to certify that the research project titled,

### "Development of 3D Printing for Tissue Engineering of Ear Pinna"

Submitted by : **Mr. Nilesh C. Bhamare**

Under the supervision of appointed Guide (if any): **Dr. Meghnad G. Joshi**

Has been studied by the Institutional Ethics Committee (IEC) at its meeting held on **14/05/2018**  
and granted approval for the study with due effect with the following caveats:

1. If you desire any change in the protocol or standard recording document at any time, please submit the same to the IEC for information and approval before the change is implemented.
2. All serious and/or unexpected adverse events due to the drug/procedures tested in the study must be informed to the IEC within 24 hours and steps for appropriate treatment must be immediately instituted.
3. In case of injury/disability/death of any participant attributable to the drug/procedure under study, all compensation is to be made by the sponsor of the study.
4. The Chief investigator/Researcher must inform the IEC immediately if the study is terminated earlier than planned with the reasons for the same.
5. The final results of the study must be communicated to the IEC within 3 months of the completion of data collection.
6. The researcher must take all precautions to safeguard the rights, safety, dignity and wellbeing of the participants in the study.
7. The researcher must be up to date about all information regarding the risk/benefit ratio of any drug/procedure being used and any new information must be conveyed to the IEC immediately. The IEC reserves the right to change a decision on the project in the light of any new knowledge.
8. Before publishing the results of the study, the researcher must take permission from the Dean of the Institution.
9. Annual progress report should be submitted for all sponsored projects to the committee.
10. Unethical conduct of research in non-sponsored projects will result in withdrawal of the ethics approval and negation of all data collected till that date.

**Dr. Mrs. Shimpa R. Sharma**  
(Member Secretary, IEC)  
**Dr. (Mrs) Shimpa Sharma**  
Member Secretary,  
Institutional Ethics Committee  
D. Y. Patil Medical College,  
Kolhapur - 416 006

869, 'E' Kasaba Bayada, Kolhapur - 416 006 (MS) INDIA. Phone No. : (0231) 2601235-36, Fax : (0231) 2601238,  
Email : shimpasharma@gmail.com

## INDEX

<b>Chapter No.</b>	<b>Title</b>	<b>Page No.</b>
1	<p>Introduction to ear pinna and Review of literature of auricular deformities</p> <p>1.1 Ear Pinna Embryology, Anatomy and Physiology</p> <p>1.2 Ear Pinna Cellular Organization and Extra Cellular Matrix</p> <p>1.3 Ear Pinna Function</p> <p>1.4 Abnormalities in ear pinna and its consequence</p> <p>1.5 Surgical techniques for reconstruction of ear pinna</p> <p>1.6 Limitation of surgical techniques</p> <p>1.7 Tissue engineering for Ear Pinna</p> <p>1.8 Biological TE scaffold</p> <p>1.9 Synthetic TE scaffold</p> <p>1.10 3D Bioprinting for Reconstruction of Ear Pinna</p> <p>1.11 Gap in existing research</p> <p>1.12 Objectives</p> <p>1.13 Scope of work</p> <p>References</p>	1-42
2	<p>Synthesis, characterization and in vivo studies of goat ear pinna scaffold of tissue engineered human ear pinna</p> <p>2.1 Introduction to the need of advancement in auricular reconstruction treatments</p> <p>2.2 Material and Methods</p> <p>2.3 Preparation of Scaffold: Decellularization Process</p> <p>2.4 Histochemical Characterization of Decellularized Scaffold</p> <p>2.4.1 Haematoxyline and Eosin (HE)</p> <p>2.4.2 4', 6-diamidino-2-phenylindole (DAPI)</p> <p>2.4.3 Masson's trichrome (MT)</p>	43-67

	<p>2.4.4 Glycosaminoglcans (GAG)</p> <p>2.4.5 DNA quantification</p> <p>2.5 Physical Characterization of Decellularized Scaffold</p> <p>2.5.1 Mechanical Properties</p> <p>2.5.2 Scanning Electron Microscopy (SEM) analysis</p> <p>2.6 Fabrication of human ear pinna mold</p> <p>2.6.1 Patented molding technology</p> <p>2.7 <i>In vivo</i> Study of Engineered Human Ear Pinna</p> <p>2.7.1 Histological assessment</p> <p>2.7.2 Mechanical testing</p> <p>2.7.3 SEM analysis</p> <p>2.7.4 Statistical analysis</p> <p>2.8 Histochemical Characterization of decellularized Scaffold</p> <p>2.8.1 HE staining</p> <p>2.8.2 DAPI staining</p> <p>2.8.3 MT staining</p> <p>2.8.4 AB pH-2.5 staining</p> <p>2.8.5 DNA quantification</p> <p>2.9 Physical Characterization of Decellularized Scaffold</p> <p>2.9.1 Mechanical Properties</p> <p>2.9.2 SEM analysis</p> <p>2.10 Patented Molding Pinna</p> <p>2.11 <i>In vivo</i> Study of Engineered Human Ear Pinna</p> <p>2.11.1 Mechanical testing after biocompatibility study</p> <p>2.11.2 SEM analysis</p> <p>2.11.3 Histological assessment after biocompatibility study</p> <p>References</p>	
3	<p>Synthesis, Characterization and <i>in vivo</i> studies of 3D Printed Ear Pinna</p> <p>3.1 Introduction to tissue engineering by 3D printing of pinna</p> <p>3.2 Materials and methods</p> <p>3.3 Preparation of Bioink</p>	68-109

	<p>3.4. Physical characterization of bioink</p> <p>3.4.1 FTIR analysis of bioink</p> <p>3.4.2 Rheological analysis of bioink</p> <p>3.4.3 Spreadability analysis of bioink</p> <p>3.5 3D printing of ear pinna</p> <p>3.6. Physical characterization of 3D printed ear pinna</p> <p>3.6.1 Thermogravimetric analysis (TGA)</p> <p>3.6.2 X-ray diffraction (XRD) analysis</p> <p>3.6.3 Swelling behaviour</p> <p>3.6.4 Surface wettability (Contact angle)</p> <p>3.6.5 <i>In vitro</i> biodegradability</p> <p>3.7. Biocompatibility testing of 3D printed ear pinna in check embryo (<i>in ovo</i>).</p> <p>3.7.1 Histological assessment</p> <p>3.7.2 SEM analysis</p> <p>3.8 Transplantation of 3D printed ear pinna</p> <p>3.8.1 Ultrasound Sonography of Transplanted Ear Pinna</p> <p>3.8.2 CT scans of Transplanted Ear Pinna</p> <p>3.8.3 Biomechanical characterization (Tensile testing)</p> <p>3.8.4 Histological assessment</p> <p>3.8.5 SEM analysis</p> <p>3.8.6 IHC</p> <p>3.9 Statistical Analysis</p> <p>3.10 Physical characterization of bioink</p> <p>3.10.1 FTIR analysis</p> <p>3.10.2 Rheological analysis</p> <p>3.10.3 Spreadability analysis</p> <p>3.10.4 Printing of 3D printed ear pinna</p> <p>3.11 Physiochemical characterization of 3D printed ear pinna</p> <p>3.11.1 Thermogravimetric analysis (TGA)</p> <p>3.11.2 XRD analysis</p>	
--	---	--

	3.11.3 Swelling behaviour 3.11.4 Surface wettability (Contact angle) 3.11.5 <i>In vitro</i> biodegradability 3.12 Biocompatibility study <i>in ovo</i> 3.13 <i>In vivo</i> study of 3D printed ear pinna 3.13.1 Biomechanical characterization of 3D printed native rat pinna and transplanted pinna 3.13.2 Histological assessment 3.13.3 SEM analysis 3.13.4 IHC 3.14 Discussion 3.15 Conclusions References	
4	General Discussion References	110-113
5	Conclusions	114-115
6	Future scope of work	116-117

## LIST OF FIGURES

Figure 1.1: Ear pinna functions.....	7
Figure 1.2: Ear abnormalities.....	8
Figure 1.3: General autologous surgical procedure for ear reconstruction and its post-operative problems.....	13
Figure 1.4: Progress in Tissue engineering.....	21
Figure 2.1: A- Control goat ear pinna cartilage, B- Decellularized goat ear pinna.....	46
Figure 2.2: Histochemical study of decellularization process.....	51
Figure 2.3: DNA quantification.....	52
Figure 2.4: Scanning electron microscopy of decellularized goat cartilage .....	55
Figure 2.5: Shape of human ear pinna.....	56
Figure 2.6: Biocompatibility testing.....	57
Figure 2.7: Mechanical testing of human ear shaped pinna done after transplantation.....	58
Figure 2.8: Scanning electron microscopy of goat cartilage after transplantation.....	59
Figure 2.9: Histochemistry of scaffold after transplantation.....	60
Figure 2.10: VAP expression in scaffold after transplantation.....	60
Figure 2.11: CD90+ expression in scaffold after transplantation.....	61
Figure 3.1: Synthesis of Bioink.....	71
Figure 3.2: Fourier Transform Infrared spectroscopy (FTIR) of bioink.....	82
Figure 3.3: Rheological behaviour of bioink.....	83
Figure 3.4: Spreadability analysis.....	83
Figure 3.4C: Spreading rate of bioink.....	84
Figure 3.5: 3D printing of ear pinna .....	85
Figure 3.6: Thermo Gravimetric Analysis (TGA) of 3D printed pinna.....	86
Figure 3.7: X-ray diffraction (XRD) analysis of 3D printed pinna.....	87
Figure 3.8: Swelling behavior of 3D printed pinna.....	88
Figure 3.9: Surface wettability of 3D printed pinna.....	88

Figure 3.10: <i>In vitro</i> Biodegradability study of 3D printed ear pinna.....	89
Figure 3.11: 3D printed ear pinna graft biocompatibility and CAM assay.....	90
Figure 3.12: Histology (HE) of CAM.....	91
Figure 3.13: SEM of pinna graft.....	92
Figure 3.14: 3D printed ear.....	77
Figure 3.15: 3D printed pinna transplant biocompatibility.....	78
Figure 3.16: Ultrasound sonography (USG) of transplanted 3D printed ear pinna.....	93
Figure 3.17: Computed Tomography (CT) of transplanted 3D printed ear pinna.....	93
Figure 3.18: 3D printed ear transplant angiogenesis.....	94
Figure 3.19: 3D printed ear pinna transplant.....	79
Figure 3.20: Biomechanical characterization 3D printed ear pinna, native rat ear pinna and transplanted 3D ear pinna.....	95
Figure 3.21: Histology of negative, positive control and transplanted 3D printed ear pinna.....	97
Figure 3.22: SEM images of transplanted 3D printed ear pinna.....	98
Figure 3.23: Immunohistochemical study of negative control, positive control and transplanted 3D printed ear pinna.....	99

## LIST OF TABLES

Table 2.1: Decellularization protocols for goat ear pinna.....	45
Table 2.2: Mechanical testing of decellularized scaffold.....	53
Table 2.3: Mechanical testing of recellularized scaffold.....	57
Table.3.1: Spreadability of bioink.....	84
Table 3.2: Swelling of 3D printed pinna.....	87
Table 3.3: Biodegradability of 3D printed pinna.....	89
Table 3.4: Biomechanical characterization (tensile testing) of 3D printed ear pinna, native rat ear pinna and transplanted 3D printed ear pinna.....	95

## LIST OF ABBREVIATIONS

ATP	Adenosine 5'-Triphosphate
AER	Autologous Ear Reconstruction
ACI	Autologous Chondrocyte Implantation
AM	Additive Manufacturing
ASCs	Adipose Derived Stem Cells
ALH	Adipocyte Laden Hydrogel
ACI	Autologous Chondrocyte Implantation
AM	Additive Manufacturing
ASCs	Adipose Derived Stem Cells
ALH	Adipocyte Laden hydrogel
AB	Alcian Blue
ACM	Acellular Cartilage Matrix
BMPs	Bone Morphogenetic Proteins
BST-1	Bone Marrow Stromal Cell Antigen-1
CT	Computerized Tomography
CD	Cluster of Differentiation
CAD/CAM	Computer-Aided design/Computer-Aided Manufacturing
CLH	Chondrocyte Laden Hydrogel
CFM	Craniofacial Microsomia
CAM	Chorioallantoic Membrane
CPCSEA	Committee for the Purpose of Control and Supervision of Experiments on Animals
DNA	Deoxyribonucleic Acid
DMSO	Dimethyl Sulfoxide
DW	Distilled Water
DAPI	4', 6-Diamidino-2-Phenylindole
dECM	Decellularized Extra Cellular Matrix
ETO	Ethylene Oxide
EAC	External Auditory Canal
ECM	Extra Cellular Matrix

FGFs	Fibroblast Growth Factors
FDM	Fused Deposition Modelling
GAG	Glycosaminoglycan
GT	Gelatin
HE	Haematoxyline And Eosin
Hox a 2	Homeobox a 2
IAEC	Institutional Animal Ethical Committee
ICD	International Classification For Diseases
IHC	Immunohistochemistry
Irf6	Interferon Regulatory Factor 6
MSCs	Mesenchymal Stem Cells
MtoBS	Multi-Head Tissue/Organ Building System
MT	Masson's Trichrome
NES	Nestin
OCT4	Octamer-binding transcription factor 4
PE	Polyethylene
PMMA	Polymethyl Methacrylate
PVC	Polyvinyl Chloride
PGA	Polyglycolic Acid
PEG	Polyethylene Glycol
PCL	Polycaprolactone
PLA	Polylactic Acid
PVA	Poly (Vinyl Alcohol)
P-4HB	Poly 4-Hydroxybutyrate
PCR	Polymerase Chain Reaction
PVDF	Polyvinylidene Fluoride
PBS	Phosphate Buffer Saline
STL	Stereolithography
SLS	Selective Laser Sintering
SDS	Sodium Dodecyl Sulfate
SEM	Scanning Electron Microscopes
SO/FG	Safranin-O/Fast Green
Sox2	SRY-Box Transcription Factor 2
Six1	Sineoculis homeobox 1

TGF	Transforming Growth Factor
Tbx1	T-box 1
TCS	Treacher Collins Syndrome
TE	Tissue Engineering
TB	Toluidine Blue
TGA	Thermogravimetric Analysis
UV	Ultraviolet
USG	Ultrasound Sonography
UTM	Universal Testing Machine
VAP	Vascular Associated Protein
VEG	Verhoeff Elastic Stain
XRD	X-Ray Diffraction

## Chapter-1

# Introduction to Ear Pinna: Review of Literature of Tissue Engineering of Ear Pinna

## 1. Introduction:

Ear is a sensory organ necessary for the hearing purpose. It is located on the both sides of the face. Some genetic, physical or accidental causes can cause the deformities in the shape of ear pinna. Protruding or eye-catching shape of ear pinna because of deformity makes the life of the patient difficult. The social, physical, psychological effects on the patient's life states the need of treatment for restoration of pinna shape. There are various treatments available in medical practice by plastic surgeons. Even if the numerous methods are available such as surgical methods, they have their own limitations which are still needed to be overcome. In this chapter, we studied the auricular deformities, various available treatments and their limitations in detail.

### 1.1 Ear Pinna Embryology, Anatomy and Physiology:

Ears are paired organs, one on each side of the head (Schuknecht 1988). The vertebrate ear is divided into the outer pinna or auricle or external ear (Visible part of the ear), middle, and inner ear. The ear is one of the sensory organs used for hearing. Hearing ability is necessary for distant warning and communication (Schuknecht 1988; Mota and Danti 2019).

The pinna begins its development throughout the 5<sup>th</sup> week, and the hillocks are initially distinguishable during the 6<sup>th</sup> week of embryo development (Bartel-Friedrich and Wulke 2007; Luquetti et al. 2011) The pinna hillocks gradually grow into pinna during the foetal development. They are initially at low position on the embryonic neck and eventually rise to re-position little by little to dorsal ward (Luquetti et al. 2011). Additionally, facial growth covers the pharyngeal ectoderm plays a key role in defining the overall morphology of the auricle (Luquetti et al. 2011).

The anatomy of the ear pinna is complex (Hunter et al. 2009). The major makers of the external ear are skin (with adnexa), cartilage, and six intrinsic muscles. The external rim of

## **Development of 3D Printing for Tissue Engineering of Ear Pinna**

ear pinna is known as helix and curves slightly inward towards the external acoustic meatus providing concave shape to the pinna (Lanz and Wood 2004). The opposite side of helix is known as antihelix which is convex in shape. The scaphoid fossa lies in the cavity between helix and antihelix. The external auditory canal continues in the skull in sigmoid fashion until it meets the tympanic membrane (Bartel-Friedrich and Wulke 2007). The lobes are soft, fleshy and inferior part of the pinna. The earlobes vary in size and are attached to the anteroinferior portion to the face (Hunter et al. 2009). This auricle is composed of elastic cartilage providing the skeletal framework. Cartilage is connective tissue having flexible nature. It is supplied with less vascularization with respect to other connective tissues. The cartilage receives its nutrients directly from its overlying perichondrium (Oseni et al. 2011).

The head in humans is large in contrast to the size of the outer ear so the role of the outer ear is non-significant compared to other mammals. It also collects some higher frequency sound from behind, serving to find whether the sound comes from the front or the back (Schuknecht 1988). Pinna is made up of cartilage, collects sound and channels it into the ear canal. Pinna is covered with a layer of skin consisting of sebaceous glands protecting the ear from cracking (Lanz and Wood 2004). The ear canal is about 4 centimetres long and comprises of an external and inner portion. The external portion is lined with hairy skin covering sweat glands and oily sebaceous glands which produces ear wax. The skin of the ear canal is thin and attached firmly to the bone of the inner ear canal, a cavity which absorbs low frequency sound but leads it to the drum head (eardrum or tympanic membrane) at its base. The external layer of the drumhead is formed of skin in continuity with that of the ear canal (Schuknecht 1988). During the course of life, skin sheds and is repetitively renewing. Ear canal skin develops like a fingernail from the depths to the outside so that the skin is shed into the waxy excretions in the external part and falls out (Schuknecht 1988). This is why cotton buds should not be used to clean the ear canal as due to its push the shed skin and wax goes deep

into the canal and obstructs hearing. The ear canal has a minor bend where the external cartilaginous part connects with the bony thin skinned internal part, so that the outer part runs slightly backwards and the inner part somewhat forwards. The tympanic membrane divides the ear canal from the middle ear and is fashioned somewhat like a loudspeaker cone (which is a perfect shape for diffusing sound between solids and air). The entire membrane is less than a  $1/10^{\text{th}}$  of millimetre thick. It covers a round opening about 1 cm in diameter into the middle hollow ear (Schuknecht 1988).

Ear (Principle mechanism like microphone) transforms collected physical sound vibration into a determined nervous impulse which in turn is then processed by the central auditory pathways of the brain (Schuknecht 1988). Once the sound waves pass through pinna, they move 2-3 cm into the auditory canal before hitting the eardrum. The resulting vibrations are transmitted by the three ossicles, producing the oval window covering the cochlea to vibrate. The vibrations are sensed by the cilia (flexible hair cells) and initiate a nervous impulse sent via the auditory nerve to the auditory cortex (Schuknecht 1988). Vibration is less transmitted at the line between two carriers which vary prominently in variable characteristic such as air and water (Schuknecht 1988). Humans need to hear only up to 4 kHz to understand speech; our 60- dB high-frequency hearing limit is 17.6 kHz because our pinnae require frequencies above 6 kHz can provide directional signals. Pinnae (Both ears) of mammals hear upper frequencies than non-mammalian tetrapods, that is, above 10 kHz (Heffner and Heffner 2018).

### **1.2 Ear Pinna Cellular Organization and Extra Cellular Matrix (ECM):**

The chondrocytes are the only cells found in cartilage. Chondrocytes are unique in nature, having no direct contact to the vascular organization (Phull et al. 2016). Ear Pinna chondrocytes which are found in lacunae surrounded by ECM (Barrett-Jolley et al. 2010). Multipotent mesenchymal stem cells (MSCs) arise from lateral plate mesoderm,

cranial neural crest, and somite. Various molecular mechanism involved in the differentiation of the MSCs towards chondrocytes are yet not fully understood. Growth factors are involved in chondrogenic differentiation such as transforming growth factor (TGF)- $\beta$  and fibroblast growth factor (FGF). Signalling pathways involved in chondrogenic development are Wnts, and Notch signalling pathways (O'Sullivan et al. 2011). Chondrocytes within cartilage primal continue to express Sox9 transcription factor and then undergo its maturation (Phull et al. 2016). Chondrogenic differentiation potential markers are cluster of differentiation (CD)105+, CD73+, CD44+, CD90+, CD13+, CD166+ (O'Sullivan et al. 2011). Specific CD44+/CD90+ progenitor/stem cells were identified in the auricular perichondrium layer (O'Sullivan et al. 2011). Progenitor cell differentiate in order as chondroprogenitor cell, chondroblasts, chondrocytes, and finally hypertrophic chondrocytes (Phull et al. 2016).

Chondroblasts (young cells) are relatively irregular and small while chondrocytes (mature cells) are larger which become spheroid or polygonal with flattened edges with age and lose the extensions (Oseni et al. 2011; Phull et al. 2016). Chondrocytes lack cell-to-cell contacts therefore; these cells show changes in phenotype when developed in monolayer cultures (Phull et al. 2016). Location and origin control the fate of chondrocytes. Chondrocytes go through apoptotic cell death or metaplasia or trans differentiate to osteoblast causing in formation of the cartilage to bone (Phull et al. 2016).

The chondrocytes are providing elastic support as a key functional element and allow smooth pain-free movement in cartilage (Phull et al. 2016). Chondrocytes are responsible for the formation of cartilage specific ECM by secreting proteoglycans, collagen and non-collagenous proteins (Oseni et al. 2011). Chondrocytes contains lipid droplets; mitochondria, golgi complex, and cytoplasm which are significant in cartilage or ECM regeneration. Chondrocytes are metabolically active which is required for upholding the traits of ECM (Phull et al. 2016).

The ECM of pinna cartilage consists of fibrous elastin, type II (most abundant matrix) and V collagen and proteoglycans (aggrecan) (Oseni et al. 2005). ECM macromolecules are significant mediators of cartilage formation (Krishnan and Grodzinsky 2018). Fibrous proteins in the ECM are responsible for the connective tissue's tensile strength (Correia et al. 2011). Negative charge molecules aggrecan such as glycosaminoglycan (GAG) consists of chondroitin sulphate forming a gel-like ground substance that provides elasticity and the ability to resist against compression. These components provide lubrication and shock absorption (Oseni et al. 2005). When aggrecan monomers and GAG bind to hyaluronic acid can induce water, growth factors and cytokines (Barrett-Jolley et al. 2010; Phull et al. 2016). Collagen network provides tensile strength to cartilage and structural skeleton for auricle (Oseni et al. 2011; Phull et al. 2016) Collagen Type II is produced by chondroblast activity. The fibres of type II collagen are thin and have profuse amount of proteoglycan entangled in between fibrils. Cartilaginous ECM is constantly under pressure due to the swelling nature of the tissue and high tensile collagen network reinforcing it (Akkiraju and Nohe 2015). Elastin protein displays the ability to recoil after being stretched, therefore provides resilience to the fibre and it can withstand into a considerable degree of bending. Microfibrils are suggested to have an anchoring function at various anatomical locations (Utomo et al. 2015a). Having the different relative amount of elastin and microfibrils between elastic, elaunin and oxytalan fibers contain different mechanical properties (Utomo et al. 2015a).

ECM acts like scaffold and play major role in new tissue formation due to its biodegradability and biocompatible nature (Correia et al. 2011). ECM is responsible for inducing cytokine, responding to cell-signals, providing ideal conditions for cell adhesion, growth (Bartel-Friedrich and Wulke 2007; Chinnasamy et al. 2018; Jung et al. 2018). ECM should give network of a surface microporous structure, mechanical support, exchange of nutrients and waste products (Oseni et al. 2005).

Chondrocytes generate adenosine 5'-triphosphate (ATP) during anaerobic respiration and lowering the pH which can continue in anoxic conditions. Chondrocytes embedded within the ECM have negative ionic environment can affect the mechanism of ion channels, which is directly affected on chondrocyte metabolism, proliferation and ability to synthesize matrix (Barrett-Jolley et al. 2010). Regeneration of elastic cartilage is restricted due to its aneural, nonvascular, alymphatic nature as well as the little to no mitotic activity of chondrocytes hence reconstruction of ear pinna treatment makes challenging (Storck et al. 2014; Krishnan and Grodzinsky 2018; Borrelli et al. 2020). This makes regeneration and reconstruction of ear pinna an object for research.

### **1.3 Ear Pinna Function:**

The main function of pinna is to collect sound just like a funnel (Fig. 1.1A) from the environment and transfers it to the internal ear, in order to do this, the signal must reach to the brain via central auditory pathways (Mota and Danti 2019). Without pinna the sound waves would take a more direct route into the auditory canal. The pinna has a curvature in order to collect sound from surroundings (Schuknecht 1988). The pinna is essential for collection of sound as there is variance in air pressure inside and outside the ear. The resistance of the air is greater on inner ear than outside as the air inside the ear is compressed and hence provides greater pressure. Pinna is capable of overcoming the variance in pressure inside and outside the ear. The pinna serves the purpose of bridge which makes the alteration easy allowing more sound to move into the ear canal (meatus). The function of the meatus is to transfer sound from the pinna to the eardrum (tympanic membrane). Eardrum is delicate and pressure from sound waves creates vibrations in eardrum. Hence, ears are able to recognize low as well as high frequency sound waves. Ear canal functions as a natural hearing support which amplifies low frequency sound waves. Meatus is somewhat bent, provides hair and the cerumen (earwax) that collectively help as a defensive barrier against contaminations

(Unwanted things such as clay, dust and insects). The earwax is used to grease the skin of the meatus, and to transport contaminant out of the ear (Schuknecht 1988).

Pinna provides symmetry to the face which is necessary for social acceptance (Ali et al. 2017). The ear pinna has major impact on the facial appearance of a person which directly has effect on his/her social and psychological wellbeing (Ali et al. 2017). Pinna provides an anchoring place for typical hearing aids (External listening devices), ear jewellery (Fig. 1.1B) frames spectacles and facial mask (Fig. 1.1C) (Eng and Chiu 2002).

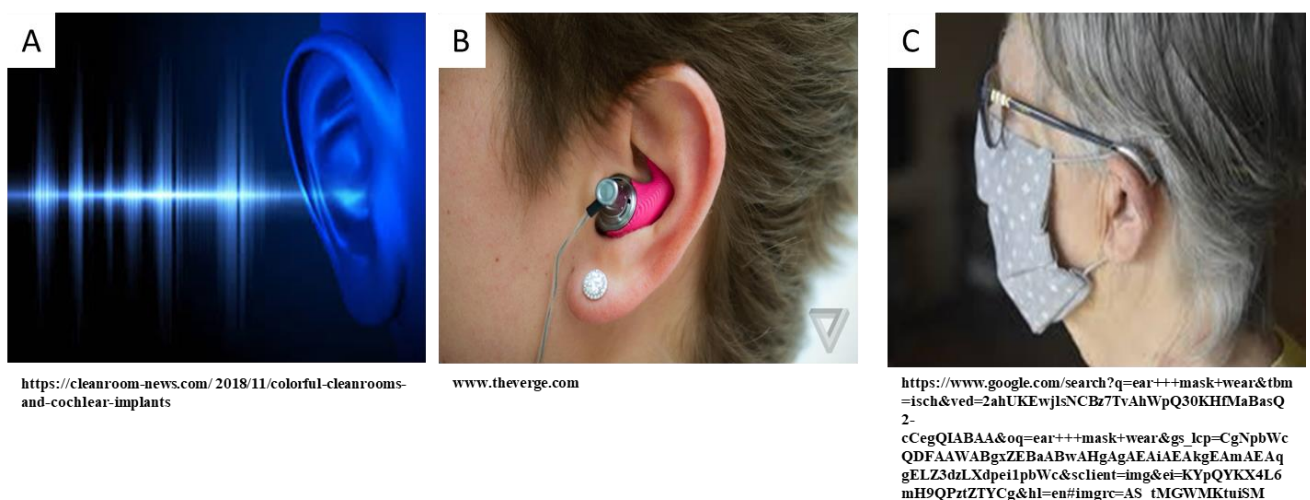


*Figure 1.1: Ear pinna functions*

*A. Collection of sound, B. Typical hearing aids and ear jewellery, C. Frames spectacles and facial mask*

### 1.4 Abnormalities in ear pinna and its consequence:

Ear abnormalities can be characterized based on shape and size of auricle which can possibly cause loss of hearing (Odat et al. 2016). Abnormalities of ear pinna encompasses four grades such as congenital auricular malformation with grade I microtia (Ear size is slightly small), grade II microtia (Size of one ear is one half), grade III microtia ('Peanut' shape ear size) and grade IV microtia (Anotia: absence of pinna) (Luquetti et al. 2012; Storck et al. 2014; Krishnan and Grodzinsky 2018; Mussi et al. 2019) Such a coding system used for register

## Development of 3D Printing for Tissue Engineering of Ear Pinna

microtia according to International Classification for Diseases (ICD) (Luquetti et al. 2011) (Fig.1.2 A).

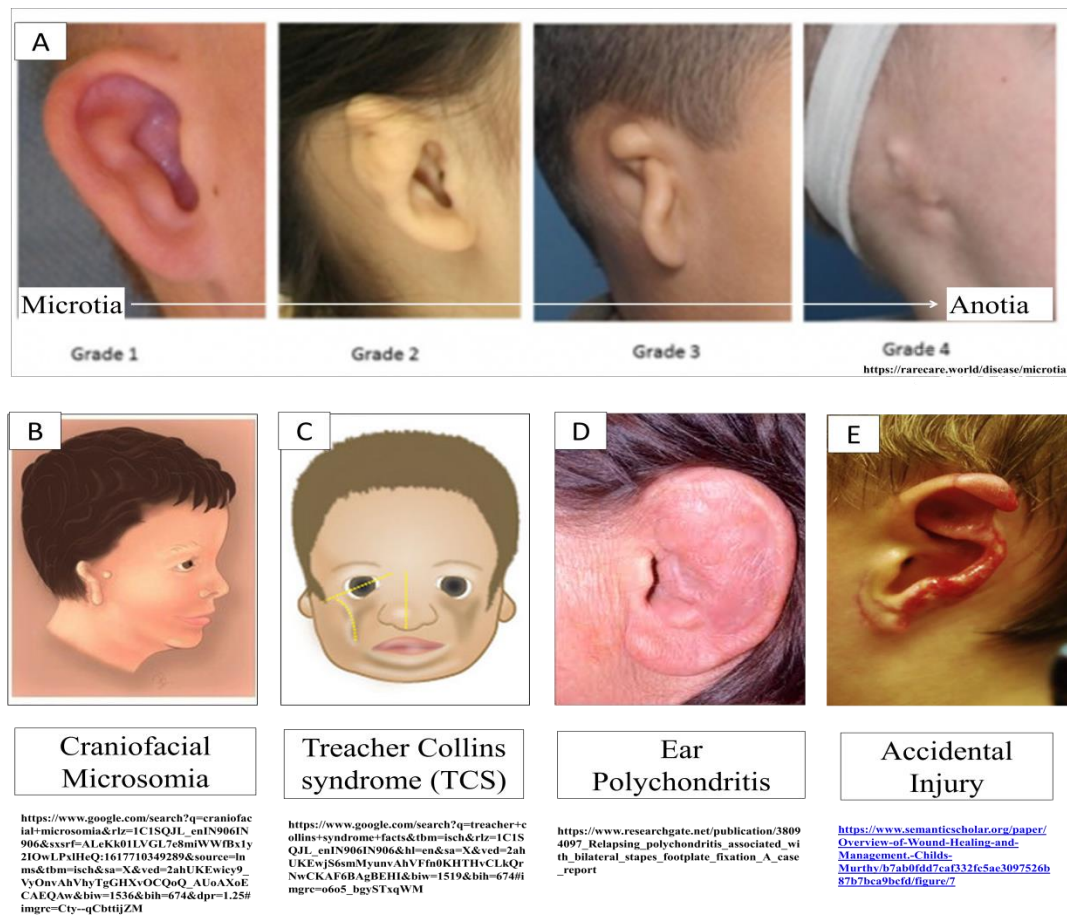


Figure 1.2: Ear abnormalities

- A. Ear abnormalities: Grade 1: Smaller than normal, Grade 2: usually lower half, Grade 3: pea nut shaped cartilage and Grade 4: anotia
- B. Craniofacial Microsomia: Gestational abnormalities
- C. Treacher Collins syndrome (TCS): Uneven ears
- D. Ear polychondritis: Autoimmune rheumatic disorder
- E. Accidental injury: Animal Bite or cuts

A craniofacial microsomia (CFM) which is a congenital deformity (Fig.1.2 B) which affects one or both auricles (Primarily affecting the anatomical areas that developed from first and second branchial arches during the 5<sup>th</sup>–6<sup>th</sup> weeks of gestation) (Mussi et al. 2019). Strong confirmation supports the link between gestational exposure to specific medications such as thalidomide, and the immune suppressant link to microtia (Luquetti et al. 2012). The mechanisms by which these exposures cause microtia have not been fully clarified. Other risk factors recognized low birth weight, low maternal education, advanced maternal age,

maternal acute illness, maternal diabetes mellitus and multiple births (Luquetti et al. 2012). A number of genes have now been recognized on conditions associated with microtia (Luquetti et al. 2012). The gene expression markers involved in pinna growth include SRY-Box Transcription Factor 2 (Sox2), Nestin (NES), Bone marrow stromal cell antigen-1 (BST-1), and Octamer-binding transcription factor 4 (OCT4). Person with microtia shows a decline in these gene markers (Ishak et al. 2011). Microtia has been testified in persons with autosomal trisomies, such as trisomy 18, 21, and 22, as well as with mosaicism of trisomy 13 and 18 and aneusomies, as in deletion of 4p, 5p, and 18p, 18q, and 22q. Chromosomal translocations connecting the 6 p24 region is related with orofacial clefting and bilateral microtia (Luquetti et al. 2012). Animal models studies suggest that knockout homeobox gene such as homeobox a-2 (Hoxa 2) or sineoculis homeobox 1(Six1/ Six4) or interferon regulatory factor 6 (Irf6) or mutation T-box 1(*Tbx1*) gene mice link with microtia (Luquetti et al. 2012). Signalling paths link in the pinna synthesis such as bone morphogenetic proteins (BMPs), Wnts, fibroblast growth factors (FGFs), and retinoic acid. Deregulations of these signalling pathways initiated by genetic or environmental influences create a possible source of microtia (Luquetti et al. 2012). In summary, although most of studies have found genetic variations possibly related with microtia, no causal genetic mutation has been definite to date (Luquetti et al. 2012).

Microtia happens more commonly in males, with an estimated 20–40% increased risk compared to females (Luquetti et al. 2012). Additionally, microtia affects the right ear twice as often as the left (Mussi et al. 2019). Microtia usually occurs due to aural atresia (Absence of the ear canal) or stenosis with conductive hearing loss (80% of cases) (Mussi et al. 2019). Hispanic ethnicities have also been described as risk factors for microtia in population-based studies (Luquetti et al. 2012). Microtia prevalence rate is up to 2 to 3 per 10,000 births in Asian population (Yamaguchi et al. 2017; Mussi et al. 2019).

Treacher Collins syndrome (TCS) consists of uneven ears (*Fig.1.2C*) together that may present as rotated, and occur in 77% of patients with TCS (Ma et al. 2019). Along with pinna deformity, there is mandibular under development. These malformations happen together because both grow embryonically from the first and second brachial arches (Ma et al. 2019). Polychondritis is an autoimmune rheumatic disorder in which destructive inflammation of cartilage is observed (*Fig.1.2D*) along with painful episodes. As the disease progresses anatomical deformation and functional impairment of the affected part occurs. Almost 80% of the population diagnosed with relapsing polychondritis experiences auricular chondritis. Although the clear cause of chondritis is still unknown, autoantibodies against collagen II have been detected (Borgia et al. 2018).

The pinna consists of chondrocytes and study has determined that there are some variances in normal chondrocytes and those collected from patients with microtia. These variances lead to reduced migration and causing hypoplasia (Ishak et al. 2011). The pinna may subject to injury caused by freezing of the skin and underlying cartilage, in case of people working in extreme weathers such as mining operations in the Arctic or sub-Arctic in winter (Schuknecht 1988). Various trauma or accidents such as burning and cutting can destroy the shape of pinna (*Fig.1.2 E*) and damage the tissue (Krishnan and Grodzinsky 2018). The pinna may get disfigured, either from heat shock due to high temperature. Traumas can lead to hemorrhage between the cartilage and its covering sheath producing cauliflower ear (Storck et al. 2014). Cavernous hemangiomas are benign tumors where assemblage of dilated blood vessels forms a lesion (Odat et al. 2016).

Current studies have revealed that the ear abnormalities consist of roughly 50% shrinkage in ear volume, approximately 19% shrinkage in ear length, and about 28% shrinkage in ear width (Ma et al. 2019). Perhaps, the pinna abnormalities lead to the most overall distress because of the cosmetic appearance (Ma et al. 2019).

The consequence of congenital deformities or trauma of the external ear reported in individuals has been associated with issues such as psychological negative impact (Johns et al. 2017). Especially in children, anotia/microtia can lead to speech and language interruptions, trouble while learning at school, problems in human communication and certain physical difficulties such as, for example, in wearing glasses (Mussi et al. 2019). These abnormalities also affect the patient's life due to reduced self-esteem, anxiety, depression, poor interpersonal skills (Johns et al. 2017). Fifty two percent of patients with microtia get suffer with anxiety and the quality of life is compromised (Mussi et al. 2019).

### **1.5 Surgical techniques for reconstruction of ear pinna:**

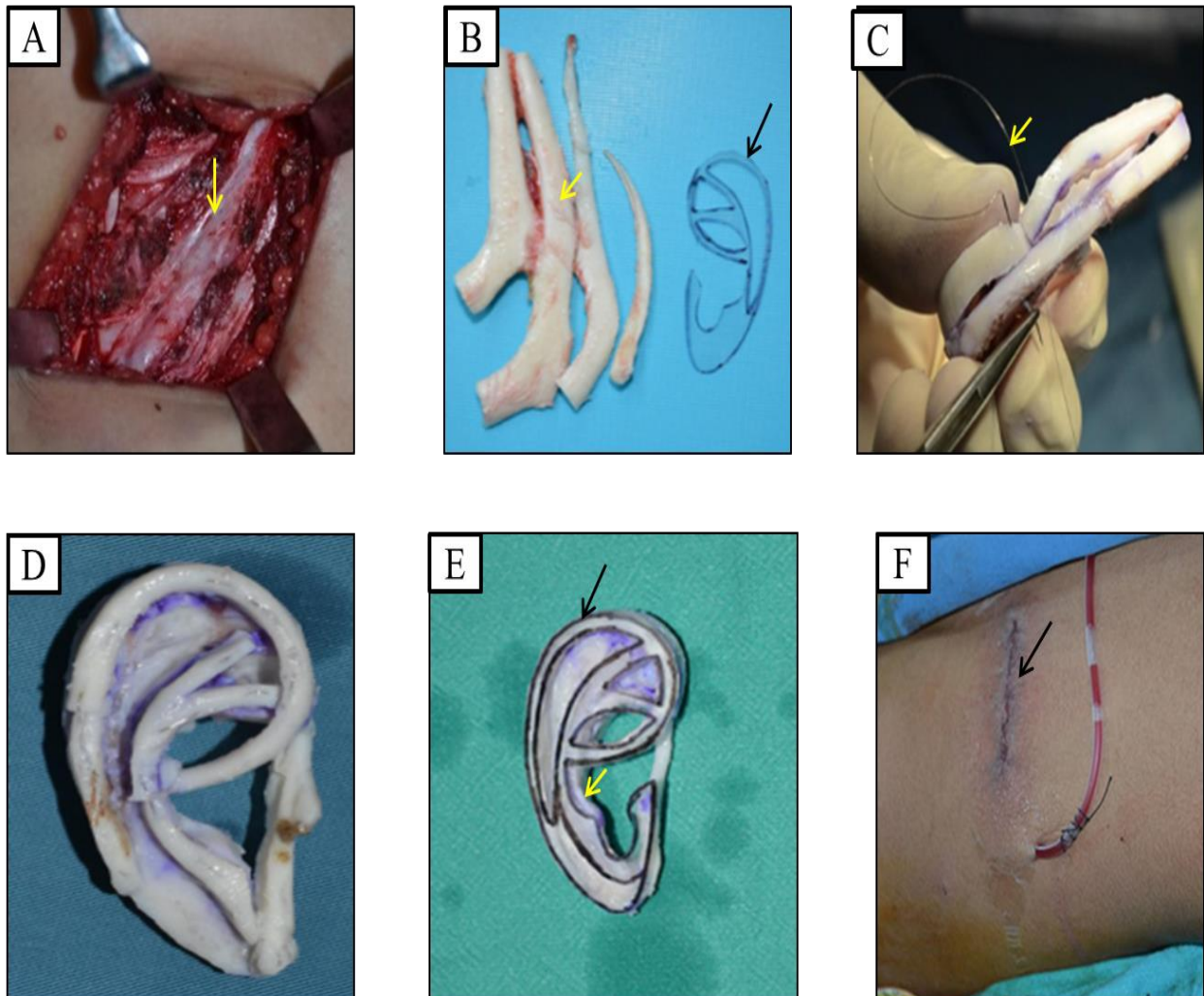
As early as 600 BC, physicians have been dealing with the problem of treating structural defects of the auricle. The current therapy for auricular reconstruction is still, greatest challenge for reconstructive plastic surgeons (Storck et al. 2014; Sharma et al. 2015; Mota and Danti 2019). The current procedure involves autologous ear reconstruction (AER) (patient's own rib cartilages) or allogeneic (genetically non-identical donor of the same species)/ (different species donor) xenogeneic costal cartilage or nasal septal cartilage or (artificial) prosthetic material is being used to create a framework of pinna (Rotter et al. 2008; Nayyer et al. 2012a; Borrelli et al. 2020).

The Nagata and Firmin techniques, refined from the original approaches described by Tanzer and Brent, are considered the current gold standards of AER (Rotter et al. 2008). The ideal time for reconstruction of the ear is after the child is 7 to 10 years old when the physical development of the ear has already reached a certain size or chest circumference is of 60 cm at the xiphisternum, which is necessary to avoid causing severe distortion between the reconstructed ear and the normal one (Chauhan and Guruprasad 2012; Sharma et al. 2015). Before the age of seven, pinna is still very fragile and thin. The final decision on the timing for repair depends on the physical development and the thickness of the lower chest so as to

obtain an ideal costal cartilage complex (Chauhan and Guruprasad 2012). The enlarged thickness of the Indian skin may also serve as important criteria, for framework holding and its reabsorption. Hence reconstruction of the ear pinna is suitable for patients above the age of 10 years (Sharma et al. 2015).

Principle of surgical operations technique is almost same but before operation there is need for inspection of the surrounding skin for scars, evidence of previous surgery and the hair-line. At first stage surgery, template of the cartilaginous scaffold is carved from the explanted sixth, seventh, and eighth rib. Sixth and seventh costal cartilages are used to build the base frame according to the previously measured ear pinna, and the eighth costal cartilage is recycled to form the rim or helix (Using scalpels and disinfected wood-carving chisels the basic template was carved from the main cartilage block, then the helical rim was carved by thinning of the piece from the floating eighth rib on its external convex surface to cause deliberate wrapping in a satisfactory direction). Fine-gauge wire or stainless steel wires or 6-0 prolene or 3-0 polydioxanone sutures used to assemble the constructed elements and create the one-piece, 3D framework (Chauhan and Guruprasad 2012).

## Development of 3D Printing for Tissue Engineering of Ear Pinna



Sharma M, Dudipala RR, Mathew J, et al. Objective analysis of microtia reconstruction in Indian patients and modifications in management protocol. *Indian J Plast Surg.* 2015;48(2):144-152. doi:10.4103/0970-0358.163050

*Figure 1.3: General autologous surgical procedure for ear reconstruction (A-E) and its post-operative problems (F).*

*A-E: Reconstruction procedure using surgical techniques (A- yellow arrow indicated for costal rib cartilage, B- black arrow indicated for patient specific template, C- sutures used to assemble the constructed elements, D- constructed 3D framework, E- template with constructed 3D framework). F: Post-operative chest Scars.*

The operative ear position was marked using the film template and preoperatively determined measurements. A small incision was made along the ear vestige dissecting the skin pocket and removing the cartilage remnant beneath the skin pocket (A small incision is given at the site of designated normal ear position) formation. Newly created framework is

inserted in the pocket and closed it with the help of skin (Chauhan and Guruprasad 2012; Sharma et al. 2015). The Nagata technique has the basics remain the same fewer stages and has been shown to yield more consistent outcomes in the hands of some surgeons. During the first stage a complete framework, including the tragus, is inserted into a skin pocket, and the lobule is transposed. This stage corresponds to the three first stages of Brent's technique (Firmin 1998). After first stage surgery patients were discharged on the second post-operative day on pain prescription and antibiotics. Patients are advised for ear dressing after 5 days and the sutures are removed on the usual after 7 days. At the completion of the first stage task all the structures visible in a normal human ear should be recognizable in the reconstructed ear (Chauhan and Guruprasad 2012; Sharma et al. 2015).

The second stage is usually done 5–6 months after the first stage (Chauhan and Guruprasad 2012; Sharma et al. 2015). In second stage ear framework is elevated (lifted from the base) by giving an incision in the scalp. An additional piece of rib cartilage, which was placed under the chest wall skin at the period of first stage surgery was taken out, designed and used as a support for the elevated ear framework by exactly suturing it behind the ear. It helps in providing stability to framework of the ear (Chauhan and Guruprasad 2012; Sharma et al. 2015). The superior part and posterior of the ear is then enclosed by taking a layer of tissue from the below surface of the scalp (temporoparietal fascial flap). It is vascularized and it benefits in providing the nutrition of the cartilage thus maintaining the reconstructed ear over a long period (Sharma et al. 2015). After that back side of ear is further enclosed with a section of skin which is taken from the scalp and it finally closes the surgical wound. The skin graft was sutured and followed by ear dressings for 7 days (Sharma et al. 2015).

This stage was optional based on patient's need but when performed gives the reconstructed ear a better aesthetic and natural look. Third stage was performed 3- 4 months after the second stage surgery. This stage involves procedures like correction of minor rotational and

positional defects of the reconstructed ear. This helped in revising the scar at the previous harvest site (Chauhan and Guruprasad 2012). General principles of surgical procedure for ear reconstruction shown in (*Fig.1.3 A-E*).

An alternative treatment option to surgical reconstruction is the use of bone-anchored prostheses (Rotter et al. 2008). Various prosthetics such as silicon framework, porous polyethylene (PE), polymethyl methacrylate (PMMA), teflon, polyvinyl chloride (PVC), polyurethane, hydroxyapatite, titanium implants have been used as an ear pinna framework reconstruction (Nayyer et al. 2012a; Storck et al. 2014). The first stage involves rotating a superficial temporoparietal flap over the framework with skin graft and pocket. The second stage was a lobule transposition and ear elevation (Chauhan and Guruprasad 2012).

Advantage of current surgical techniques is that autologous costal cartilage graft provides blood supply and minimal risk of resorption of grafted cartilage. The color and texture can be well matched compared with surrounding tissues. The most important benefit of this surgical technique is the autologous objects used reduce the risk of infection or extrusion of the graft (Storck et al. 2014). Allogenic/prosthetic surgical materials two stage technique advantages are less invasive and reliable method of total ear reconstruction in comparison to other techniques (Chauhan and Guruprasad 2012). Prosthetic surgical material can be easy to shape, placed immediately, without surgery, and cost-effective (Nayyer et al. 2012a; Chinnasamy et al. 2018).

### **1.6 Limitation of surgical techniques:**

The current surgical autologous costal cartilage treatment is requires skilled surgeons to obtain excellent results, Harvesting of autologous costal cartilage is time consuming process, associated Post-operative chest Scars (*Fig.1.3 F*) and postoperative discomfort (Nayyer et al. 2012a). Other obstacles such as variable cosmetic results, donor-site morbidity, risk of

pneumothorax, deformities of the thorax and considerable postoperative pain (Rotter et al. 2008; Nayyer et al. 2012a). Surgical autologous costal cartilage treatment is also age dependent. The surgeries have to be done between 7 to 10 years of age otherwise severe distortion may occur in chest. Autologous Brent's technique does not show good results after surgeries (probably due to the thicker Indian skin) (Sharma et al. 2015).

Xenogenic/ allogenic/ alloplastic surgical material or graft needs continuous monitoring post-surgery. Complications for alloplastic material include the risk of extrusion with possibility of alopecia (hair to fall out in small patches), lifelong immunosuppression to avoid the risk of infection and ultimately graft rejection (Storck et al. 2014; Borrelli et al. 2020).

Prosthetic materials such as silicone framework may induce contamination, porous skin, bleeding and framework displacement (Nayyer et al. 2012a; Storck et al. 2014). Various prosthetic materials produce great variation in size and shape that must be produced to match the opposite normal ear (Chauhan and Guruprasad 2012). Prosthetic pinna are supposed to be replaced every few years as the old one wears off (Chinnasamy et al. 2018).

Generation of ear framework is done using Two-dimensional (2D) template (placing a 2D X-ray film over the normal ear and tracing the outlines). 2D template does not offer sufficient data such as thickness and gravity features of the normal ear framework due to compression applied on the ear to track the contour changes the shape (Facchini et al. 2020). Three-dimensional (3D) ear model is simply a visual aid for the plastic surgeon used to find and cut from the cartilage in the reconstruction method. But result is dependent on the surgeon's technical abilities, visual capacity to draw replica of ear (Facchini et al. 2020). This surgical technique requires multiple operations which makes it expensive for patient.

These limitations of surgical procedures can be overcome by using Tissue Engineering (TE). Using TE, providing a patient specific solution for ear abnormalities becomes easier and

cheaper. The cartilage used for reconstruction of ear pinna can be created artificially without performing surgery which makes it a hassle-free technique for pinna reconstruction (Chauhan and Guruprasad 2012).

### **1.7 Tissue engineering for Ear Pinna:**

TE provides a viable alternative for reconstructive surgeries of the external ear (Ikada and Ikada 2006; Borrelli et al. 2020). Regenerative Medicine (RM) is a growing area which associations with TE as principle based on self-healing in the regeneration of cells, tissues, and organs, to restore their impaired function (Borrelli et al. 2020). TE deals with methods of regeneration using chondrocytes or chondrogenic precursors, stem or progenitor cells, growth factors TGF and BMPs and scaffold (Adelola O. Oseni, Claire Crowley, Maria Z. Boland 2005; Kim and Evans 2005; Oseni et al. 2011; Borrelli et al. 2020).

In the first Autologous Chondrocyte Implantation (ACI) clinical trial anchorage autonomous growth and the appearance of COL2A1, FGFR-3 and BMP-2 were evaluated to substantiate the expansion of chondrocytes. Xenogeneic and allogeneic chondrocyte were studied as an alternative cell sources. However, these cells can get involved in immune responses. Therefore, more studies are needed to alleviate such issues. Now, a technique for optimization of *ex vivo* selection and expansion of chondrocytes is an active research area in the field of TE. However, combinatorial approaches of cell with TE and scaffold are increasing these days. Chondrocytes cell source along with biocompatible scaffolds and growth factors are being used in RM for treating cartilage related defects.

Finding a suitable scaffold material (naturally and synthetic) like ECM is essential for the ability to support cell growth, to withstand stress, vasculogenesis, non-immunogenic response for successful auricular tissue engineering (Bichara et al. 2012; Nayyer et al. 2012a). Allogeneic or xenogeneic or synthetic scaffold can lead to adverse reaction. Hence, acellular

ECM or cell-free decellularized ECM (dECM) scaffolds are the primary necessities of tissue regeneration with minimization of an adverse host reaction and promotion of constructive remodelling of host tissue for clinical applications (Crapo et al. 2011; Utomo et al. 2015a; Kawecki et al. 2018). dECM was obtained by decellularization techniques including physical procedures (agitation, freeze-thaw cycles), chemical procedures (ionic –non-ionic detergents, antioxidant agent, acids and alkali), and biological procedures (enzymes) (Crapo et al. 2011; Kawecki et al. 2018).

Physical methods such as mechanical agitation along with detergent, and/or enzymatic solutions for dense tissues like cartilage require longer time. Freeze–thaw cycles form ice crystals which punctures cell membrane, preserve glycosaminoglycan and collagen content, and also does not alter the mechanical and viscoelastic properties of the cartilage ECM and (Szarko et al. 2010; Kim et al. 2019). Chemical procedures such as using ionic detergents Sodium dodecyl sulfate (SDS) and sodium deoxycholate are strong detergents that can completely disrupt cartilage cell membranes and fully denature proteins (Szarko et al. 2010; Kim et al. 2019). Dimethyl sulfoxide (DMSO) is a cryopreservative and used as a solvent to decellularize tissues which improves the diffusivity of other detergents in cells, which consequently reduces the reaction time and improve the quality of decellularized tissue (Guler et al. 2018). Non-ionic detergents (Triton X-100) are generally considered to solubilize proteins while preserving native protein organization (Porzionato et al. 2018).

Alkaline bases like sodium hydroxide (NaOH) (Bałakier et al. 1991), ammonium hydroxide denature genetic materials can also eliminate minute growth factors from the subsequent ECM (Porzionato et al. 2018). Acids can also denature ECM proteins including GAGs, collagen, and growth factors. It is important to optimize the dose and exposure time when acids are used for decellularization (Porzionato et al. 2018). Effect of an extreme pH can increase the efficacy of cell elimination but can impart substantial variations to the ECM

ingredients. The use of alkaline or acidic solutions during decellularization needs a neutral pH approach to attain effective decellularization without severe loss to the ECM constituents (Porzionato et al. 2018). Combination of physical and chemical decellularization techniques can reduce the exposure time of cartilage to decellularizing agents (Szarko et al. 2010).

Enzyme (trypsin) mostly used as decellularizing agents for cell removal due to its lack of specificity toward native collagen. Trypsin does not induce a cytotoxic effect and eliminates peptides of non-helical collagen responsible for the stimulation of the immune reaction (Porzionato et al. 2018).

Ineffective decellularization can reduce growth factor content, denature and loss of collagen network has been shown to be associated with graft rejection response which can inhibit a constructive remodelling outcome (Porzionato et al. 2018). Optimization of decellularization techniques for getting dECM are different among tissues or organs due to tissue specific ECM and geometric concerns (Porzionato et al. 2018). However, number of cycles or days are required to achieve optimum decellularization of ear cartilage is yet not specified (Gong et al. 2011; Rahman et al. 2018).

Decellularized tissue can be transformed into formation of solubilized dECM in slurry form. Its slurry form of pulverized molecules so does not preserve the architecture of the natural ECM but preserve its in molecular forms (Kim et al. 2019). These solubilized bioink (dECM slurry) was used for formation of cartilage scaffold using mould (Kim et al. 2019; Facchini et al. 2020). There are two main classes of bioink resources which are used in 3D bioprinting of tissue/organ constructions. One is the cell-scaffold built approach and the other one is a scaffold-without cell (Jose et al. 2016; Gopinathan and Noh 2018).

Molds can be used to produce biomaterials or cell-biomaterial constructs in the shape of ear (Rotter et al. 2008). It is required to apply the molding scaffold in an accurate and pressure

free mode, to take into account the elastic stability of the auricle (Rotter et al. 2008). The application of various ECM act like scaffolding materials such as synthetic (Polyglycolic acid (PGA), Polyethylene glycol (PEG), Polycaprolactone (PCL) based polyurethanes, Poly (vinyl alcohol) (PVA), Polylactic acid (PLA) and biological (dECM cartilage, collagen, fibrin, alginate and silk polymer and gelatin) hydrogel or bioink form application is possible in a relatively short time, at low cost, recyclable, easily extruded into matrix or gel, and were able to construct molds (Rotter et al. 2008; Hwang et al. 2014). The positive or negative molding techniques and framework for support were used to produce human ear pinna shape. Computer-aided design/computer-aided manufacturing (CAD/CAM) virtual molding is used for constructing accurate molds as well as titanium wires were used for stable framework to gain the shape. The general progress of tissue engineering contributing in reconstruction is shown in (*Fig.1.4*).

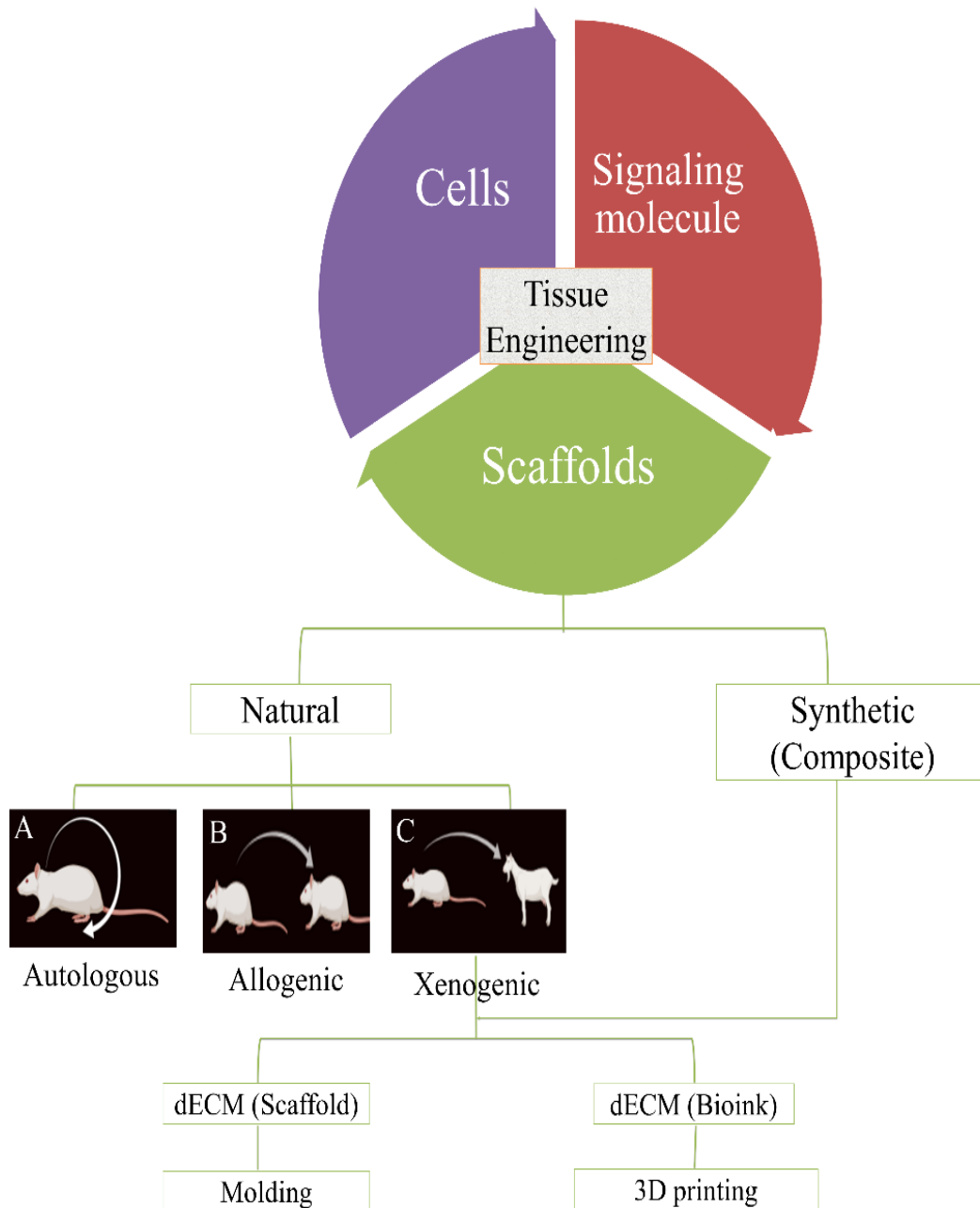


*Figure 1.4: Progress in Tissue engineering*  
*Tissue engineering key factors such as cells, signaling molecules, scaffold sources with its current progress techniques such as molding and 3D printing.*

### 1.8 Biological TE scaffold:

Ting et al 1998 first reported TE neocartilage in vitro utilizing natural scaffold fibrin gel for formation of ear template seeded with bovine chondrocytes. *In vitro* preculture for 28 days helped maintain the original shape of ear constructs (Ear shape was generated from hand cut positive (Ting v 1998). *In vivo*, implanted subcutaneously in female nude mice after 4 weeks implant was taken for histology and mechanical analysis. GAG expression was observed with mechanical character as almost similar to native (Ting v 1998).

Ear shape was generated from prefabricated molds bone wax and injection molding techniques. The hand-sculpted positive mold was allowed to dry for 48 hours then used to generate two pieces of the negative mold. The negative mold worked as the external stent used for manufacturing of the auricle cartilage. Chondrocyte-fibrin polymer suspension added between layers of lyophilized swine perichondrium was placed in the bone wax and allowed polymerize. The 3 layers ear shape construct was implanted after 12 weeks into a subcutaneous pocket on the back of an athymic male rat and stented externally for 6 weeks. Tissue engineered ear construct histology was similar to native auricular cartilage including presence of abundant sulphated GAGs and elastin fibres. Experimental ear construct on both surfaces were capable to undergo almost 180° of both torsion and winding in either direction without sign of fracture and recovered their preliminary shape after testing (Xu et al. 2005).

A silicone block in the shape of a human auricle was placed in the wistar rats in a subcutaneous pocket. The femoral vascular pedicle is transposed onto the silicone to prefabricate the ensuing capsule creation. 4 weeks after implantation of the chondrocytes into the capsule, the construct is isolated on its pedicle. The construct was vascularized created on the fused transposed vessels (Neumeister et al. 2006).

Human adult half size ear was imprinted by hand in clay and used to create polydimethylsiloxane molds. Coiled metallic titanium wire bent was prepared to mimic the

outline of the human auricle and was fixed in half of the fabricated collagen scaffolds, while left over collagen scaffolds was made without wire support. Constructs were sterilized with ethylene oxide (ETO) gas before 14 days of seeding with chondrocytes and implanted subcutaneously on the backs of female athymic mice up to 6 weeks. In constructs, with and without wire support neocartilage formation, it was confirmed by histological and biochemical analysis were similar to that of native sheep pinna cartilage (Zhou et al. 2011).

Computerized tomography (CT) derived ear data used for to produce CAD-Stereolithography (STL) 3D ear image. The 3D image of the ear was sent to the 3D impression and through laser impression produced first positive mold overlapping layer by layer. The negative mold created by silicone, based on the 3D first positive mold. Mesenchymal perichondrocytes isolated from auricular cartilage of New Zealand White rabbits. Inside negative mold the cells were seeded with biodegradable alginate and silk-fibroin (*Bombyx mori* silkworm) polymer for one week of *in vitro* culture. The ear shaped fibrin-based scaffold was implanted into the *in vivo* subcutaneous pocket of immunocompetent rabbits. After 8 weeks of implantation constructs were harvested for examination. TGF- $\beta$  growth factor and BMP-2 were used in this research for chondrogenic expression and ear cartilage construct that resembles the human ear (Sterodimas and De Faria 2013).

Ear images were obtained using a 3D digitizer and these images were converted to STL files. Negative 3D ear mold of acrylonitrile butadiene styrene (ABS) was printed out through fused deposition modeling (FDM) 3D printer. Collagen for implant molding was extracted from sprague rat-tails mixed with the cells. Collagen cell suspension inserted into ear molds and simultaneously acellular constructs culture for 3–5 days. Construct were implanted subcutaneously of nude rats while construct harvested after 1 and 3 months were native

auricle and construct. Biomechanically and histologically examination was revealed that construct mimic to native ear (Reiffel et al. 2013).

### 1.9 TE synthetic (Composite) scaffold:

First report of synthetic biodegradable, porous polymers PGA + PLA and its derivative copolymers fabricated in the human ear shape scaffold was created using silicone rubber prosthetic ear mold. The synthetic ear was seeded with bovine chondrocytes and implanted 7 weeks *in vivo* (nude athymic mice). Ear transplant resorbed during *in vivo* implant period and implanted ear examination revealed that recellularized chondrocytes were morphologically similar to native ear (Vacanti 1992).

The PGA and PLA synthetic biodegradable ear shape template (Ear shape plaster cast used as alginate impression material) was seeded with bovine articular cartilage chondrocytes and subcutaneous implanted 10 weeks *in vivo* (Nude athymic male mice). Harvested implant histo-immunochemistry revealed that new cartilage formation and collagen II expression (Cao Y 1997).

PGA/PLA copolymer was used in the formation of ear pinna shape templates (Ear shape was sculpted into using polymethyl methacrylate mold). Templates were allowed to vacuum dry for evaporation of residual methylene chloride. Ear templates seeded with chondrocytes *in vitro* 5<sup>th</sup> day's culture. Experimental and control grafts (Rabbit nasal tip graft, a cross, and form ear template) were subcutaneously implanted (4 or 8 weeks) or (6 to 12 months) into the *in vivo* (New Zealand white rabbits) and after harvesting were transplanted for 4 weeks. All white rabbits accepted implantation and no graft extrusions were observed. Implanted auricle was characterized by morphological histological and biomechanical (Britt and Park 2015).

Auricular-shaped construct were molded 6 weeks within an ear-shaped silicone mold, and bioresorbable PGLA-PLLA fleece soaked with human nasal septal chondrocytes were mixed

with human fibrinogen. After *in vitro* incubation silicone cylinder the auricular-shaped fabricated implant were implanted in subcutaneous areas *in vivo* model (Nude mouse) up to 12 weeks. The implants were investigated for macroscopic and microscopic features. Microscopic inspection confirmed chondrocyte, collagen and low level of GAG synthesis and that all of the implants showed stability in shape to an excessive extent (Haisch et al. 2002).

Pure gold inert molds (24 carat) were structured in two distinct halves, which were fixed with minor gold screws. Frequent perforating holes of 0.5 to 0.7 mm diameter were drilled in gold mold. Alginate was cross linked in the presence of calcium to become a thicker gel, pluronic F-127 and PGA to form hydrogel. Combinations of chondrocytes and each separated biodegradable polymers were used inside a perforated, ear shaped, hollow gold mold. These molds, along with a control gold mold, were implanted for 8 to 20 weeks *in vivo* subcutaneously of immunocompetent large-animal models (pigs and sheep). Histological examination showed areas of cartilage mixed with fibrous tissue and synthesis GAGs. Implants of calcium alginate maintained human ear shape, pluronic F-127 noted cartilage generation (Kamil et al. 2004).

Vinyl polysiloxane was used as a negative impression mold obtained from a 1-year-old child. PLLA + PCL was introduced into the molds and lyophilized at 40°C for 12 hrs. Finally, molds were placed under vacuum at 60°C for 12 h to obtain a shape as a small human ear. Bovine articular chondrocytes were seeded and without cell seeded ear polymer mold alone were each implantated in dorsal skin flaps of athymic mice for up to 40 weeks. Retrieved constructs examined were cartilage, vasculature and configuration was maintained while cell seeded copolymer expresses aggrecan. Chondrocyte-seeded ear polymer mold retained their original configuration over the 40-week time period (Utilizing et al. 2004).

3D human ear model was formed by hand using clay modeling. Three types of auricular polymeric scaffolds PLLA, PCL and poly 4-hydroxybutyrate (P-4HB) were used in this

## Development of 3D Printing for Tissue Engineering of Ear Pinna

experiment used for shape of a human ear using the negative mold (vinyl polysiloxane). Granular sucrose was mixed with a minimal quantity of water and transferred into the negative ear mold to form into an ear shape sucrose template. Autologous chondrocytes were collected from adult sheep ears and white rabbit, and were 4 weeks cultured with the ear-shaped scaffolds. Each animal nude mice (40 weeks) while in New Zealand white rabbits (12 weeks) received one human ear-shape cell-polymer construct on the back. After 4 and 8 weeks, each sheet constructs were harvested and observed some degree of neocartilage formation. PCL ear were preserved a better gross architecture than PGA and P-4HB ears evaluated (Shieh et al. 2004a).

CAD/CAM was employed to generate 3D printed negative resin ear molds as per the shape of the patient's normal ear was scanned by CT. The negative mold outer portion was replaced by a silicon rubber, which was molded according to the inner portion of the resin negative mold. Fabric PGA fibers were pressed using the negative mold for over 12 h. PLA solution was evenly added onto the PGA scaffold, dried in a 65°C oven, weighed, and pressed again with the negative mold. Finally edge of the ear-shaped scaffold was carefully shaved as per the positive CT scan ear. 3D laser surface scanning system was used for the shape analysis of construct and negative molds. Swine articular derived chondrocyte was *in vitro* seeded into the scaffold and were harvested at 4 weeks, 8 weeks and 12 weeks for shape and histology study. Scaffold maintains the ear-shape throughout the *in vitro* culture period. 20% PLA scaffolds beneficial expressions of cell seeding, ECM synthesis, and cartilage development (Liu et al. 2010).

Human auricle shaped negative impression silicone mold created through rapid prototyping directly from CAD, via an STL file. PCL based mixture was injected into a silicone mold and heated at 67 to 68°C for 2h for formation of 3D human auricle shaped scaffold. Pinna cartilage-based chondrocyte were harvested from chinchilla-bastard rabbits and seeded in 3D

human auricle shaped scaffold for 6 days *in vitro* culture. These constructs were initially implanted in the skin flaps (rabbits) and then neovascularized using vascular loops with terminal arteriovenous anastomosis. These constructs were then developed as connective tissue flaps and re-implanted in the same location, micro surgically. There was evidence of cartilage-like tissue formation and the presence of newly formed collagen type II was seen (von Bomhard et al. 2013).

Ultrafine composite fibers of gelatin (GT) /PCL were fabricated as membrane sheet via electrospinning technology in that GT/PCL (50:50) delivered by a syringe pump to metal needle, used as the spinneret and mounted in the form of membranes. Thus, ready GT/PCL membranes sheets were dried in a vacuum oven for 1 week at 37°C and then lyophilized in a vacuum freeze-drier. Chondrocytes were harvested from pig ears and seeded onto GT/PCL sheets for 7 days culture. Cell seeded GT/PCL sheets were stacked on top one by one 20 layers like the sandwich model contained between chondrocyte suspension. Sandwich model was incubated at 37°C for 4 weeks of culture *in vitro*. An auricle -shaped titanium alloy model was prepared and was used as mold. The model was positioned in the culture and GT/PCL sheet was then sited on top, to cover the entire model. The whole ear sheet titanium model, was cultured for 2 weeks, and then subcutaneously implanted into nude mice. After 6 weeks of implantation GT/PCL ear pinna constructs harvested and confirmed its biocompatibility. Constructs were recellularized and maintained their shape. During *in vitro* membranes gradually degraded, although the seeded cells proliferated and secreted ECM to maintain the 3-D structure (Xue et al. 2013a).

PE human ear shaped alloplastic surgical implants (commercially available) were immersed in the oxidation solution (sulfuric acid/water/chromium trioxide) after acetone wash then were dried and stored in a desiccator until use. Surface modified and unmodified (Control) Implants were implanted subcutaneously of Sprague-Dawley rats while Implants were

harvested after 2 weeks. Harvested ear implants were seeded with the chondrocytes and fibrin solution was performed with the applying cell-spraying system (Gas-assisted applicator and a dual syringe). The chondrocyte-fibrin-covered implants were placed into the subcutaneous space of male athymic mice. Constructs were retrieved at 2, 4, 8, and 12 weeks after implantation for analyses. Cell-spraying was system allowed for homogenous cell matrix. Surface modification of *in vitro* and *in vivo* revealed functionalized implant surface. No evidence of *in vivo* necrosis or extrusion was seen (Kim et al. 2016).

### 1.10 3D Bioprinting for Reconstruction of Ear Pinna:

Scientists studied 3D printing technology to develop the reconstruction of ear pinna which can eliminate the limitations of traditional methods to some extent. 3D printing techniques allows to design desired scaffold characteristics with layer-by-layer deposition of polymer from computer-controlled nozzle accurately (Jessop et al. 2016).

In FDM/Extrusion printing techniques biomaterials are extruded from the nozzle creating a definite object (Shen et al. 2019). Material jetting / Inkjet are methods in which deposition of droplets by droplets and displacement of material with or without cells is used to develop a 3D object (Lee et al. 2014a). Selective laser sintering (SLS) based on laser scanning is performed under the computer in command to melt and bond powdered polymer on a 3D working platform (Shen et al. 2019). Stereolithography is a 3D printing system that selectively polymerizes layers of a photopolymer via computer-controlled ultraviolet (UV) light contact (Shen et al. 2019).

If 3D bioprinting is combined with RM, it can overcome current problems of reconstruction of pinna to reduce time and cost (Jessop et al. 2016; Shen et al. 2019). Additive manufacturing (AM) involves certain steps which are initially a CAD based virtual model for pinna is created and then converted to STL file. This file slices the CAD object into thin

cross-sectional layers for printing the bioink by printer. Further interpretation of STL to G-code on the host computer and controls are sent to the printer that allowed the object to be 3D printed (Saxena and Kamran 2016).

Multi-head tissue/organ building system (MtoBS) based on CAD/CAM was used to construct a porous 3D structure and placed various hydrogels into the structure. The MtoBS had a specific regulator for motion, temperature, the plunger and pneumatic system. Ear pinna framework made up of PCL and PEG was synthesized by layer-by-layer deposition. Pre-osteoblasts were seeded framework culture for 7 days and after checked its tensile property. Human Adipose Derived Stem Cells (ASCs) were isolated and cultured for one week were chondrocytes and adipocytes, differentiated. Alginate hydrogel mixed with chondrocyte laden hydrogel (CLH) and Alginate hydrogel mixed adipocyte laden hydrogel (ALH) were prepared. Cell laden hydrogel mix or each separately or without were printed on PCL framework using the MtoBS through the layer-by-layer deposition process and incubated at 37°C. After a week of incubation polymerase chain reaction (PCR) were performed for Deoxyribonucleic acid (DNA), sox9, collagen type II, and aggrecan expression level. 3D printing sacrificial layer was effective for completely synthesizing the porous framework (Lee et al. 2014b).

FDM 3D printer nozzle was heated to melt the polyvinylidene fluoride (PVDF) and the auricle is produced in order to form layer by layer onto the build plate according to STL ear data. Analytical testing done at conditions of applying different stimuli (electric current), pressure, temperature and cold (imitating human skin receptors) gives high stability of printed pinna (Suaste-Gómez et al. 2016). Printed pinna shows piezoelectric and pyroelectric properties. PVDF also contribute for biocompatibility, degradability, temperature sensor, pressure sensor and non-toxic.

Fabricated 3D hybrid scaffold by using PCL for regenerating auricle shape was designed using CAD software. Human adult stem cell and chondrocytes (rabbit articular) cells -laden alginate solution seeded on the auricle PCL framework for 28 days culture. PCL auricle scaffold was implanted subcutaneously in sprague-dawley rats while construct was harvested after 12 weeks. 3D hybrid scaffold was examined with and without the presence of chondrocytes. *In vitro* and *in vivo* experiments showed that the construct enhanced mechanical properties and chondrogenesis was definitely occurred (Jang et al. 2020a).

In research by Jia et al 2020, cartilage was freeze-dried, pulverized and decellularized in the form of acellular cartilage matrix (ACM) powder. Designing of scaffolds with ACM/Gelatin were mixed and decanted into cylindrical molds, then freeze-dried to construct 3D porous ACM/Gelatin scaffolds. Goat ears derived chondrocytes were isolated and was seeded into each scaffold for 14 days of culture and revealed ECM development. ACM/Gelatin scaffolds integrating with 3D printed PCL inner core designing, silicone cast molding, and followed by pre-cooling and freeze-drying. Chondrocyte suspension was seeded into the ACM/Gelatin ear-shaped scaffold and incubated for 2 weeks. Constructs were subcutaneously implanted into nude mice. ACM/Gelatin fabricated into human-ear shape and proper mechanical strength. By optimizing proportion and concentration of ACM and gelatin, the presented scaffolds gain required pore structure and degradation rate as well as biocompatibility. Histology highlights the intact lacuna structure and ECM deposition (Jia et al. 2020a).

### 1.11 Gap in existing research:

A number of gaps or boundaries have been recognized with current tissue-engineered pinna like low success rate of accuracy in shape and size of pinna (Nayyer et al. 2012a; Hwang et al. 2014). According to researchers, chondrocytes are needed to be cultured beforehand and then seeded in the scaffold which is time consuming and the possibility of contamination increases. The techniques which are (Zhou et al. 2011; Xue et al. 2013b) or external mold

required (Neumeister et al. 2006; Bomhard et al. 2013) got better shape otherwise without external mold of the human pinna shape getting distorted or shrink (Vacanti 1992; Haisch et al. 2002; Neumeister et al. 2006; Zhou et al. 2011; Sahakyants and Vacanti 2020). Less tensile strength than native pinna (Britt and Park 2015), complete cartilage replacement was not always achieved, inflammatory reaction after transplant (Shieh et al. 2004a; Britt and Park 2015), antigenicity and fibrosis (Kamil et al. 2004), longer time for ECM deposition after transplant (Isogai et al. 2005), cost increase for reconstruction due to patient-specific molds (Sterodimas and De Faria 2013) and less clinical utility (Xu et al. 2005) are the restrictions of traditional reconstruction methods of ear pinna. Traditional ear pinna reconstruction mold was not capable to mimic the efficient characteristics of native ears and consumes time compromising quality of natural pinna for patient. Touch-free laser optic scanning of the auricle are an interesting alternative. However, this digitizer is not applicable for direct scanning of the patient auricle due to high cost (Xue et al. 2013a). The human transplant is not done till date to know whether the mechanical strength, shape, size, and tissue composition will be retained or not after transplant considered as human trial (Kamil et al. 2004; Liu et al. 2010; Reiffel et al. 2013). Considering all these gaps, a clear need exists to develop alternative strategies to reconstruct auricle.

### 1.12 Objectives:

1. To develop and optimize bioink (Combination of polymer PVA/PLA/PEG + biological goat ear pinna cartilage) for 3D printing of ear pinna.
2. To study histology and mechanical properties of 3D printed of ear pinna.
3. To test biocompatibility of the 3D printed ear pinna.
4. To study transplantation of 3D printed ear pinna.

### 1.13 Scope of work

The scope of TE human ear pinna through molding technology related material for implant containing xenogenic decellularized ECM with improved biocompatible and biomechanical properties. This molding pinna or implants or graft can be used for the replacement of damaged ear pinna or elastic cartilage and more specifically without graft versus host reaction. Scope also related to a method comprising the generation of patient specific ear pinna using molding techniques followed by surgically implanting the graft. Primary scope of the patented molding research is to construct human ear pinna using goat ear cartilage ECM. Another scope of research is to develop method of decellularizations using use physicochemical and enzymatic to remove all the cellular content (Protein and DNA) of goat ear cartilage. Other importance of work is to fabricate poly vinyl chloride mold for customized ear shape using CT image.

The scope of printed ear pinna through 3D printing related material for graft or implant containing xenogeneic decellularized ECM slurry with composite polymers improved biodegradability, biocompatible and tensile properties. The scope of this research is the bioink preserved the intrinsic ECM, attained viscosity for bioink formation and attained well nature for printing. Primary scope of the patented bioink research that printable bioink can attain well anatomical pinna shape, biomechanical properties, biodegradability and biocompatibility. This study highlighted the *in vitro*, *in ovo* and *in vivo* biocompatibility of 3D printed auricular constructs as a scaffold, for purposes of cartilage TE.

Hence in this research innovative molding scaffold and 3D printable bioink significantly scope in overcome problems that capacity of pinna cartilage to less regeneration, cartilage donor limitation, maintenance of tissue specific ECM, *in vivo* regeneration, and biocompatibility. This study molding pinna and printing pinna can be applied as an ear pinna cartilage substitute for clinical applications in the future.

### References:

- Adelola O. Oseni, Claire Crowley, Maria Z. Boland PEB and AMS (2005) Cartilage Tissue Engineering: the Application of Nanomaterials and Stem Cell Technology Adelola O. Oseni, Claire Crowley, Maria Z. Boland, Peter E. Butler and Alexander M. Seifalian. *Curr Opin Biotechnol* 16:503–509. <https://doi.org/10.1016/j.copbio.2005.08.004>
- Akkiraju H, Nohe A (2015) Role of chondrocytes in cartilage formation, progression of osteoarthritis and cartilage regeneration. *J Dev Biol* 3:177–192. <https://doi.org/10.3390/jdb3040177>
- Ali K, Meaike JD, Maricevich RS, Olshinka A (2017) The Protruding Ear: Cosmetic and Reconstruction. *Semin Plast Surg* 31:152–160. <https://doi.org/10.1055/s-0037-1604241>
- Balakier H, Zenzes M, Wang P, et al (1991) The effect of cryopreservation on the development of S- and G2-phase mouse embryos. *J Vitro Fertil Embryo Transf* 8:89–95. <https://doi.org/10.1007/BF01138661>
- Barrett-Jolley R, Lewis R, Fallman R, Mobasheri A (2010) The emerging chondrocyte channelome. *Front Physiol* 1 OCT: <https://doi.org/10.3389/fphys.2010.00135>
- Bartel-Friedrich S, Wulke C (2007) Classification and diagnosis of ear malformations. *GMS Curr Top Otorhinolaryngol Head Neck Surg* 6:Doc05
- Bichara DA, O’Sullivan NA, Pomerantseva I, et al (2012) The tissue-engineered auricle: Past, present, and future. *Tissue Eng - Part B Rev* 18:51–61. <https://doi.org/10.1089/ten.teb.2011.0326>
- Borgia F, Giuffrida F, Guarneri F, Cannavò SP (2018) Relapsing polychondritis: An updated review. *Biomedicines* 6:1–14. <https://doi.org/10.3390/biomedicines6030084>

- Borrelli MR, Hu MS, Longaker MT, Lorenz HP (2020) Tissue Engineering and Regenerative Medicine in Craniofacial Reconstruction and Facial Aesthetics. *J Craniofac Surg* 31:15–27. <https://doi.org/10.1097/SCS.00000000000005840>
- Britt JC, Park SS (2015) Autogenous Tissue-Engineered Cartilage. 124:671–677
- Chauhan DS, Guruprasad Y (2012) Auricular Reconstruction of Congenital Microtia Using Autogenous Costal Cartilage: Report of 27 Cases. *J Maxillofac Oral Surg* 11:47–52. <https://doi.org/10.1007/s12663-011-0290-1>
- Chinnasamy A, Gopinath V, Jain AR (2018) Ear Prosthesis for Postburn Deformity. *Case Rep Otolaryngol* 2018:1–6. <https://doi.org/10.1155/2018/2689098>
- Correia CR, Moreira-Teixeira LS, Moroni L, et al (2011) Chitosan scaffolds containing hyaluronic acid for cartilage tissue engineering. *Tissue Eng - Part C Methods* 17:717–730. <https://doi.org/10.1089/ten.tec.2010.0467>
- Crapo PM, Gilbert TW, Badylak SF (2011) An overview of tissue and whole organ decellularization processes. *Biomaterials* 32:3233–3243. <https://doi.org/10.1016/j.biomaterials.2011.01.057>
- Eng H, Chiu RSF (2002) Spectacle fitting with ear, nose and face deformities or abnormalities. *Clin Exp Optom* 85:389–391. <https://doi.org/10.1111/j.1444-0938.2002.tb02391.x>
- Facchini F, Morabito A, Buonamici F, et al (2020) Autologous ear reconstruction: Towards a semiautomatic cadbased procedure for 3D printable surgical guides. *Comput Aided Des Appl* 18:357–367. <https://doi.org/10.14733/cadaps.2021.357-367>
- Firmin F (1998) Ear reconstruction in cases of typical microtia. Personal experience based on

352 microtic ear corrections. *Scand J Plast Reconstr Surg Hand Surg* 32:35–47.

<https://doi.org/10.1080/02844319850158930>

Gong YY, Xue JX, Zhang WJ, et al (2011) A sandwich model for engineering cartilage with acellular cartilage sheets and chondrocytes. *Biomaterials* 32:2265–2273.

<https://doi.org/10.1016/j.biomaterials.2010.11.078>

Gopinathan J, Noh I (2018) review 5 2018 Recent trends in bioinks for 3D printing.pdf. 1–15

Guler S, Aydin HM, Lü LX, Yang Y (2018) Improvement of Decellularization Efficiency of Porcine Aorta Using Dimethyl Sulfoxide as a Penetration Enhancer. *Artif Organs*

42:219–230. <https://doi.org/10.1111/aor.12978>

Haisch A, Kläring S, Gröger A, et al (2002) A tissue-engineering model for the manufacture of auricular-shaped cartilage implants. *Eur Arch Oto-Rhino-Laryngology* 259:316–321.

<https://doi.org/10.1007/s00405-002-0446-1>

Heffner HE, Heffner RS (2018) The evolution of mammalian hearing. *AIP Conf Proc* 1965:.

<https://doi.org/10.1063/1.5038516>

Hunter A, Frias JL, Gillessen-Kaesbach G, et al (2009) Elements of morphology: Standard terminology for the ear. *Am J Med Genet Part A* 149:40–60.

<https://doi.org/10.1002/ajmg.a.32599>

Hwang CM, Lee BK, Green D, et al (2014) Auricular reconstruction using tissue-engineered alloplastic implants for improved clinical outcomes. *Plast Reconstr Surg* 133:360–369.

<https://doi.org/10.1097/01.prs.0000438460.68098.4b>

Ikada Y, Ikada Y (2006) Challenges in tissue engineering. 589–601.

<https://doi.org/10.1098/rsif.2006.0124>

- Ishak MF, Chua KH, Asma A, et al (2011) Stem cell genes are poorly expressed in chondrocytes from microtic cartilage. *Int J Pediatr Otorhinolaryngol* 75:835–840.  
<https://doi.org/10.1016/j.ijporl.2011.03.021>
- Isogai N, Morotomi T, Hayakawa S, et al (2005) Combined chondrocyte-copolymer implantation with slow release of basic fibroblast growth factor for tissue engineering an auricular cartilage construct. *J Biomed Mater Res - Part A* 74:408–418.  
<https://doi.org/10.1002/jbm.a.30343>
- Jang CH, Koo Y, Kim G (2020) Jo ur l P re of. *Carbohydr Polym* 116776.  
<https://doi.org/10.1016/j.carbpol.2020.116776>
- Jessop ZM, Javed M, Otto IA, et al (2016) Combining regenerative medicine strategies to provide durable reconstructive options: Auricular cartilage tissue engineering. *Stem Cell Res Ther* 7:1–12. <https://doi.org/10.1186/s13287-015-0273-0>
- Jia L, Zhang Y, Yao L, et al (2020) Regeneration of human-ear-shaped cartilage with acellular cartilage matrix-based biomimetic scaffolds. *Appl Mater Today* 20:100639.  
<https://doi.org/10.1016/j.apmt.2020.100639>
- Johns AL, Lewin SL, Im DD (2017) Teasing in younger and older children with microtia before and after ear reconstruction. *J Plast Surg Hand Surg* 51:205–209.  
<https://doi.org/10.1080/2000656X.2016.1222294>
- Jose RR, Rodriguez MJ, Dixon TA, et al (2016) Evolution of Bioinks and Additive Manufacturing Technologies for 3D Bioprinting. *ACS Biomater Sci Eng* 2:1662–1678.  
<https://doi.org/10.1021/acsbiomaterials.6b00088>
- Jung BK, Kim JY, Kim YS, et al (2018) Ideal scaffold design for total ear reconstruction using a three- dimensional printing technique. 1–9. <https://doi.org/10.1002/jbm.b.34222>

- Kamil SH, Vacanti MP, Aminuddin BS, et al (2004) Tissue Engineering of a Human Sized and Shaped Auricle Using a Mold. *Laryngoscope* 114:867–870.  
<https://doi.org/10.1097/00005537-200405000-00015>
- Kawecki M, Łabuś W, Klama-Baryla A, et al (2018) A review of decellurization methods caused by an urgent need for quality control of cell-free extracellular matrix' scaffolds and their role in regenerative medicine. *J Biomed Mater Res - Part B Appl Biomater* 106:909–923. <https://doi.org/10.1002/jbm.b.33865>
- Kim JS, Hong S, Hwang C (2016) Bio-ink Materials for 3D Bio-printing. *J Int Soc Simul Surg* 3:49–59. <https://doi.org/10.18204/jissis.2016.3.2.049>
- Kim M, Evans D (2005) Tissue Engineering : The Future of Stem Cells. *Top Tissue Eng* 2:1–22
- Kim YS, Majid M, Melchiorri AJ, Mikos AG (2019) Applications of decellularized extracellular matrix in bone and cartilage tissue engineering. *Bioeng Transl Med* 4:83–95. <https://doi.org/10.1002/btm2.10110>
- Krishnan Y, Grodzinsky AJ (2018) Cartilage diseases. *Matrix Biol* 71–72:51–69.  
<https://doi.org/10.1016/j.matbio.2018.05.005>
- Lanz OI, Wood BC (2004) Surgery of the ear and pinna. *Vet Clin North Am - Small Anim Pract* 34:567–599. <https://doi.org/10.1016/j.cvsm.2003.10.011>
- Lee J-S, Hong JM, Jung JW, et al (2014a) 3D printing of composite tissue with complex shape applied to ear regeneration. *Biofabrication* 6:024103.  
<https://doi.org/10.1088/1758-5082/6/2/024103>
- Lee JS, Hong JM, Jung JW, et al (2014b) 3D printing of composite tissue with complex

shape applied to ear regeneration. *Biofabrication* 6:.. <https://doi.org/10.1088/1758-5082/6/2/024103>

Liu Y, Zhang L, Zhou G, et al (2010) In vitro engineering of human ear-shaped cartilage assisted with CAD/CAM technology. *Biomaterials* 31:2176–2183.  
<https://doi.org/10.1016/j.biomaterials.2009.11.080>

Luquetti DV, Leoncini E, Mastroiacovo P (2011) Microtia-anotia: A global review of prevalence rates. *Birth Defects Res Part A - Clin Mol Teratol* 91:813–822.  
<https://doi.org/10.1002/bdra.20836>

Luquetti D V., Heike CL, Hing A V., et al (2012) Microtia: Epidemiology and genetics. *Am J Med Genet Part A* 158 A:124–139. <https://doi.org/10.1002/ajmg.a.34352>

Ma X, Xie F, Zhang C, et al (2019) Correlation between mandible and external ear in patients with Treacher-Collins syndrome. *J Craniofac Surg* 30:975–979.  
<https://doi.org/10.1097/SCS.00000000000005216>

Mota C, Danti S (2019) *Ear tissue engineering*, Third Edit. Elsevier

Mussi E, Furferi R, Volpe Y, et al (2019) Ear reconstruction simulation: From handcrafting to 3D printing. *Bioengineering* 6:1–19. <https://doi.org/10.3390/bioengineering6010014>

Nayyer L, Patel KH, Esmaeili A, et al (2012) Tissue engineering: Revolution and challenge in auricular cartilage reconstruction. *Plast Reconstr Surg* 129:1123–1137.  
<https://doi.org/10.1097/PRS.0b013e31824a2c1c>

Neumeister MW, Wu T, Chambers C (2006) Vascularized tissue-engineered ears. *Plast Reconstr Surg* 117:116–122. <https://doi.org/10.1097/01.prs.0000195071.01699.ce>

O’Sullivan J, D’Arcy S, Barry FP, et al (2011) Mesenchymal chondroprogenitor cell origin

- and therapeutic potential. *Stem Cell Res Ther* 2:1–7. <https://doi.org/10.1186/scrt49>
- Odat H, Al-Qudah M, Al-Qudah MA (2016) Cavernous Hemangioma of the External Canal, Tympanic Membrane, and Middle Ear Cleft: A Case Report. *Head Neck Pathol* 10:261–264. <https://doi.org/10.1007/s12105-015-0650-0>
- Oseni AO, Crowley C, Boland MZ, et al (2011) Cartilage Tissue Engineering : the Application of Nanomaterials and Stem Cell Technology. *Tissue Eng Tissue Organ Regen* 233–266. <https://doi.org/10.5772/22453>
- Phull AR, Eo SH, Abbas Q, et al (2016) Applications of Chondrocyte-Based Cartilage Engineering: An Overview. *Biomed Res Int* 2016:. <https://doi.org/10.1155/2016/1879837>
- Porzionato A, Stocco E, Barbon S, et al (2018) Tissue-engineered grafts from human decellularized extracellular matrices: A systematic review and future perspectives. *Int J Mol Sci* 19:. <https://doi.org/10.3390/ijms19124117>
- Rahman S, Griffin M, Naik A, et al (2018) Optimising the decellularization of human elastic cartilage with trypsin for future use in ear reconstruction. *Sci Rep* 8:1–11. <https://doi.org/10.1038/s41598-018-20592-x>
- Reiffel AJ, Kafka C, Hernandez KA, et al (2013) High-Fidelity Tissue Engineering of Patient-Specific Auricles for Reconstruction of Pediatric Microtia and Other Auricular Deformities. *PLoS One* 8:. <https://doi.org/10.1371/journal.pone.0056506>
- Rotter N, Steiner A, Scheithauer M (2008) Reconstruction of auricular cartilage using tissue-engineering techniques. *Oper Tech Otolaryngol - Head Neck Surg* 19:278–284. <https://doi.org/10.1016/j.otot.2008.10.004>

- Sahakyants T, Vacanti JP (2020) Tissue engineering: from the bedside to the bench and back to the bedside. *Pediatr Surg Int* 36:1123–1133. <https://doi.org/10.1007/s00383-020-04722-z>
- Saxena A, Kamran M (2016) A Comprehensive Study on 3D Printing Technology. *MIT Int J Mech Eng* 6:63–69
- Schuknecht HF (1988) Otologic medicine and surgery (vol. 1). *Laryngoscope* 98:1359. <https://doi.org/10.1288/00005537-198812000-00020>
- Sharma M, Dudipala RR, Mathew J, et al (2015) Objective analysis of microtia reconstruction in Indian patients and modifications in management protocol. *Indian J Plast Surg* 48:144–152. <https://doi.org/10.4103/0970-0358.163050>
- Shen S, Chen M, Guo W, et al (2019) Three dimensional printing-based strategies for functional cartilage regeneration. *Tissue Eng - Part B Rev* 25:187–201. <https://doi.org/10.1089/ten.teb.2018.0248>
- Shieh S, Terada S, Vacanti JP (2004) Tissue engineering auricular reconstruction : in vitro and in vivo studies. 25:1545–1557. [https://doi.org/10.1016/S0142-9612\(03\)00501-5](https://doi.org/10.1016/S0142-9612(03)00501-5)
- Sterodimas A, De Faria J (2013) Human auricular tissue engineering in an immunocompetent animal model. *Aesthetic Surg J* 33:283–289. <https://doi.org/10.1177/1090820X12472902>
- Storck K, Staudenmaier R, Buchberger M, et al (2014) Total reconstruction of the auricle: Our experiences on indications and recent techniques. *Biomed Res Int* 2014:1. <https://doi.org/10.1155/2014/373286>
- Suaste-Gómez E, Rodríguez-Roldán G, Reyes-Cruz H, Terán-Jiménez O (2016) Developing

an ear prosthesis fabricated in polyvinylidene fluoride by a 3D printer with sensory intrinsic properties of pressure and temperature. *Sensors (Switzerland)* 16:1–11.

<https://doi.org/10.3390/s16030332>

Szarko M, Muldrew K, Bertram JE (2010) Freeze-thaw treatment effects on the dynamic mechanical properties of articular cartilage. *BMC Musculoskelet Disord* 11:.

<https://doi.org/10.1186/1471-2474-11-231>

Utilizing M, Chondrocyte C, Isogai N, et al (2004) Tissue Engineering of an Auricular Cartilage. 10:

Utomo L, Pleumeekers MM, Nimeskern L, et al (2015) Preparation and characterization of a decellularized cartilage scaffold for ear cartilage reconstruction. *Biomed Mater* 10:.

<https://doi.org/10.1088/1748-6041/10/1/015010>

Vacanti JP (1992) Polymer matrices. 252:367–374

von Bomhard A, Veit J, Bermueller C, et al (2013) Prefabrication of 3D Cartilage Constructs: Towards a Tissue Engineered Auricle - A Model Tested in Rabbits. *PLoS One* 8:.

<https://doi.org/10.1371/journal.pone.0071667>

Xu JW, Shane Johnson T, Motarjem PM, et al (2005) Tissue-engineered flexible ear-shaped cartilage. *Plast Reconstr Surg* 115:1633–1641.

<https://doi.org/10.1097/01.PRS.0000161465.21513.5D>

Xue J, Feng B, Zheng R, et al (2013a) Engineering ear-shaped cartilage using electrospun fibrous membranes of gelatin/polycaprolactone. *Biomaterials* 34:2624–2631.

<https://doi.org/10.1016/j.biomaterials.2012.12.011>

Xue J, Feng B, Zheng R, et al (2013b) Biomaterials Engineering ear-shaped cartilage using

electrospun fibrous membranes of gelatin / polycaprolactone. *Biomaterials* 34:2624–2631. <https://doi.org/10.1016/j.biomaterials.2012.12.011>

Yamaguchi T, Sato H, Kato-ito M, et al (2017) Interspecies organogenesis generates autologous functional islets. *Nature* 1–15. <https://doi.org/10.1038/nature21070>

Zhou L, Pomerantseva I, Bassett EK, et al (2011) Engineering ear constructs with a composite scaffold to maintain dimensions. *Tissue Eng - Part A* 17:1573–1581. <https://doi.org/10.1089/ten.tea.2010.0627>

## Chapter-2

Synthesis, characterization and *in vivo*  
studies of goat ear pinna scaffold of  
tissue engineered human ear pinna

### 2.1. Introduction:

Congenital deformities of the external ear (pinna or auricle and External Auditory Canal (EAC)) are collectively termed microtia. Congenital auricular malformations range from smaller than normal pinna (Grade I), partial ear with closed-off external ear canal (Grade II), small peanut shaped cartilage with relatively well-formed ear lobe (Grade III) and total absence of ear (Grade IV). Higher grades are accompanied by different levels of hearing loss and EAC abnormalities too (Barron and Pandit 2003; Arora et al. 2016). Occurrence reported varies from 0.83 to 17.4 per 10,000 births with higher incidence reported in Hispanics, Asians, and native Americans and associated consequences such as lack of confidence, poor interpersonal skills and antagonism increasing with age have been reported (Duisit et al. 2018).

Current therapies use the autologous intercostal cartilage hand-carved to serve as grafts for ear reconstruction. Remodeling of cartilage to the appropriate shape falls to the operating surgeon. However, this autologous graft is associated with several unwanted ramifications such as inflammation, lack of neo-cartilage maturation, donor site morbidity, risk of pneumothorax and costochondritis (Kim and Evans 2005; Hasan et al. 2014; Kshersagar et al. 2018b; Reighard et al. 2018). A xenogeneic graft would demonstrate enhanced compliance but is accompanied with the higher chance of immune rejection with reduced patency (Nayyer et al. 2012a). Allografts, though promising, also have their own limitations such as host versus graft reaction, chances of opportunistic infectious diseases or premature degradation of the implants. Non-biological source implants or alloplastic/prosthetics made of silicone, hydroxyapatite, nonporous materials, polyethylene implants do not appear natural but can be biometric. The synthetic implants have a higher chance of secondary tissue infection at the site of implantation, framework fracture and extrusion (Ten Koppel et al. 2001; Tardalkar et al. 2017). Recent trends in reconstructive surgery involve use of preformed implants to

construct an external ear or custom source implants at the time of surgical implantation. These are plagued with the challenge of ensuring mechanical stability of the implant (Arora et al. 2016). The present status of cell-based therapies, with the dangers of dedifferentiation, preclude their application in creation of an intact and complete functioning model (Youngstrom et al. 2013).

Tissue engineering (TE) provides a viable alternative for reconstructive surgeries of the external ear (Chiu et al. 2019). TE involves combining living cells with a natural/synthetic support or scaffold to build a three-dimensional living construct that is functionally, structurally and mechanically equal to or better than the tissue that is to be replaced (Hasan et al. 2014). Tissue Engineered technologies, where the scaffold is generated through a decellularization process followed by cell seeding, could meet scientific and clinical needs faster than other methods (Duisit et al. 2018).

Cartilage tissue engineering is an area that warrants greater attention in this respect. A nascent area of investigation, it faces the dilemmas of scaffold maintenance, unstable biomechanical properties, preservation of ECM and biocompatibility (Barron and Pandit 2003). The decellularized ECM scaffolds serve as a natural template for organ regeneration without immunogenic reaction (Youngstrom et al. 2013; Díaz-Moreno et al. 2018; Kshersagar et al. 2018a). They have the ability to support cell adherence and proliferation by allowing nutrition and gas exchange resulting in new tissue generation in the requisite shape. The efficiency of the TE ear pinna scaffold has been evaluated in *in-vivo* experiments mainly at subcutaneous implantation sites (Ten Koppel et al. 2001).

In this study, a physico-chemical and enzymatic methods of decellularization of goat ear cartilage to generate a scaffolds was used. The processes did not alter the cartilage-specific ECM. The derived construct was evaluated in xeno transplant model *in vivo* with reference to

biocompatibility, functional recellularization and tensile strength using histology, Scanning Electron Microscopes (SEM) and mechanical testing.

## 2.2 Materials and Methods

### Sample Collection

Goat ear pinna (n=30) samples were harvested at the slaughterhouse. The entire dermis and epidermis were removed carefully. All cartilages were rinsed in 70% alcohol followed by normal saline containing antibiotics solution of 100 ug/ml Streptomycin (Abbott Healthcare, India), 100 U/ml Penicillin (Alembic Pharmaceuticals Ltd, India), and 2.5 ug/ml Gentamycin (Cadilla Pharmaceuticals Ltd, India). The rinsed cartilages (*Fig. 2.1A*) were stored at -40°C until further use.

### 2.3. Preparation of Scaffold: Decellularization Process:

Goat ear cartilage samples were decellularized using protocol developed to remove all cellular components from ear pinna to make it nonimmunogenic. Decellularization comprised of cycles carried out by five methods (*Table 2.1*).

*Table 2.1: Decellularization protocols for goat ear pinna*

Method 1	Method 2	Method 3	Method 4	Method 5
2% SDS (w/v) treatment for 12hrs.	2% sodium deoxycholate (w/v) treatment for 6hrs.	5% DMSO (v/v) treatment for 6 hrs.	Distilled water (DW) treatment for 2hrs, followed by freeze and thaw	1% trypsin (v/v) treatment for 12hrs
All treatment (M1-M5) cycles were carried out in a sterile box on the shaker [REMI RX-12R-DX] at 180 revolutions per minute (rpm).				
Distilled water for 12 hrs	2 % SDS treatment for 6hrs	2 % SDS treatment for 6hrs	Overnight 5% DMSO	Distilled water for 12 hrs
After a specific time point run samples stored - 40 °C in the deep freezer overnight.				
Every treatment sample was thawed the next morning at room temperature and the cycle was repeated.				

For the five methods, the goat ear cartilages were treated using a sterile box in different solutions on shaker (REMI RX-12R-DX, India) at 180 rpm. Method 1 (M1) used a solution of 2% sodium dodecyl sulphate (SDS) for 12 hours followed by distilled water for 12 hours.

## Development of 3D Printing for Tissue Engineering of Ear Pinna

Method 2 (M2) used 2% sodium deoxycholate for 6 hours followed by 2% SDS treatment for 6 hours. Method 3 (M3) used 5% Dimethyl sulfoxide (DMSO) (v/v) for 6 hours followed by 2% SDS treatment for 6 hours. Method 4 (M4) used distilled water treatment for 2 hours followed by freeze and thaw and overnight treatment with 5% DMSO thereafter. Method 5 (M5) used 1% trypsin (v/v) treatment for 12 hours followed by distilled water (DW) for 12 hours. At completion of the treatments as specified, the ear cartilages were stored at -40°C in the deep freezer overnight. All samples were thawed the next morning at room temperature and the cycle repeated till complete decellularization was achieved.

After decellularization, prepared scaffolds (*Fig. 2.1B*) were stored in distilled water containing antibiotics at -40°C.

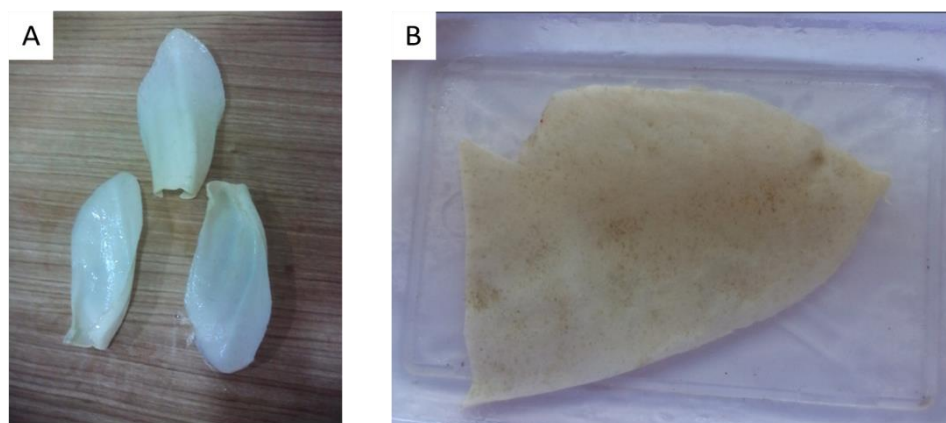


*Figure 2.1: A- Control goat ear pinna cartilage, B- Decellularized goat ear pinna:*

*After removal of all cellular components of goat ear pinna becomes delicate and soft in texture.*

### 2.4 Histochemical Characterization of Decellularized Scaffold

Native ear pinna of goat serves as a Control and decellularized ear pinna were investigated at every 10<sup>th</sup> cycle by histology. Specimens were fixed with 10% neutral-buffered formalin, dehydrated through alcohol grades and embedded in paraffin wax.

2.4.1. Haematoxyline and Eosin (HE): The sections were stained for chondrocyte nuclear structures using HE.

2.4.2. 4', 6-diamidino-2-phenylindole (DAPI): Sections were stained with DAPI (Invitrogen, CA, USA) to stain adenine–thymine rich regions in DNA.

2.4.3. Masson's trichrome (MT) : Demonstration of collagen was made by MT stain (Rieppo et al. 2019).

2.4.4. Glycosaminoglcans (GAG) content of samples was determined using Alcian blue (AB) pH-2.5 (Sigma, A5268) staining.

### **2.4.5 DNA quantification**

DNA was quantified spectrophotometrically with optical densities at 260 nm and 280 nm to yield purity of nucleic acid. Residual DNA was quantified in control and decellularized ear pinna using UV Spectrophotometer (UV-1800 UV-VIS Spectrophotometer) at 260 nm as elaborated here. Samples were collected at concentration of 1 mg/ml and allowed to freeze at - 20°C. After 15 minutes all samples were crushed with mortar pestle. 40 µl of DNA solution was transferred to 3.96 ml of DW in 4 ml cuvette. Utmost care was taken to ensure that solution was air bubble free. Solution was kept for 10 minutes to ensure the complete diffusion of DNA throughout the solution. This represented a 1: 100 dilution of the standards and DNA samples. The spectrometer was set at 260 nm and reading was noted down (Tardalkar et al. 2017).

## **2.5 Physical Characterization of Decellularized Scaffold:**

### **2.5.1. Mechanical Properties:**

Mechanical testing was performed by using displacement-controlled setup. Control and decellularized scaffold were cut into required cylindrical-shaped 4 cm strips to obtain specimens for mechanical analysis. Tensile force applied on control and decellularized scaffolds until strip were fractured. The values were digitally recorded at each pressure. This

was used to find out mechanical strain, stress, strength, deformation and elasticity of scaffold (Konig et al. 2009).

### **2.5.2. Scanning Electron Microscopy (SEM) analysis:**

SEM was performed on cross sections of goat ear pinna cartilage scaffolds to investigate cellular architecture and its porosity. After dehydration in oven at 60°C, the decellularized scaffold samples were fixed to the stage using double sided tape. Images of scaffolds in varying magnification were taken using JEOL JSM 6360 SEM model at Department of Physics, Shivaji University, Kolhapur.

## **2.6. Fabrication of human ear pinna mold:**

### **2.6.1 Patented molding technology:**

The auricle mold for the creation of human ear-like cartilage construct was prepared by a Poly Vinyl Chloride (PVC) which is a non-toxic and chemically inert material (Rahman et al. 2018). PVC sheets were converted into proper anatomical 3D human ear pinna mold in different sizes such as 55 mm, 65 mm, and 75mm using a patented method (Application filing receipt (AFR) for application no. 201921004685 Year 2019).

### **2.7 *In vivo* Study of Engineered Human Ear Pinna:**

The animal study and all experiments were approved by Institutional Animal Ethical Committee (IAEC) (Ref. - 6/IAEC/2017) of D Y Patil Education Society, Deemed University, Kolhapur. Wistar rats (male with age 5-6 months), weighing approximately 150 to 160 g were used for study. The animals were divided into control and experimental groups. The experimental Wistar rats were kept according to principles of laboratory animal care at controlled room temperature condition and humidity (~52%). After 4 weeks, animals were sacrificed by cervical dislocation.

### **Post implantation assessment of scaffolds**

This was done by histological assessment, mechanical testing, SEM and Immunohistochemistry (IHC).

#### **2.7.1 Histological assessment**

The control and samples were fixed in 10% neutral buffered formalin and embedded in paraffin. Sections were stained with HE, DAPI, MT stain, AB pH 2.5, Toluidine blue (TB) staining, to demonstrate cellular recruitment.

IHC was performed for Vascular Associated Protein (VAP) and CD90<sup>+</sup> expression. Sections (4μ) were taken on the positively charged slides (Pathnsitu biotech, India). Before processing, slides were washed with D/W containing 0.05% tween 20 followed by antigen retrieval using sodium citrate pH 7.4. Serum blocking was done by goat serum and slides were incubated with VAP (Invitrogen, India) and CD90 (Invitrogen, India) overnight at 4<sup>0</sup>C followed by wash with D/W containing 0.05% tween 20. Staining was done using anti mouse secondary antibody conjugate with Alexa 488 (Molecular Probes, USA) and counterstained using DAPI. Slides were mounted with DAKO mounting media. Stained sections were viewed under a fluorescent microscope (Nikon eclipse Ti Japan).

#### **2.7.2 Mechanical testing**

Mechanical testing was performed by tensometer, while measuring under tensile loader at room temperature. The tensometer applied tensile force to strips of biocompatible ear pinna scaffolds treated with M2, M3 and M5 successively.

#### **2.7.3 SEM analysis**

SEM was performed on cross sections of recellularized M2 (Magnification X 3500), M3 (Magnification X 3000) and M5 (Magnification X 1400) scaffold to investigate cellular architecture and its porosity.

### 2.7.4 Statistical Analysis

Data are reported as the mean  $\pm$  SD. Differences between three or more groups were assessed using one-way Analysis of variance). Significance level  $p = 0.05$  was set for all the tests. In the figures, statistical significance is denoted as \* for  $p$ -value  $\leq 0.05$ , \*\* for  $p$ -value  $\leq 0.001$ , \*\*\* for  $p$ -value  $\leq 0.0001$ .

### 2.8 Histochemical Characterization of decellularized Scaffold:

Histological examinations of the control and decellularized scaffolds were done at every 10<sup>th</sup> cycle with HE, AB pH-2.5, DAPI, and MT to ascertain whether the cellular components were totally removed and histoarchitecture was preserved.

2.8.1 HE staining of the scaffold showed that complete decellularization was achieved at 40<sup>th</sup> cycle for M5 and for M1-M4 80<sup>th</sup> cycle was needed for complete decellularization as shown in Figure 2.2A with progressive reduction in sequential cycles. Methods M2, M3 and M5 showed negligible nuclear material compared to M1 and M4. Control cartilage showed differentiated chondrocyte with lacunae and nucleus was better organized (Fig 2.2E-A)

2.8.2 DAPI staining used to crosscheck the decellularization process revealed complete removal of cellular material in all methods (Fig 2.2B). Control revealed abundant bluish stained nucleus (Fig. 2.2E-B)

## Development of 3D Printing for Tissue Engineering of Ear Pinna

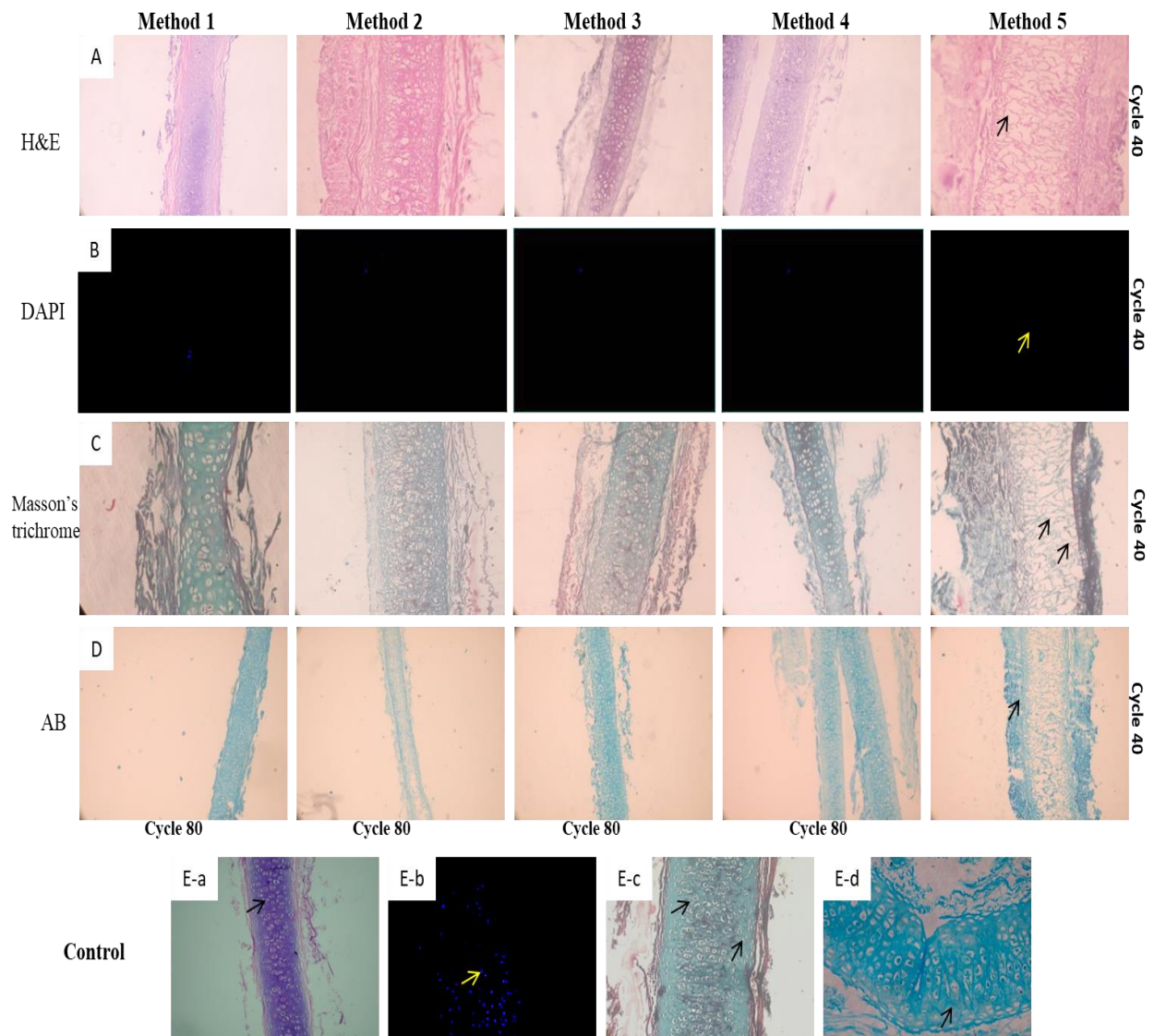


*Figure 2.2: Histochemical study of decellularization process*

*[E-a] HE stained in control showed well-organized blue nucleus chondrocytes resides in lacunae and preserved ECM. [A] HE stained decellularized ear pinna in [M1-M5] methods showed no cells. M2, M3, M5 method showed fast decellularizaion as compared to other, while at 80th cycle no any nucleus showed. [E-b] DAPI staining in native ear pinna showed prominent blue fluorescents nucleus. [B] DAPI staining in decellularized scaffold showed no nucleus. Method 5, M2, and M3 showed complete decellularization earlier than other methods. [E-c] Massiontrichrome staining in native showed a well-organized form of ECM blue-green color collagen and elastin. [C] The organization and mass of collagen fibers remain unaffected after decellularization in all methods. [E-d] AB pH 2.5 staining in native ear pinna. [D]AB pH 2.5 staining confirmed that the GAG has been preserved and its organization appeared to remain unaffected after decellularization*

2.8.3 MT staining showed intact appearance of collagen and ECM in decellularized goat ear pinna cartilage scaffolds (Fig. 2.2C) with no obvious disruptions to histoarchitecture. Scaffolds treated with methods 2 and 3 showed better preservation of collagen and ECM compared to other methods. Control showed normal bundle of collagen and ECM (Fig. 2.2E-

C). 2.8.4 AB pH-2.5 staining demonstrated that the major structural components via GAGs showed no disruption following treatment with preserved architecture (Figure 2.2D). Control showed well organized ECM and GAGs (Fig. 2.2E-D).

### 2.8.5 DNA quantification:

The DNA content of samples in experimental group showed reduction with each subsequent cycle compared to control (Fig. 2.3). Scaffolds processed with Method 2 showed the most reduction while Methods 1 and 4 yielded the least reductions in DNA content.

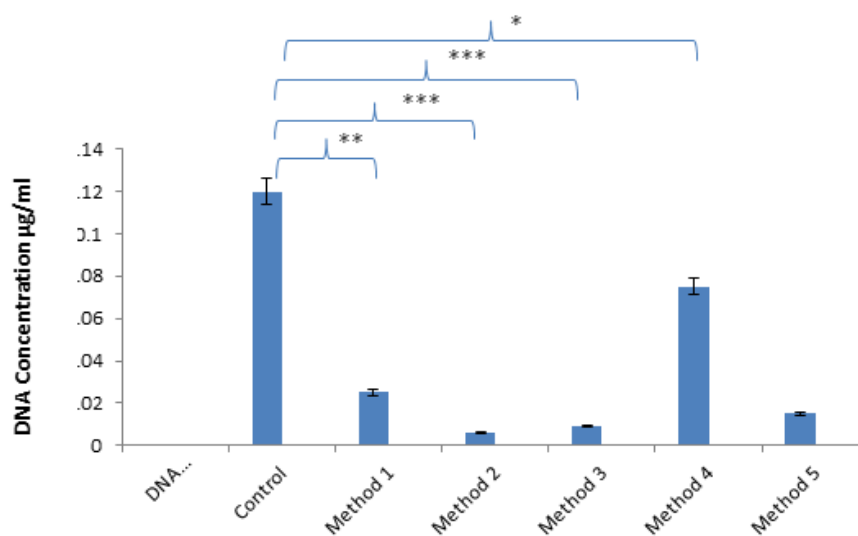


Figure 2.3: DNA quantification

Overall decellularized goat ear pinna cartilage such as M2, M3, and M5 significantly showed negligible DNA content ( $p < 0.0001$ ) compared to control (0.12 µg/ml), M1 and M4. \*Significant difference with  $p < 0.05$ .

## 2.9 Physical Characterization of Decellularized Scaffold:

### 2.9.1 Mechanical Properties:

Elasticity, stress rupture and ultimate stress limit of control and decellularized scaffold were confirmed by mechanical testing (Table 2.2). The mechanical testing analysis showed that the ultimate stress, strain and elasticity for control and decellularized ear scaffold were not significantly different. Ultimate stress and tensile strength in samples treated by M2 and M5

were similarly good. Significant elasticity was seen in samples treated by M2 and M5. Overall M2 and M3 showed better retention of mechanical properties compared to M1, M4 and M5.

Decellularized scaffold prepared by method 2, 3 and 5 showed the significantly biophysical stable, elastic and load-bearing object. Elasticity, stress rupture and ultimate stress limit of control and decellularized scaffold were confirmed by mechanical testing and summarized in Table 2.2.

*Table 2.2: Mechanical testing of decellularized scaffold*

Decellularized Scaffold	Control goat Ear Pinna	M1	M2	M3	M4	M5
Strain	00.32±0.01	0.55±00.01	00.27±00.01	00.35±00.01	00.25±00.01	00.34±00.01
Stress	60.17±01.20	20.33±01.80	98.00±02.00	18.21±01.00	13.01±01.00	20.00±02.50
Deformation	05.50±01.00	05.50±01.00	05.50±00.50	07.00±01.50	05.50±00.50	08.50±00.80
Elasticity	21.90±17.12	71.21±18.00	45.94±02.00	55.57±04.12	95.56±18.00	72.17±05.00

The mechanical testing analysis showed that the ultimate stress, strain and elasticity for control and decellularized ear scaffolds were not significantly different.

Strain of decellularized scaffold was 0.32±0.015 mm, 0.55±0.018 mm, 0.27±0.011 mm, 0.35±0.014 mm, 0.25±0.010 mm and 0.34±0.011 mm in control, method 1, method 2, method 3, method 4 and method 5 respectively. There was no significant difference ( $p<0.0001$ ) in control and control and M3, M4. Ultimate stress (N/mm<sup>2</sup>) of decellularized scaffold was 60.17±1.20, 20.33± 1.80, 98.00± 2.00, 18.21± 1.00, 13.01± 1.00 and 20± 2.50 N/mm<sup>2</sup> in control, method 1, method 2, method 3, method 4 and method 5 respectively. There was significant difference ( $p<0.0001$ ) between control and M2, M4, M5. Ultimate

stress and tensile strength in samples treated by M2 and M5 were good and similar. Significant elasticity was seen in samples treated by M2 and M5. Overall M2 and M3 showed better retention of mechanical properties compared to M1, M4 and M5. Deformation (mm) study of scaffold showed  $6.5 \pm 0.5$ ,  $5.5 \pm 1$ ,  $5.5 \pm 0.5$ ,  $7.0 \pm 1.5$ ,  $5.5 \pm 0.5$ , and  $8.5 \pm 0.8$  in control, method 1, method 2, method 3, method 4 and method 5 respectively (Fig. 2.10 Graph 3). Elasticity (N/mm<sup>2</sup>) of decellularized scaffold was  $21.90 \pm 17.12$ ,  $71.21 \pm 18.000$ ,  $45.94 \pm 20$ ,  $55.57 \pm 11$ ,  $95.56 \pm 18$ , and  $72.17 \pm 25$  in control and all methods 1, 2, 3, 4, 5 respectively ( $p < 0.05$ ). Method 2 and method 5 showed no significant difference in elasticity.

Overall method 2 and 3 maintained mechanical properties as compared to method 1, 4, 5. Decellularized scaffold prepared by method 2, 3 and 5 showed the significantly biophysical stable, elastic and load-bearing object. Moreover, scaffolds prepared by these methods have more stability, elasticity and flexibility to attain human ear shaped pinna. Hence scaffolds prepared by 2, 3 and 5 were selected for *in vivo* experiment.

### 2.9.2 SEM analysis

SEM of decellularized ear pinna scaffold (Fig. 2.4) by M2 showed 3D network of ECM in overall morphology (Magnification, 1000X), M3 sample (Magnification, 1700X) and M5 sample (Magnification, 1000X). SEM results proved that M2 and M3 showed an excellent result to maintain 3D network of ECM and overall morphological porosity as compared to M5.

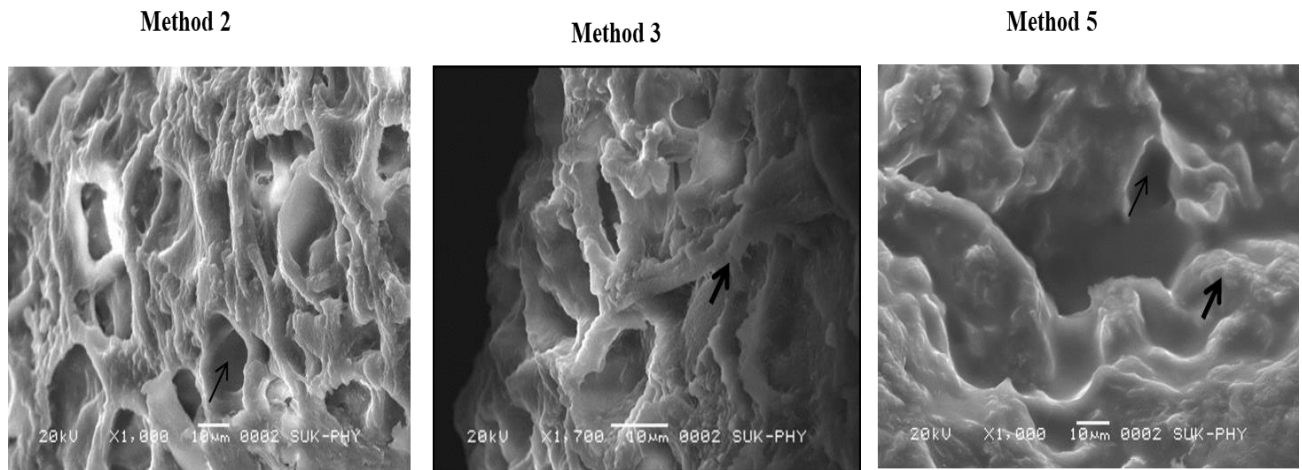


*Figure 2.4: Scanning electron microscopy of decellularized goat cartilage*

*SEM analysis of decellularized ear pinna scaffold by M2 (Magnification 1000X), M3 (1700X) and M5 (1000X) methods revealed not many obvious changes in the architecture of ECM and with clear surface porosity, however by method 2 and M3 showed good surface porosity and fibrous.*

### 2.10 Patented Molding Pinna:

The engineered auricle was resilient and smooth and had maintained its structural integrity and texture. Human ear shape scaffold obtained at 3-5 days after incubation. The auricular-shaped scaffold produced by decellularizing goat ear pinna cartilage had a very similar anatomical shape to human auricle with an almost identical size (Fig. 2.5).



*Figure 2.5: Shape of human ear pinna*

*Using mold, decellularized goat ear pinna scaffold shaped into human ear pinna.*

### **2.11 *In vivo* Study of Engineered Human Ear Pinna:**

Selection: Scaffolds achieved by M2, M3 and M5 showed well preserved ECM (Collagen and GAG), porous microstructure, superior mechanical stability and elasticity compared to the decellularized ear pinna generated via M1 and M4. These could harbor potential to attain shape desired for the human ear pinna. Hence ear pinna generated by these methods was used for biocompatibility studies. Method: The scaffolds (n=3) developed from M2, M3 and M5 were transplanted into the peritoneal cavity of Wistar rats (*Fig.2.6*) for four weeks.

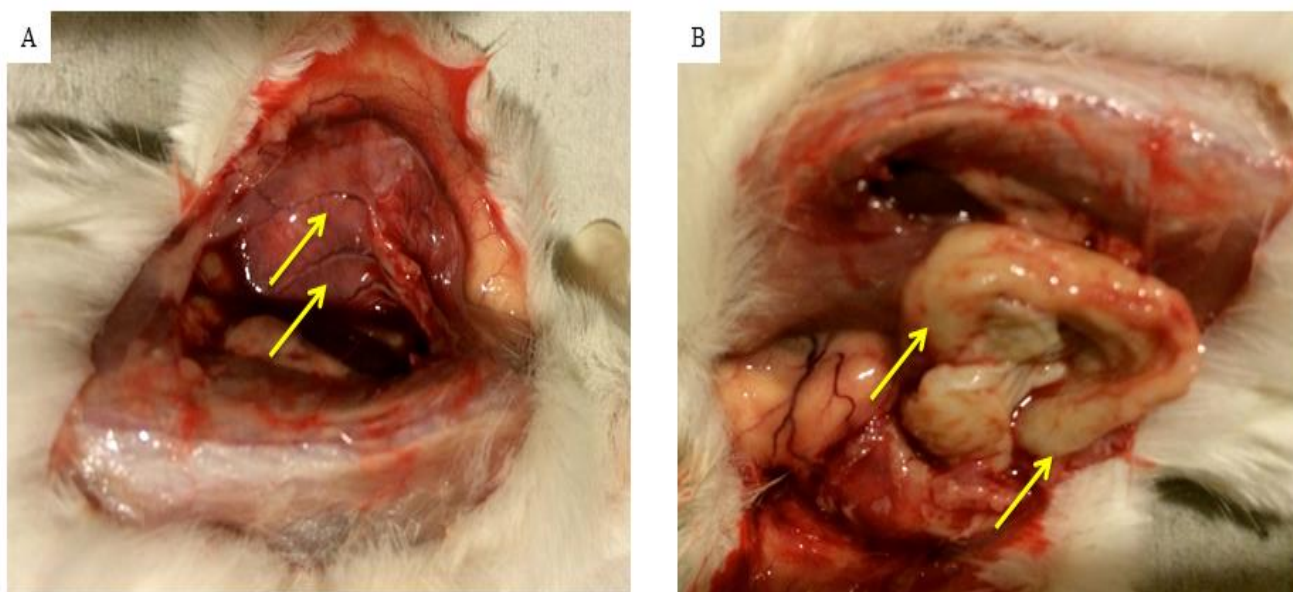


*Figure 2.6: Biocompatibility testing*  
*[A] Peritoneal cavity of Wistar rats, showed grafted ear pinna scaffold. [B] After four weeks of grafting angiogenesis showed without any immune rejection.*

### 2.11.1 Mechanical testing after biocompatibility study

Grafted scaffolds showed good mechanical strain, stress, deformation and elasticity as compared to control. The value of mechanical properties of recellularized pinna was summarized in (Table 2.3 and Fig. 2.7).

*Table 2.3: Mechanical testing of recellularized scaffold*

Pinna cartilage	Control goat Ear Pinna	M2	M3	M5
Strain	00.32±00.01	00.20±00.01	00.32±00.02	00.17±0.005
Stress	60.17± 01.20	59.02± 01.00	34.79± 01.50	57.93 ± 01.30
Deformation	05.50± 01.00	10.00± 00.50	16.00± 00.50	08.50 ± 00.20
Elasticity	21.90±01.12	25.01±03.40	13.28± 01.13	20.90± 02.35

## Development of 3D Printing for Tissue Engineering of Ear Pinna

The Graph 1 showed strain (mm) of recellularized pinna as  $0.20 \pm 0.10$  mm,  $0.32 \pm 0.02$  mm and  $0.17 \pm 0.005$  for method 2, method 3 and method 5 respectively. Ultimate stress (N/mm<sup>2</sup>) of control and *In vivo* decellularized ear pinna were similar. M5 decellularization showed highest ultimate stress bearing capacity which was decreased significantly after recellularization (Graph 2). Deformation (mm) did not show much alteration during decellularization and recellularization process in M2 and M5 (Graph 3). *In vivo* decellularized ear pinna generated by M3 showed highest deformation. The Graph 4 showed elasticity (N/mm<sup>2</sup>) of biocompatible scaffold was  $25.01 \pm 23.40$  and  $20.90 \pm 12.35$  as compared to control ( $21.90 \pm 17.12$  N/mm<sup>2</sup>). M5 decellularization showed significant increase in elasticity, which was decreased to ( $20.9 \pm 5.35$ ) after *in vivo* recellularization.

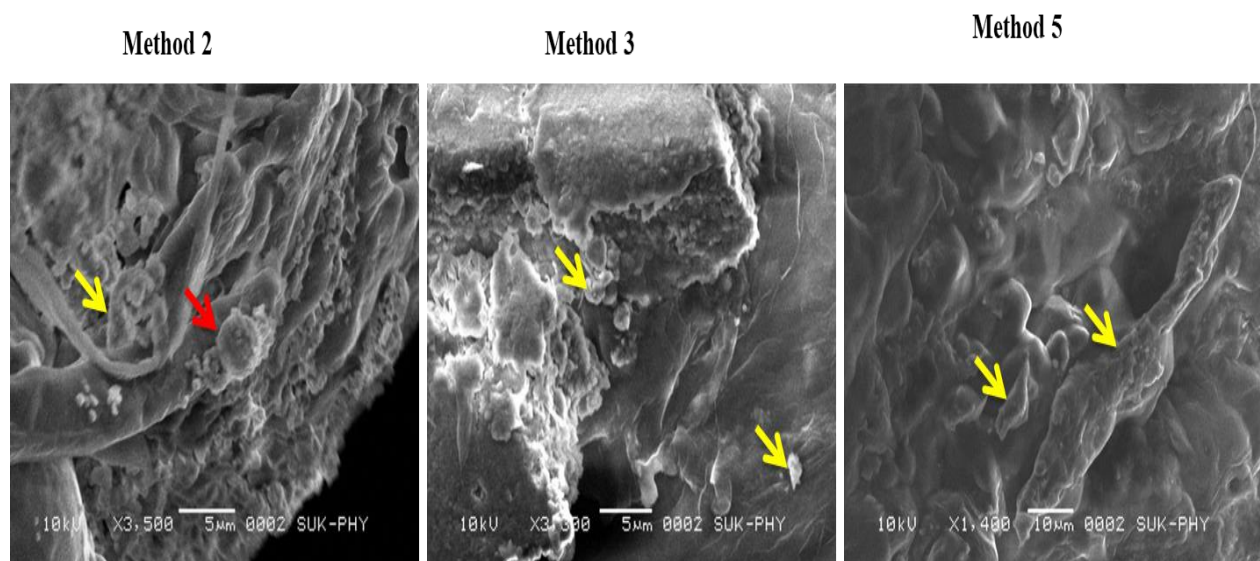


Figure 2.7: Mechanical testing of human ear shaped pinna done after transplantation

Graph 1. Ultimate strain, Graph 2. Ultimate stress, Graph 3. Deformation, Graph 4. Elasticity. In graph 1-4, Methods 2 and M 3, M 5 of grafted ear pinna scaffold showed as remarkable stable mechanical properties as compare to native pinna. Overall recellularization M2 and M5 significantly enhanced elasticity as compared to native cartilage. However, recellularized scaffold from Method 2, M3 and M5 should maintain elastic properties and significance one way analysis (\*\*\*)  $p < 0.0001$  in comparison to Control. All the decellularised and re-cellularised M2, M3 and M5 groups were compared with control for elastic (Young's modulus) properties.

### 2.11.2 SEM analysis

SEM of scaffold showed the 3D network of ECM cell structure in transplanted M2 (Magnification X 3500), M3 (Magnification X 3000) and M5 (Magnification X 1400) scaffold (Fig. 2.8). SEM analysis revealed that transplanted scaffolds were maintained ECM collagen, elastic fibers and significantly showed bunch of chondrocyte cell recruitment. It showed very excellent results of regeneration of and recellularization with chondrocyte cells.



*Figure 2.8: Scanning electron microscopy of goat cartilage after transplantation*

*SEM analysis of grafted ear pinna scaffold by methods M2 (Magnification X 3500), M3 (Magnification X3000) and M5 (Magnification X 1400) revealed well-organized recellularization of chondrocytes and its secreted ECM.*

### 2.11.3 Histological assessment after biocompatibility study

HE staining used to monitor the recellularization process showed that the ear pinna supported the chondrocyte growth as manifested by visible nuclei (Fig. 2.9A). Complete recellularization was achieved at 4 weeks after grafting, when the scaffolds showed well organized 3D ECM and collagen in MT staining (Fig. 2.9B), presence of GAGs on AB pH 2.5 staining (Fig. 2.9C) and recruitment of live chondrocyte cell (Fig. 2.9D) on toluidine blue staining.

## Development of 3D Printing for Tissue Engineering of Ear Pinna

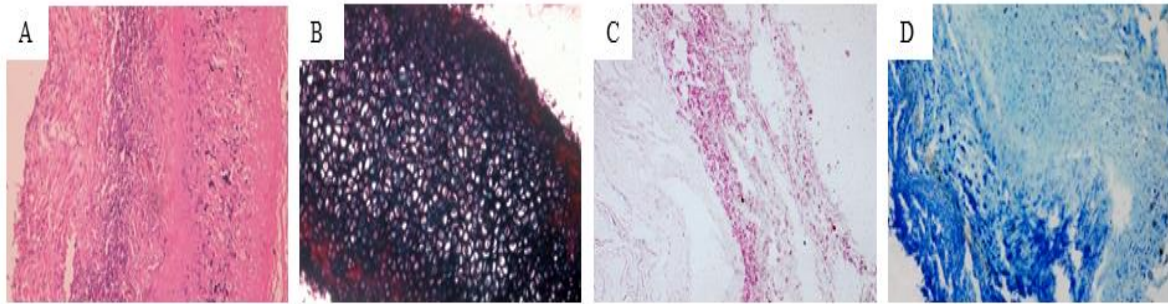


Figure 2.9: Histochemistry of scaffold after transplantation

[A] HE stained in grafted ear pinna showed recruited chondrocytes ECM and chondrocytes with its lacunae. [B] Masson's trichrome staining shows a columnar type of chondrocyte in most places and has an abundant collagen matrix. [C] AB pH 2.5 staining confirmed that the GAG organization. [D] Toluidine blue staining confirmed in grafted ear pinna chondrogenic differentiation.

IHC staining revealed expression of VAP representing vasculogenesis (Fig. 2.10).

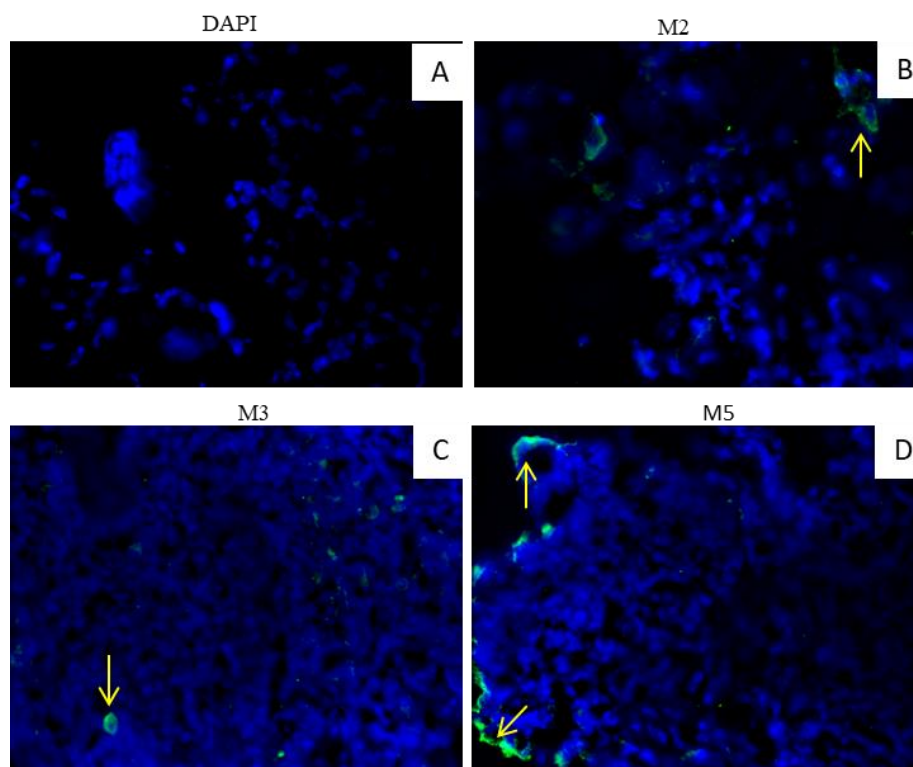
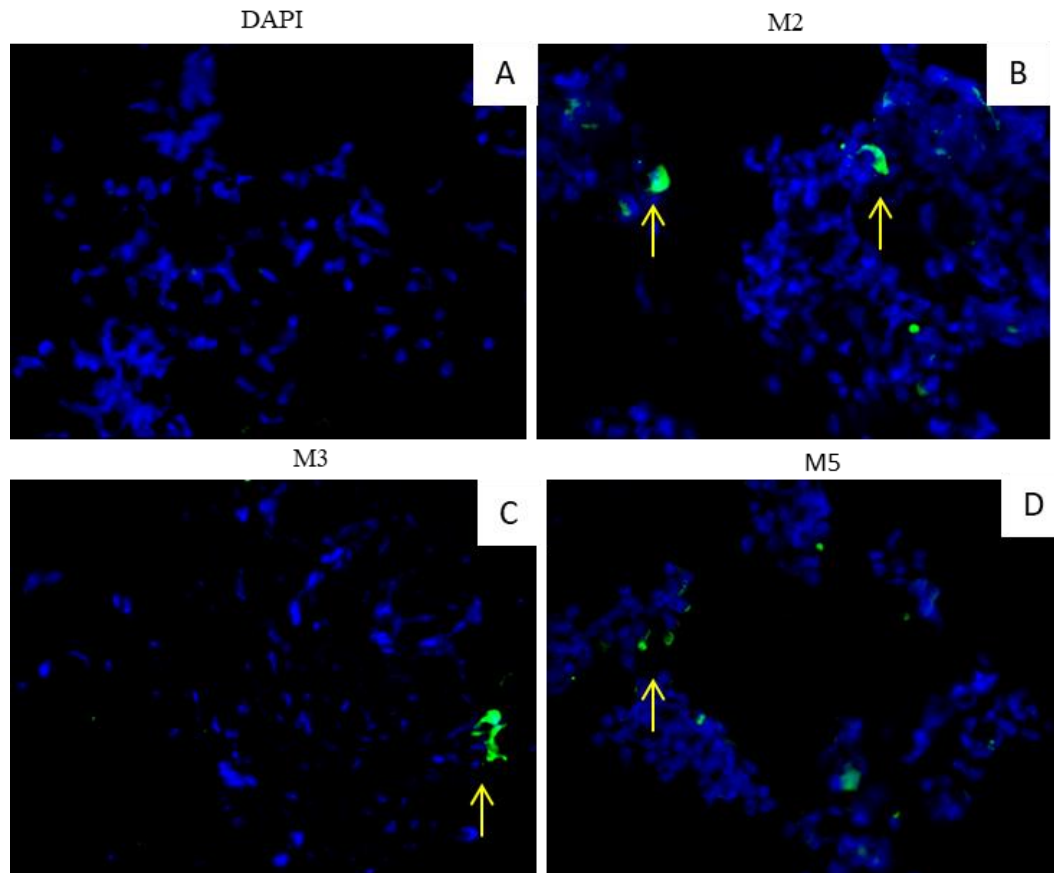


Figure 2.10: VAP expression in scaffold after transplantation

[A] DAPI staining in grafted ear pinna showed blue fluorescent nuclei. VAP-1: B) M2, C) M3, D) M5 treatment showed green fluorescent expression of vascular-associated protein marker.

## Development of 3D Printing for Tissue Engineering of Ear Pinna

CD 90<sup>+</sup> (Fig. 2.11) representing stromal markers and recruitment of chondrocyte specific progenitor cells.



*Figure 2.11: CD90<sup>+</sup> expression in scaffold after transplantation*

*[A] DAPI staining in grafted ear pinna showed blue fluorescent nucleus. CD90<sup>+</sup>: [B] M2, C) M3, D) M5 seen green fluorescent expression as chondrocyte progenitor cell (Mesenchymal stromal cell).*

### 2.12 Discussion

This study assessed the tissue engineered scaffold of ear pinna cartilage by decellularization using different chemical treatments methods. The study also extended to biocompatibility and recellularization of the scaffold on implantation into an animal model. Chemical and enzymatic detergents solubilize cell membranes and remove DNA thus proving to be effective agents to remove immunogenic tissue material.

These different decellularization methods proved efficacy to generate ideal ear pinna scaffold. Current decellularization protocols are designed to overcome the previous limitations (Utomo et al. 2015b)(Cervantes et al. 2013). Rahman S et al presented a protocol to decellularization of cartilage using trypsin followed by freeze and thaw cycles (Rahman et al. 2018). The present study found that antioxidant treatment in method 3 followed by freeze and thaw cycles can efficiently remove the DNA content and also preserve the ECM and mechanical properties. This protocol does require more cycles (80 cycles) for decellularization compared to the enzymatic method 5. However, it has been found to generate stable human ear pinna shaped cartilage with better mechanical properties. It also provides high specificity for removal of antigenic material. On the other hand, enzymatic decellularization protocol was quick and was able to achieve complete decellularization at the 40th cycle. However, this rapid decellularization was at the cost of not maintaining the mechanical properties. The resultant scaffold was more elastic, thin and more time was needed to generate the desired human ear pinna.

The present study shows that scaffold prepared by Methods 2, 3 and 5 were ideal scaffolds with excellent porosity and mechanical properties that retain excellent anatomical ear pinna shape molded in different size and shapes- 55, 65, and 75mm.

The ECM was characterized by histochemistry in this study. HE staining revealed a well-maintained structure of the scaffold with preserved ECM. The residual DNA content after

decellularization was greatly reduced compared to that found in native tissue. M5 showed faster decellularization compared to other methods. This is significant as DNA is a sensitive indicator of cell debris due to its high stability and as a marker strongly correlates with adverse host immunogenicity. MT and AB staining demonstrated no obvious disruption to the overall histo-architecture following treatment and were found to maintain collagen and GAGs structure receptively. The results of decellularization methods were promising and appreciable as the amounts of collagen remain unchanged. This outcome is desirable as collagen molecules play a vital role in maintaining ECM and also determining tissue functions. SEM analysis reported a preserved ECM of ear pinna cartilage without evidence of any damaged area. Biocompatible testing conducted on animal models (Wistar rats) found satisfactory vasculogenesis and angiogenesis in graft (Figure. 2.6B). Biocompatibility and recellularization detected through MT and AB staining pH 2.5, revealed maintenance of ECM architecture *in vivo*. Scaffolds prepared by Methods 2, 3 and 5 subjected to surface topography confirmed good elasticity. Biocompatibility Biocompatible testing of grafted human ear pinna found fully vascularized. IHC staining with VAP revealed that the transplanted ear pinna express vasculogenesis and angiogenesis marker, while CD90 + marker expression revealed that chondrogenic differentiation as shown in Figure.2.10 C-D and 2.11 C-D. Expression of CD90+ is important with regard to enhanced collagen type II and chondrogenic differentiation. IHC staining revealed chondrogenic differentiation with the graft showing cells in most places amidst abundant collagen matrix and proteoglycan content after four weeks. Thus, this study provided a novel approach to generate ear pinna xenograft for clinical applications of auricle cartilage to overcome the present limitations. The decellularized scaffold is biodegradable, biocompatible, preserves ECM and it can reduce post-transplant management problem.

### **2.13 Conclusions**

Current reconstructive surgery of the entire ear pinna remains one of the biggest challenges for the plastic surgeons. Through this study, the authors propose generation of tissue-engineered ear pinna as an alternative to overcome the present limitations in clinical usage of auricle cartilage grafts such as post-transplant management ear pinna scaffold, graft biocompatibility, donor limitation, and preservation of ECM mechanical properties and limitation of cartilage recellularization.

The present study was designed to yield an ideal decellularized biocompatible scaffold whose post-transplantation recellularization was satisfactorily characterized for stem cell recruitment and mechanical properties. The decellularized scaffold that has been obtained is biodegradable, biocompatible, preserves ECM and thus can reduce post-transplant management problem.

To summarize, this study highlights a novel approach to generate xenogenic three-dimensional Tissue Engineered human ear pinna scaffold for clinical applications.

### References:

- Arora V, Sahoo NK, Gopi A, Saini DK (2016) Implant-retained auricular prostheses: a clinical challenge. *Int J Oral Maxillofac Surg* 45:631–635.  
<https://doi.org/10.1016/j.ijom.2015.12.011>
- Barron V, Pandit a (2003) Combinatorial Approaches in Tissue Engineering: Progenitor Cells, Scaffolds, and Growth Factors. *Top Tissue Eng* 1–21
- Cervantes TM, Bassett EK, Tseng A, et al (2013) Design of composite scaffolds and three-dimensional shape analysis for tissue-engineered ear. *J R Soc Interface* 10:.  
<https://doi.org/10.1098/rsif.2013.0413>
- Chiu LLY, Weber JF, Waldman SD (2019) Engineering of scaffold-free tri-layered auricular tissues for external ear reconstruction. *Laryngoscope* 129:E272–E283.  
<https://doi.org/10.1002/lary.27823>
- Díaz-Moreno E, Durand-Herrera D, Carriel V, et al (2018) Evaluation of freeze-drying and cryopreservation protocols for long-term storage of biomaterials based on decellularized intestine. *J Biomed Mater Res - Part B Appl Biomater* 106:488–500.  
<https://doi.org/10.1002/jbm.b.33861>
- Duisit J, Orlando G, Debluts D, et al (2018) Decellularization of the Porcine Ear Generates a Biocompatible, Nonimmunogenic Extracellular Matrix Platform for Face Subunit Bioengineering. *Ann Surg* 267:1191–1201.  
<https://doi.org/10.1097/SLA.0000000000002181>
- Hasan A, Ragaert K, Swieszkowski W, et al (2014) Biomechanical properties of native and tissue engineered heart valve constructs. *J Biomech* 47:1949–1963.

<https://doi.org/10.1016/j.jbiomech.2013.09.023>

Kim M, Evans D (2005) Tissue Engineering : The Future of Stem Cells. *Top Tissue Eng* 2:1–22

Konig G, McAllister TN, Dusserre N, et al (2009) Mechanical properties of completely autologous human tissue engineered blood vessels compared to human saphenous vein and mammary artery. *Biomaterials* 30:1542–1550.

<https://doi.org/10.1016/j.biomaterials.2008.11.011>

Kshersagar J, Kshirsagar R, Desai S, et al (2018a) Decellularized amnion scaffold with activated PRP: a new paradigm dressing material for burn wound healing. *Cell Tissue Bank* 19:. <https://doi.org/10.1007/s10561-018-9688-z>

Kshersagar J, Kshirsagar R, Desai S, Bohara R (2018b) Decellularized amnion scaffold with activated PRP : a new paradigm dressing material for burn wound healing Decellularized amnion scaffold with activated PRP : a new paradigm dressing material for burn wound healing. *Cell Tissue Bank*. <https://doi.org/10.1007/s10561-018-9688-z>

Nayyer L, Patel KH, Esmaeili A, et al (2012) Tissue engineering: Revolution and challenge in auricular cartilage reconstruction. *Plast Reconstr Surg* 129:1123–1137. <https://doi.org/10.1097/PRS.0b013e31824a2c1c>

Rahman S, Griffin M, Naik A, et al (2018) Optimising the decellularization of human elastic cartilage with trypsin for future use in ear reconstruction. *Sci Rep* 8:1–11. <https://doi.org/10.1038/s41598-018-20592-x>

Reighard CL, Hollister SJ, Zopf DA (2018) Auricular reconstruction from rib to 3D printing. *J 3D Print Med* 2:35–41. <https://doi.org/10.2217/3dp-2017-0017>

- Rieppo L, Janssen L, Rahunen K, et al (2019) Histochemical quantification of collagen content in articular cartilage. PLoS One 14:1–12.  
<https://doi.org/10.1371/journal.pone.0224839>
- Tardalkar K, Desai S, Adnaik A, et al (2017) Novel Approach Toward the Generation of Tissue Engineered Heart Valve by Using Combination of Antioxidant and Detergent: A Potential Therapy in Cardiovascular Tissue Engineering. Tissue Eng Regen Med 14:755–762. <https://doi.org/10.1007/s13770-017-0070-1>
- Ten Koppel PGJ, Van Osch GJVM, Verwoerd CDA, Verwoerd-Verhoef HL (2001) A new in vivo model for testing cartilage grafts and biomaterials: The “rabbit pinna punch-hole” model. Biomaterials 22:1407–1414. [https://doi.org/10.1016/S0142-9612\(00\)00298-2](https://doi.org/10.1016/S0142-9612(00)00298-2)
- Utomo L, Pleumeekers MM, Nimeskern L (2015) Preparation and characterization of a decellularized cartilage scaffold for ear cartilage reconstruction.  
<https://doi.org/10.1088/1748-6041/10/1/015010>
- Youngstrom DW, Barrett JG, Jose RR, Kaplan DL (2013) Functional Characterization of Detergent-Decellularized Equine Tendon Extracellular Matrix for Tissue Engineering Applications. PLoS One 8:. <https://doi.org/10.1371/journal.pone.0064151>

## Chapter-3

### Synthesis, Characterization and *in vivo* studies of 3D Printed Ear Pinna

### 3.1. Introduction:

The ear is a sensory organ used for auditory perception (Mota and Danti 2019). The ear consists of three sequential parts: outer (auricle or pinna) for collection, middle for transmission, and inner for transfer of sound waves from mechanical to an electrical signal (Mota and Danti 2019). The auricle is composed of elastic cartilage which is essential for the skeletal framework (Mota and Danti 2019). Pinna cartilage provides shape, structural support, and shock absorption (Oseni et al. 2011; Storck et al. 2014). The symmetry of ear and facial ratio are considered for the cosmetic presence which deals with social stigma (Storck et al. 2014).

Every 2.06 newly-born out of 10,000 are found with CFM, who often have ear abnormalities like microtia (grade I, II, III, IV) which affects the shape of one or both auricles (Mussi et al. 2019). It can lead to an asymmetric facial appearance. External ear deformities may not be always associated with the severe functional loss but the psychological impacts can retain long term (Mussi et al. 2019). Other than microtia patients with polychondritis and trauma are found with a decrease in capacity of hearing (Mota and Danti 2019; Mussi et al. 2019). The current methods involving autologous costal cartilage to create a framework of the pinna (Nayyer et al. 2012a; Borrelli et al. 2020). The success of surgical autologous costal cartilage treatment is dependent on the surgeon's skills for obtaining excellent cosmetic results, donor-site morbidity, the intensity of pain, and the risk of pneumothorax caused after surgery (Nayyer et al. 2012a). The allogenic and xenogenic grafts have the risk of infection, inflammation and need a lifelong immunosuppressant to avoid rejection of graft (Borrelli et al. 2020). Silicone framework used as surgical material for auricular treatment can contaminate, cause pores in skin, and framework displacement (Nayyer et al. 2012a; Storck et al. 2014). Traditional ear pinna reconstruction using mold cannot show effective properties

like native ear pinna (Rotter et al. 2008). This is time consuming technique, requires patient-specific mold to produce.

3D bioprinting is a developing branch in the TE domain for the biofabrication of cartilage. The current advancement in 3D printing technology was done by Jang et.al 2020 and Jia et.al 2020. using PCL based 3D printed auricle cartilage which works as a scaffold and cell-laden alginate hydrogel association with adult stem cells (Jang et al. 2020b; Jia et al. 2020b). Chondrocytes provide enhanced mechanical properties and chondrogenesis after the characterization of 3D printed ear auricle (Jang et al. 2020b). Bioconstructed acellular cartilage matrix (ACM) and gelatine combinedly used for getting 3D porous auricle scaffold using freeze-drying method after pouring into the cylindrical mold. Gelatine is added to overcome the crosslinking problems in the reconstruction of auricle cartilage with CAD or 3D laser scanning. PCL gives 3D printed internal frame for scaffold development. Integration of 3D printing, design of inner core, cast molding, freeze-drying gives effective shape and mechanical strength to reconstructed ear pinna cartilage (Jia et al. 2020b).

Considering the limitations faced during auricular reconstruction in surgical techniques and transplantations, this research work will serve as a promising alternative for pinna reconstruction using 3D bioprinting. The present research has considered all possible evaluation aspects for the compatibility check of the printed ear pinna. Bioink was prepared from goat cartilage by adding polymers and optimized for 3D printing. Bioink characterization reveals polymers cross-link with ECM biofunctional components. 3D printing of human ear shaped pinna was done with programmed software within relatively less time. Prepared pinna was having required mechanical strength and satisfactory shape. Histology and SEM analysis show results for restoration of ECM as well as recellularization of chondrocytes and elastin fibers after transplantation. Optimized ECM enriched Bioink provided desired properties to 3D printed pinna and compatibility in an animal model can

lead to medical object for future clinical trials as a cosmetic substitute to restore acid-burnt or accidental loss of pinna cartilage.

### **3.2. Materials and methods:**

### **3.3. Preparation of Bioink:**

Bioink was prepared according to the patent. Briefly, goat ear pinnas (n=500) were collected from a slaughterhouse. Goat ear pinna skin was removed carefully to detach the cartilage and cleaned with deionized water. 70% alcohol is added and kept on a shaker (Remi RS-12R Dx, India) at 80 RPM for 1hr and weight was measured after rinsing. Antibiotic and antimycotic (Penicillin, streptomycin, and amphotericin) solution (HiMedia Laboratories Pvt. Ltd, India) was added with distilled water in cartilage for another wash and kept on a shaker for 1-2 hrs. A fine paste was obtained by grinding washed cartilage in a grinder (Avenue supermarts Ltd, India). The paste of cartilage was transferred for alkaline digestion with 1N NaOH (Hi Media Laboratories) at 90°C for 48hrs. Slurry was filtered after digestion to separate nondigested and unwanted residuals. pH of the filtered slurry was adjusted to neutral. Further, 20% PVA (HiMedia Laboratories Pvt. Ltd) was added to the slurry and heated in the microwave at 900 Watt (W) for 5 minutes followed by an interval of 2 minutes until complete polymerization. 5% gelatine (HiMedia Laboratories Pvt. Ltd) was added to the slurry and was subjected to microwave heating at 900 Watt for 1 minute followed by an interval of 2 minutes until complete polymerization. The synthesized bioink was cooled at -40°C overnight. These steps were repeated 6 times. Fig. 3.1 shows flowchart of the patented protocol for bioink synthesis.

## Development of 3D Printing for Tissue Engineering of Ear Pinna

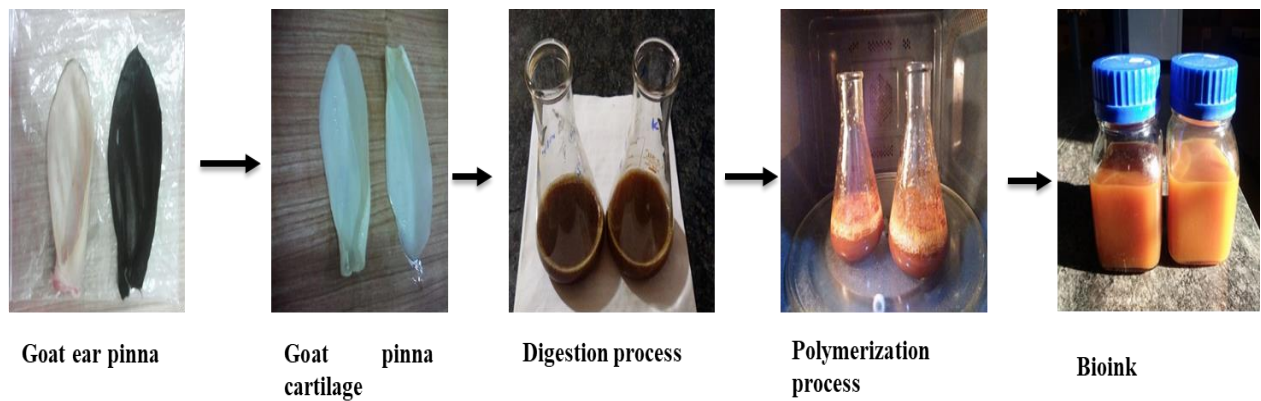


*Figure 3.1: Synthesis of Bioink*  
*Sequential steps of digestion process of goat cartilage and polymerization to make composite bioink*

### 3.4. Physical characterization of bioink:

#### 3.4.1. Fourier-transform infrared spectroscopy (FTIR) analysis of bioink:

FTIR spectroscopy (Tensor II spectral region  $450 - 4000 \text{ cm}^{-1}$ ) was used to assess the polymeric chemical groups and investigating the esterification of bioink (Pal et al. 2007; Tareq et al. 2016). Fresh bioink was prepared for FTIR analysis and placed on the crystal cell of the FTIR spectrophotometer. FTIR analysis provides a graph between transmittance (%) vs. wave number for quantitate analysis.

#### 3.4.2. Rheological analysis of bioink:

The rheological behavior of bioink (Chung et al. 2013; Pereira et al. 2018) was analyzed using the RST-CPS rheometer (7030107) equipped with an active cone/plate system. Freshly blended bioink was prepared before measurements and was loaded with small volumes of bioink on the plate. The rotational motor of the rheometer utilizes a high dynamic precision to the driving system without gearing or mechanical force transducers. Speed of block /plate was set from  $0.3300$  to  $33.3300 \text{ min}^{-1}$  for surface characterization. Shear stress (Pa)  $0.0000$  to  $4.3432$  was provided by gradually increasing the torque (mNm) from  $0.0000$  to  $0.4797$  and shear rate ( $1/\text{s}$ )  $0.9900$  to  $99.9900$ . Viscosity was measured to get profiling of viscosity vs. time by heating the plate from  $1^\circ\text{C}$  to  $11^\circ\text{C}$  at a rate of  $1^\circ\text{C min}^{-1}$  rise in temperature.

### 3.4. 3. Spreadability analysis of bioink:

The spreading ability of the bioink was examined (Al-Suwayeh et al. 2014) by spreading 0.5g of the bioink on a pre-marked circle of 2 cm diameter pre-marked on a glass plate and then a second glass plate (10 x10 cm<sup>2</sup>) was used as (Fig. 3.4A). 500g of weight was kept on the upper glass plate and checked every minute for 5 min. We have calculated the rate of spread (cm/min) and percent spread with respect to time.

The rate of spread was calculated by using the following formula (Sabale et al. 2011):

$$\text{Rate of spread} = \frac{A_2}{\text{time}} \quad \text{-----eq. (3.1)}$$

A<sub>2</sub>: Final area after spreading (cm).

time: time at measurement taken (min)

The following equation (Al-Suwayeh et al. 2014) was used to find out the percent spread (%)

$$\% \text{ spread by area} = \frac{A_2}{A_1} \times 100 \quad \text{----- eq. (3.2)}$$

Where,

A<sub>1</sub>: Circle diameter pre-marked on a glass plate (cm)

A<sub>2</sub>: Final area after spreading (cm).

### 3.5 3D printing of ear pinna:

3D printer- FDM (Rio 3D printer- R 200, India) had dimensions of 15.3 × 13.9 × 13.3 inches with an opened aluminium frame and build volume for the printer was 23 x 22.5 x 25.5 cm. At the base aluminium printer bed or platform attached with stepper motors, pulley and belt system. The main parts of extrusion bioprinter head or 3D bioprinter nozzle head were developed according to bioink requirements. Developed bio printer head consist of lead

## **Development of 3D Printing for Tissue Engineering of Ear Pinna**

screw on which big gear is mounted which is driven by small gear of stepper motor so that we can get maximum torque as we wanted. Developed 3D bio printer nozzle head attached to 3D printer with screws.

3D design of pinna was created by using CAD software for standard human ear pinna dimensions. Further, the CAD file of ear pinna was converted to STL file format represented as a triangular facet for layer-by-layer printing shown on the screen. The output was saved in the form of G-code and the microchip containing G-code was inserted in the 3D printer as printing guide. Bioink was loaded in the plunger push 20 ml syringe (plastic made) head downward direction attached to 3D bio printer nozzle head with screws. Whole 3D printer setup was maintained under air conditioner condition.

3D Bio printer power supply was on were the bioink flow rate, printer bed temperature, stepper motors speed adjusted through display knob, while press the G – code human ear pinna file for start 3D printing. All printing information was shows on its digital screen or on display board. Bio printer nozzle head was start moves in the x axis (left –right) as well as z (upward-downward) axis direction, platform moves in y (ahead-back) axis direction and motion is driven by stepper motors. Printer x axis and y axis, pulley and belt were used for transform rotation motion into linear motion whereas lead screw used in z axis. The insulated printing plunger push syringe head provided continuous flow of melted bio ink that was extrudes through its tip or nozzle (1 mm diameter). Pinna was prints with 10 mm/s – 30 mm/s speed while the speed of the motor was adjusted varying between 30 mm/s – 50 mm/s deciding the movement of the nozzle. Moving motor pushed syringe until the bioink reached to its nozzle tip which helped in printing of the ear pinna according do G code. Complete human ear pinna was synthesized layer by layer as additive based manufacturing.

### 3.6. Physical characterization of 3D printed ear pinna:

#### 3.6.1. Thermogravimetric analysis (TGA):

TGA instrument (SDT Q600 V20.9 Build 20) was used to evaluate the thermal degradation (Hirschler 1986; Sunaryono et al. 2017) of 3D printed ear pinna. The 3D printed ear pinna measuring operation was performed by dynamic mode in the nitrogen with the heating rate of 10°C/ min on the temperature until 800°C. The values of weight with increasing temperature were noted on the plot.

#### 3.6.2. X-ray diffraction (XRD) analysis:

The 3D printed ear pinna diffraction patterns were measured with an XRD analyser using Cu K $\alpha$  radiation (Pal et al. 2007; Maji et al. 2016). The sample was prepared with properties of finely ground, homogenized, and with average bulk composition for effective analysis of pinna. The graph between intensity vs. 2-theta (°) was plotted after performing the analysis.

#### 3.6.3 Swelling behavior:

The swelling behavior of bioink was assessed by examining the capacity of absorption of liquid by the material as a function of time until saturation (Hütten et al. 2014; Kim et al. 2016; Noh et al. 2019). For the swelling ability of 3D printed ear pinna (n= 3) 0.035g with 1 cm in length was immersed in 30 ml DW and incubated at 37 °C for 5 days. After every 24hrs, the water-soaked sample was taken out from distilled water; surface water was blotted off by a tissue paper and reweighed until an equilibrium weight was reached.

The percent swelling was calculated by employing the formula (Ragaert 2013; Noh et al. 2019).

$$\text{Swelling ratio (\%)} = \frac{\text{wt.of wet sample} - \text{wt.of dried sample}}{\text{wt.of dried sample}} \times 100 \quad \text{..... eq. (3.3)}$$

### 3.6.4 Surface wettability (Contact angle):

Contact angle measurements (Huhtamäki et al. 2018) were carried out by contact angle goniometer. Water contact angle measured under ambient conditions. The microsyringe needle was located close to the 3D printed ear pinna so that the tip of the needle was embedded in the water drop. The droplet was illuminated from behind, and images were recorded by the camera (Goniometer bench with F2 series digital camera). The surface wettability image was analyzed by software and a contact angle measurement was determined.

### 3.6.5 *In vitro* biodegradability:

For *in vitro* biodegradability analysis, 3.9g ( $w_i$ ) of printed pinna was immersed in Phosphate buffer saline (PBS) with 7.4 pH and incubated at 37°C with constant shaking at 100 RPM for 28 days. The PBS was changed every day. After 28 days, the 3D printed ear pinna was removed from the PBS, rinsed gently with distilled water, and dried at 37°C until exhaustion (12h) and weighed.

The *in vitro* biodegradability percentage was calculated by using the formula (Wu et al. 2014).

$$\text{Weight loss \%} = \frac{w_i - w_f}{w_i} \times 100 \quad \text{-----} \quad \text{eq. (3.4)}$$

Where,

$W_i$ : Sample weight before biodegradation.

$W_f$ : Sample weight after biodegradation.

SEM of 3D printed ear pinna before and after *in vitro* biodegradation was done and dimensions of topography images were taken at 10 $\mu$ m.

### 3.7. Biocompatibility testing of 3D printed ear pinna in chick embryo (*in ovo*):

The biocompatibility of the 3D printed ear graft was checked by using chick Chorioallantoic Membrane (CAM) model (n=12) (Burgio et al. 2018). Zero hour fertilized black leghorn chicken (*Gallus gallus*) eggs were bought from a local hatchery and cleaned with 70% alcohol. Fertilized chicken eggs were incubated at 37°C and 80% humidified ambience in a household incubator. Eggs were arbitrarily divided into two groups as a control group (n=4) and experimental groups (n=8), and incubated at 37°C and 55–65% humidity in the incubation chamber. The 3D printed ear pinna was cut into rectangular shapes as a (10mm×20mm) sample for *in ovo* study. On the 4<sup>th</sup> day of incubation, the egg's window was opened in a sterile condition and 3D printed ear graft was placed on the CAM area. The egg's window was covered by sterile paraffin film and kept in the incubator. On days 6, 8, 10, and 12, the eggs were opened and the chick embryos were observed using stereo-microscopy (Lawrence & Mayo Private Limited, India).

#### 3.7.1. Histological assessment:

The experimental eggs CAM of 6<sup>th</sup>, 8<sup>th</sup>, 10<sup>th</sup>, and 12<sup>th</sup> day were fixed in 10% neutral buffered formalin, dehydrated using alcohol grades, and embedded in paraffin wax. The sections were stained for a nuclear organization using Haematoxylin (Avoms Biotech, India) and Eosin (Nice Chemical PVT LTD, India) (HE) (Shieh et al. 2004b; Fischer et al. 2008). Images were taken in the bright field at, 20X using a (Nikon To S Eclipse TE 108) microscope (Nikon Instruments, Japan) fitted with a Nikon camera (Nikon Ds Ri 2, Japan).

#### 3.7.2. SEM analysis:

SEM photographs were taken of 3D printed ear graft the experimental on day 6, 8, 10 and 12.

### 3.8. Transplantation of 3D printed ear pinna:

The animal study was approved by Institutional Animal Ethical Committee (IAEC) (Ref. - 6/IAEC/2017) in D.Y.Patil Medical College, Deemed University, Kolhapur, MS, India. 10 Wistar rats (male with age 4-5 months), weighing approximately 250-300g were used for this study. This rat was isolated in a quarantine room for 1 week before transplantation. Animals were subjected to quarantine environments such as comfortable environment, contaminant-free bed, easy access to food (moisture and contamination free chaw), and water. Observations such as eating, drinking, or any sign of depression and stress in rats had been noted regularly. The rats were operated on in a fully sterilized room with autoclaved surgical instruments. The anesthetic process (Melo et al. 2016) was performed through intraperitoneal injections. An anesthetic dose (Abdi-Azar and Maleki 2014) of 50 mg/Kg/wt of thiopentone (Thiosol NEON, India) was given intraperitoneally to induce anesthesia which made rats anesthetized after 20 min. The breathing of anesthetized animals was checked and placed over a warm pad with feedback control at 37°C to maintain body temperature. ETO (Ethylene Oxide) sterilized 3D printed ear (Fig.3.14) was trimmed into pieces (10 mm in width), rinsed with saline containing antibiotic solution.

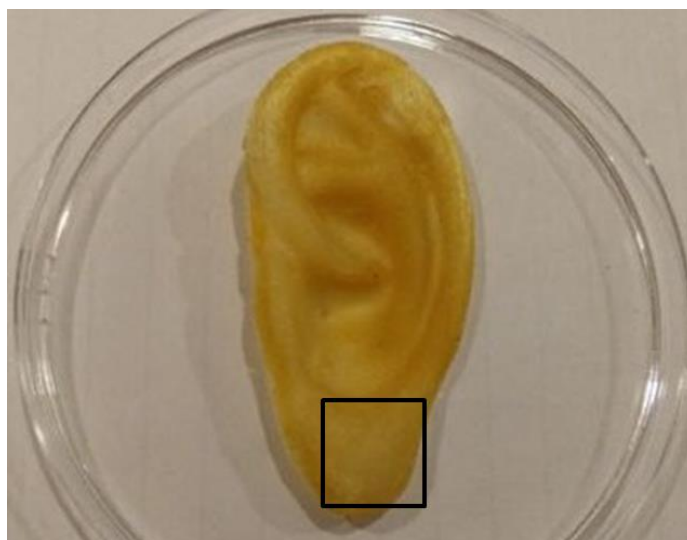


*Figure 3.14: 3D printed ear*

## Development of 3D Printing for Tissue Engineering of Ear Pinna

The right ear pinna was shaved with a trimmer then betadine solution was applied over the shaved area. By using a fine sterile blade (Surgeon Blades & Medical Devices Private Limited, India) on the base of the right ear pinna, a cut was taken on the skin. The skin was separated using ring tip forcep from both sides of the cartilage. Cartilage was dissected carefully and replaced with 3D printed pinna cartilage. Skin immediately closed with non-absorbable blue 7-0 polypropylene surgical suture (lotus surgical Pvt. Ltd. India) attached C-1 needle 10.7 mm with the help of a holder. Checked whether any gap between sutures or blood leakage from the suture. Betadine (Huns Digital Home Pvt. Ltd. India) was applied at the surgical site. Fig. 3.15 shows animal model after ear pinna transplant. Ear pinna surgery process required half hour and breathing was monitored post-transplant in rats and placed in the cage for monitoring.



*Figure 3.15: 3D printed pinna transplant biocompatibility*

### 3.8.1 Ultrasound Sonography (USG) of Transplanted Ear Pinna:

Ultrasound sonography (Wortsman and Jemec 2008; Chen et al. 2014) of the rat was performed on day 9. Ultrasound images were taken at D.Y.Patil hospital, Kolhapur by prosound  $\alpha$ -10 premier diagnostic ultrasound system (1.1 mechanical indexes, 80 transmission gains) equipped with a 5- 10MHz probe for ear pinna scans. Rats were anesthetized in a prone position with an exposed examination area. Then the probe was kept above the left and right ear pinna to observe the normal left and evolution of the right ears 3D printed transplant.

### 3.8.2 CT scans of Transplanted Ear Pinna:

CT scans (Cervantes et al. 2013; Lee et al. 2014b) were done on day 11 of the transplant. CT has a pixel size between 1  $\mu$ m to 50  $\mu$ m and allows the investigation of the microstructure of samples.

After 30 days rat was taken for scarification (euthanized) by used a high dose of thiosol sodium according to Committee for the Purpose of Control and Supervision of Experiments on Animals (CPCSEA). Transplanted graft (Fig. 3.19) and native pinna were excised for tensile testing, histological assessment, SEM analysis, and immunohistochemistry (IHC).

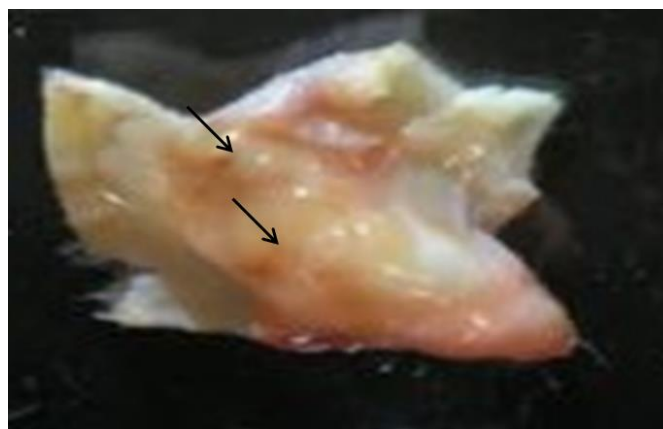


*Figure 3.19: 3D printed ear pinna transplant*

Animals were sacrificed post transplantation by cervical dislocation. A Yellow-coloured category No.2 biomedical waste management bags was used for seal scarified rat.

### **3.8.3 Biomechanical characterization (Tensile testing):**

Assessment of tensile properties (Mangera et al. 2013) of transplanted and native ear pinna was observed using a universal testing machine (UTM). Ear pinna samples were cut, measured and then the samples were clamped to the UTM. The tensile force was applied by UTM on the strips of the ear pinna up to its elongation break. Applied force and the elongation of the 3D printed ear pinna and transplanted 3D printed ear pinna and native rat pinna were used to obtain biomechanical data. The graph was taken as load vs displacement.

### **3.8.4 Histological assessment:**

The 3D printed ear pinna, native rat ear pinna and post-transplantation 3D printed ear pinna graft was fixed in 10% neutral buffered formalin, dehydrated using increasing concentrations of alcohol, washed in xylene, embedded in paraffin wax, and cut into 5 µm sections. Sections were stained for observing chondrocyte nuclear organization and cytoplasm using the HE technique according to the standard procedure (Shieh et al. 2004b; Fischer et al. 2008). Sections were stained with 0.1% Toluidine Blue (TB) for 1 minute, washed, and dehydrated. TB stain assesses for evidence of cartilage groups and chondrocytes nuclei (Bergholt et al. 2018). Sections were stained with Weigert's iron Haematoxylin and Biebrich scarlet 1% acid fuchsin solution, differentiated in phosphomolybdic phosphotungstic acid solution. It was transferred directly to aniline blue solution. For the detection of collagen fibers, Masson's trichrome (MT) stain (Copyright and Co 1984) was used. The sections were treated with a 0.1% Alcian blue (AB) acetic acid solution of pH 2.5 for 20 min, rinsed with water, dehydrated with ethanol, cleared, and mounted (Yamada 1970). GAGs cartilage matrix evaluation of samples was determined using AB pH 2.5 (Sigma, A5268, India) stain. Sections were stained with safranin-O/Fast green (SO/FG) to evaluate chondrocyte proteoglycan

distribution, picrosirius red to assess collagen association (Kahveci et al. 2000). Sections were stained with Verhoeff elastic stain (VEG), as picric acid used in the van Gieson counterstaining. VEG stain assesses the presence of elastin fibers (Copyright and Co 1984). Images were taken in the bright field at, 20x using (Nikon Ti Eclipse) microscope fitted with a Nikon camera.

### **3.8.5 SEM analysis:**

SEM (image dimension 10um) was performed on the 30th day on cross sections of ear transplants and native ear pinna for cellular morphology and topography. SEM was performed at the Department of Botany, Shivaji University, Kolhapur.

### **3.8.6 IHC:**

IHC analysis was done on 4 to 5 sections of rat ear pinna (positive control) and transplanted pinna on positively charged slides with pH 7.4. In brief, slides were deparaffinized and further antigen retrieval with sodium citrate buffer. Slides were incubated with 10% goat serum for 1 hr followed by mouse monoclonal antibody CD13 (Santa Cruz Biotechnology, Inc) with dilution 1:100, CD14 with (Santa Cruz Biotechnology, Inc) dilution 1:500, CD90 (Invitrogen) with dilution of 1:500 at room temperature for 4 hrs. Tissue without primary antibody was selected as a negative control. After wash with tween-20 for 3 times slides were incubated with goat secondary anti-mouse antibody for 1hr at room temperature. After washing with tween-20 for 3 times, slides were counterstained (30 sec.) with 4', 6-diamidino-2-phenylindole (DAPI) (Life technologies, India), and slides were mounted with Dako mounting media. Images were taken using a fluorescence microscope (Nikon s eclipse, Japan) at 20X magnification.

### 3.9 Statistical analysis:

The data for biomechanical testing has been represented as mean $\pm$  S.D. The t-test was used for finding the statistical significance of biomechanical testing. The significance level was  $p=0.01$  was set for all the tests. In the figures, statistical significance is denoted as \* as for  $p\text{-value} \leq 0.05$ , \*\* for  $p\text{-value} \leq 0.01$ .

### 3.10 Physical characterization of bioink:

#### 3.10.1 FTIR analysis:

The FTIR spectra of the bioink showed the peak around  $1094.00\text{cm}^{-1}$ ,  $1406.83\text{cm}^{-1}$ ,  $1636.29\text{cm}^{-1}$ , and  $3249.00\text{cm}^{-1}$ . FTIR analysis indicates the composition of bioink in the form of spectral arrangement as shown in (Fig. 3.2).

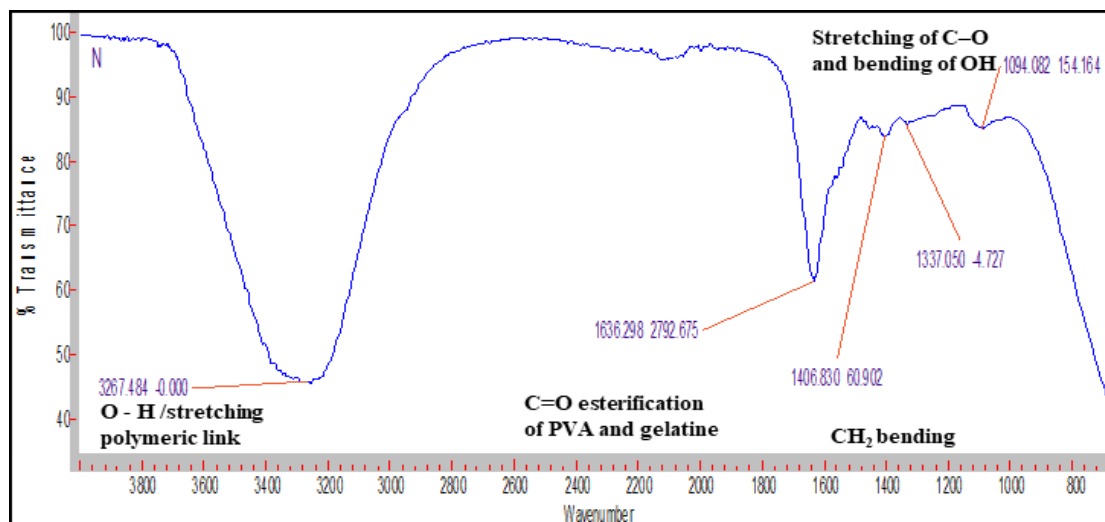


Figure 3.2: Fourier Transform Infrared spectroscopy (FTIR) of bioink

FTIR spectra of polymerized (goat ear pinna cartilage, PVA, and Gelatine) ear pinna bioink

#### 3.10.2 Rheological analysis:

Bioink surface characteristics were measured at 20 points where bioink viscosity pascal-second (Pa.s) was maximum up to 0.26 Pa.s (50 s) to average 0.04 Pa.s as shown in (Fig.3.3). At the initial time slot, the viscosity of bioink increases with time (225s - 300s) and it attains equilibrium at 1 to 2°C.

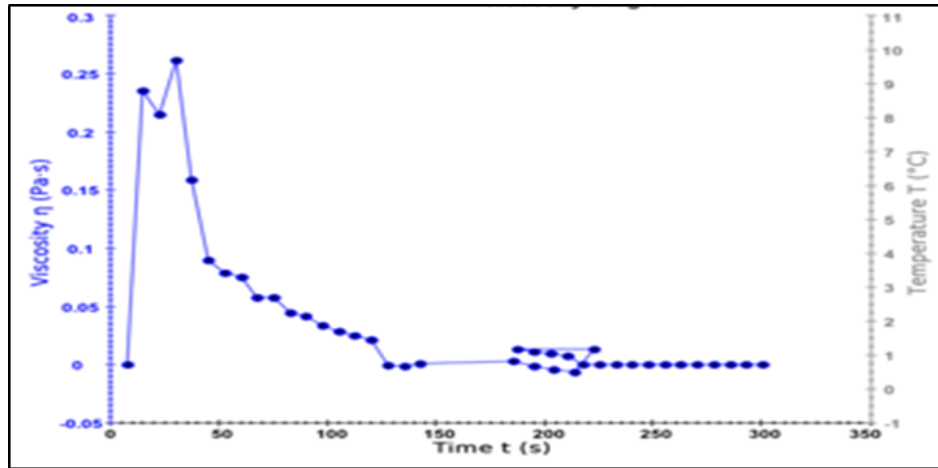


Figure.3.3: Rheological behaviour of bioink

Ear pinna bioink had shown average of 0.0405 Pa.s (250 s 300 s) viscosity

### 3.10.3 Spreadability analysis:

The diameter of the circle after spreading of the bioink was measured ( $n=5$ ) as shown in (Fig.3.4B).

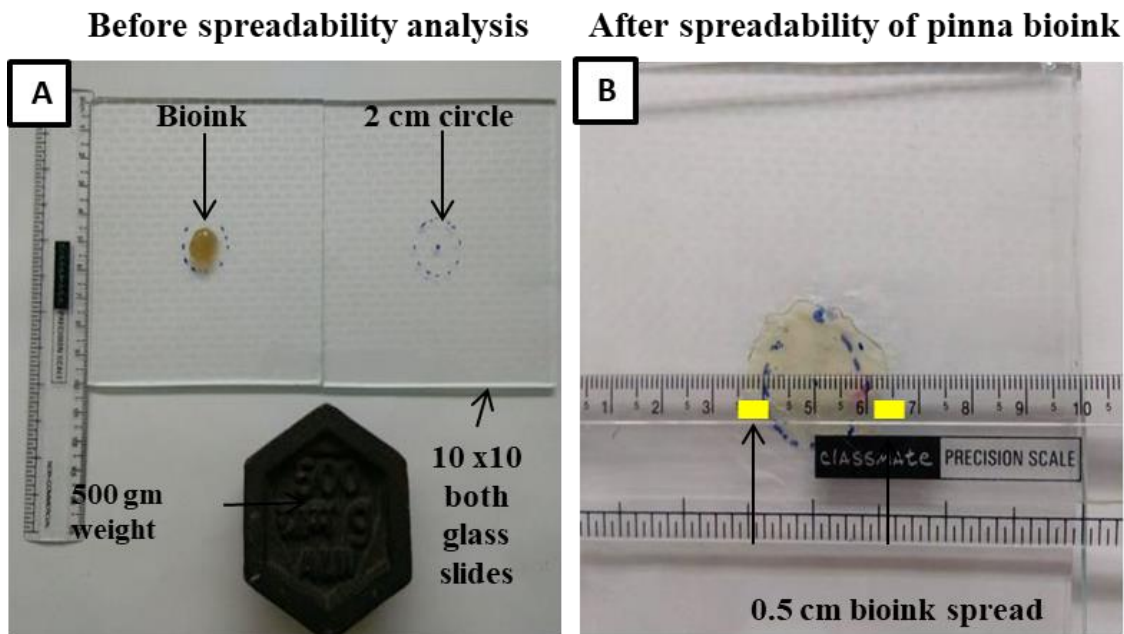


Figure 3.4: Spreadability analysis

Spread ear pinna bioink as showed [A] before spreadability analysis, [B] after spreadability of pinna bioink

## Development of 3D Printing for Tissue Engineering of Ear Pinna

The average spreading is  $0.4 \pm 0.04$  in total 5 min, while the average percent of bioink spread is 20% with decreasing rate of spread with 0.3 to 0.1 cm/min within 5 min as shown in (Table 3.1).

*Table.3.1: Spreadability of bioink*

Weight (g)	Time(min)	A1 (cm)	A2 (cm)	Bioink spreadability %	Rate(cm/min)
500	1	2	$0.3 \pm 0.04$	$15 \pm 2.2$	$0.3 \pm 0.03$
500	2	2	$0.3 \pm 0.04$	$15 \pm 2.2$	$0.15 \pm 0.03$
500	3	2	$0.4 \pm 0.04$	$20 \pm 2.2$	$0.13 \pm 0.03$
500	4	2	$0.5 \pm 0.04$	$25 \pm 2.2$	$0.12 \pm 0.03$
500	5	2	$0.5 \pm 0.04$	$25 \pm 2.2$	$0.1 \pm 0.03$
Average:			$0.4 \pm 0.04$	$20 \pm 2.2$	$0.1 \pm 0.03$

‘ $\pm$ ’ indicated the standard deviation in parameters.

The spreadability of bioink is shown in (Fig.3.4 C).

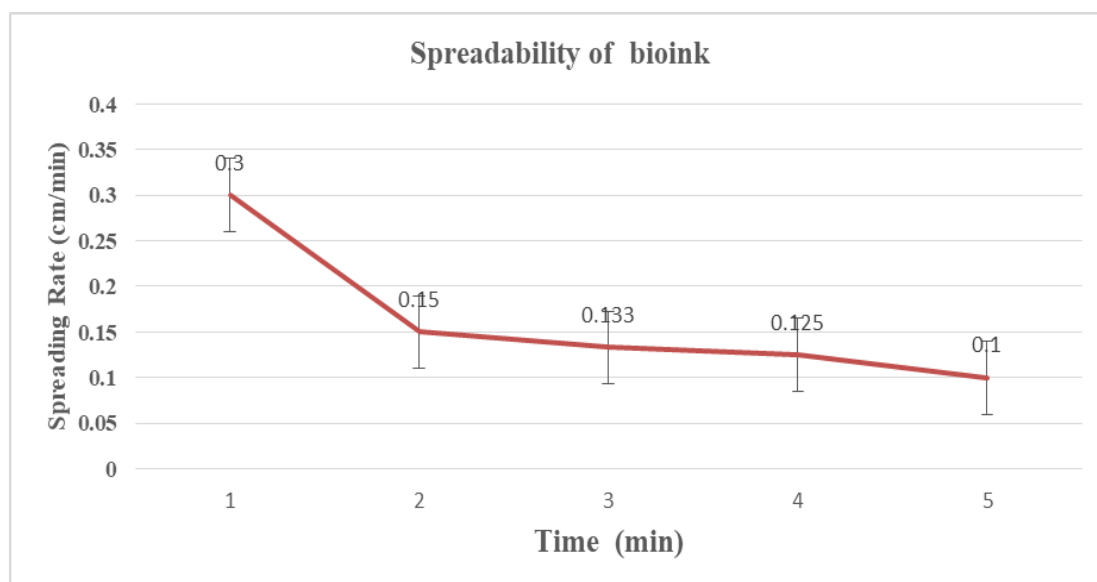


*Figure 3.4C: Spreading rate of bioink*

*Rate of bioink spreadability with respect to time (average rate of spreading of bioink: 0.1cm/min)*

### 3.10.4 Printing of 3D printed ear pinna:

Printing process of 3D pinna and whole 3D printed ear pinna was reconstructed with precise shape is shown in the Fig. 3.5

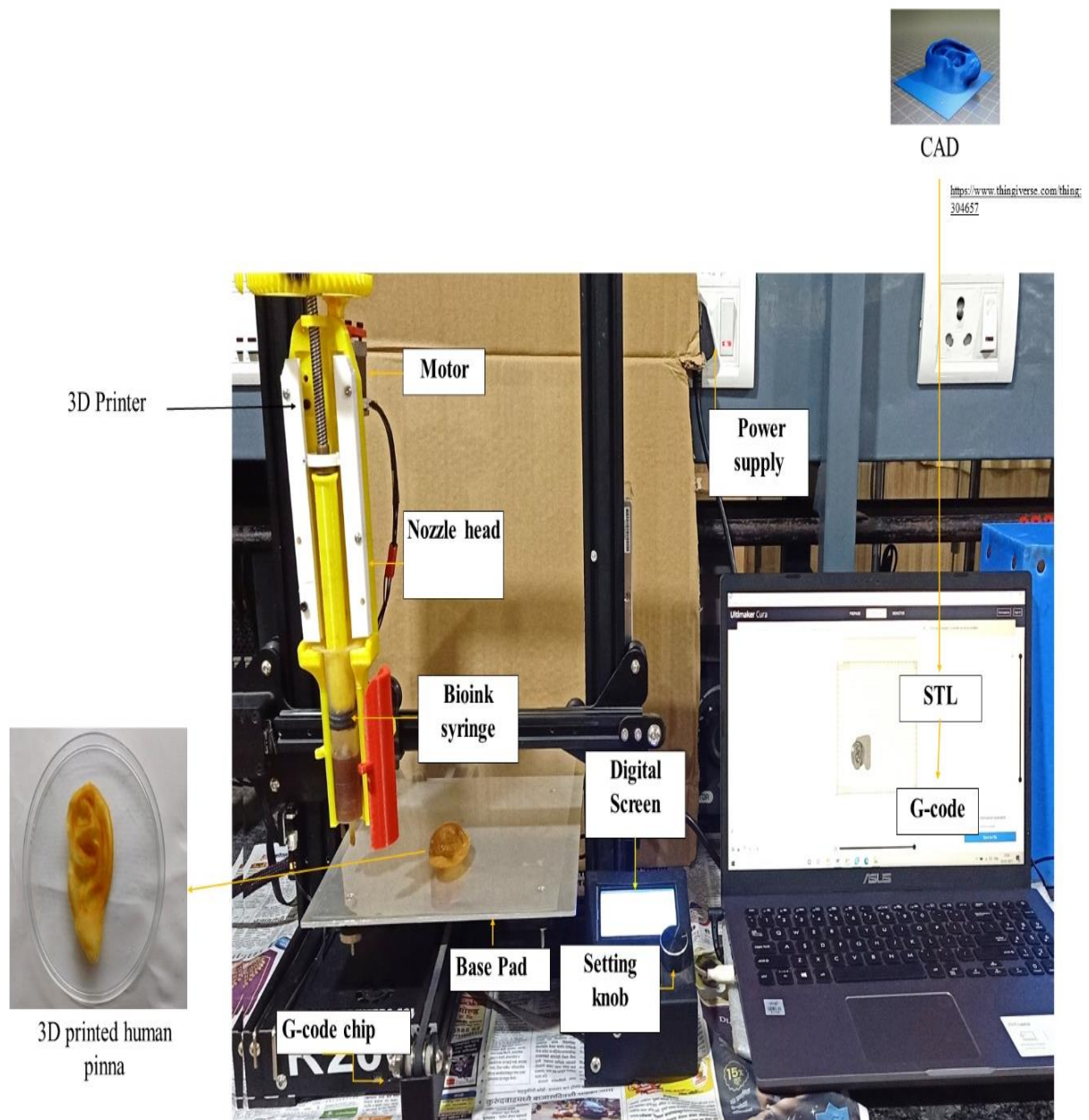


Figure 3.5: 3D printing of ear pinna

Process of 3D printing of pinna and design of the 3D printer is shown

### 3.11 Physiochemical characterization of 3D printed ear pinna:

#### 3.11.1 Thermogravimetric analysis (TGA):

The graph of thermal degradation of 3D printed ear pinna (Fig.3.6) indicates areas having different slopes: a) No weight loss b) 14.36mg weight loss of sample (80.76%) at 110 to 200°C c) 2.556mg weight loss (14.37%) 200 to 400°C d) 0.845mg weight loss (4.76%) at 400 to 800°C. Final residue after thermal degradation is 0.021mg (0.12%).

17.7850 mg (Initial weight)

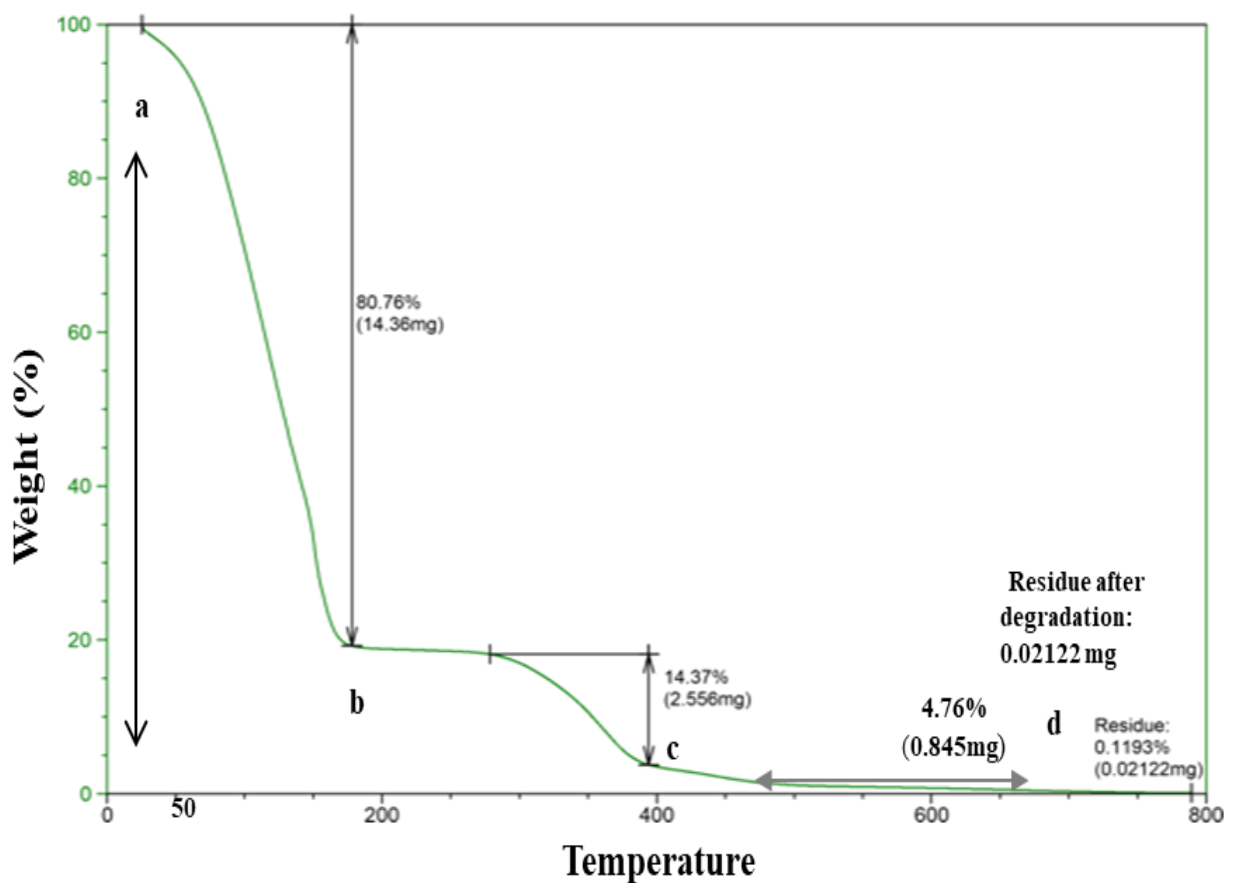


Figure 3.6: Thermo Gravimetric Analysis (TGA) of 3D printed pinna

The graph of the 3D printed pinna showing thermal degradation indicated areas of sample weight-loss for all variations of the cycle period.

### 3.11.2 XRD analysis:

The XRD pattern of the 3D ear pinna as shown in (Fig.3.7) has a prominent X-rays peak at around  $18^\circ 2\theta$  having an intensity (counts) of 10.

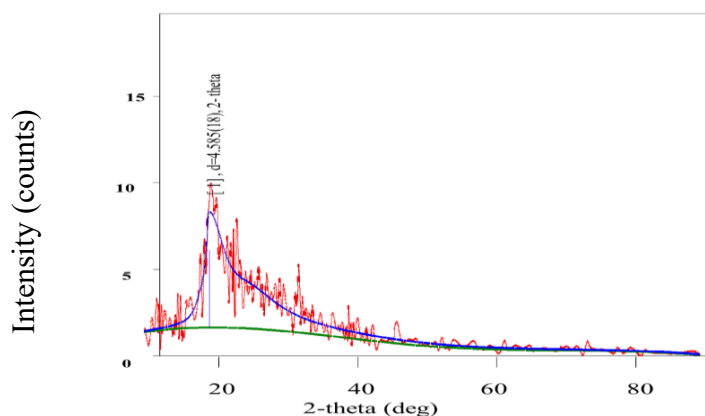


Figure 3.7: X-ray diffraction (XRD) analysis of 3D printed pinna

The XRD pattern of the 3D ear pinna having an X-ray intensity (counts) of 10.

### 3.11.3 Swelling behavior:

Results of the swelling test were given in (Table 3.2).

Table 3.2: Swelling of 3D printed pinna

Wet weight(g)	Dry weight(g)	Difference(g)	Swelling ratio (%)
0.044	0.028	0.016	57.14±00.01
0.046	0.029	0.017	58.62±00.01
0.045	0.032	0.017	60.71±00.01
0.050	0.032	0.190	61.87±00.01
0.050	0.032	0.190	61.81±00.01
Average:			60.11±00.01

‘±’ indicated the standard deviation in parameters.

## Development of 3D Printing for Tissue Engineering of Ear Pinna

3D printed ear showed an average  $60.11\% \pm 00.01\%$  expansion as shown in (Fig.3.8).

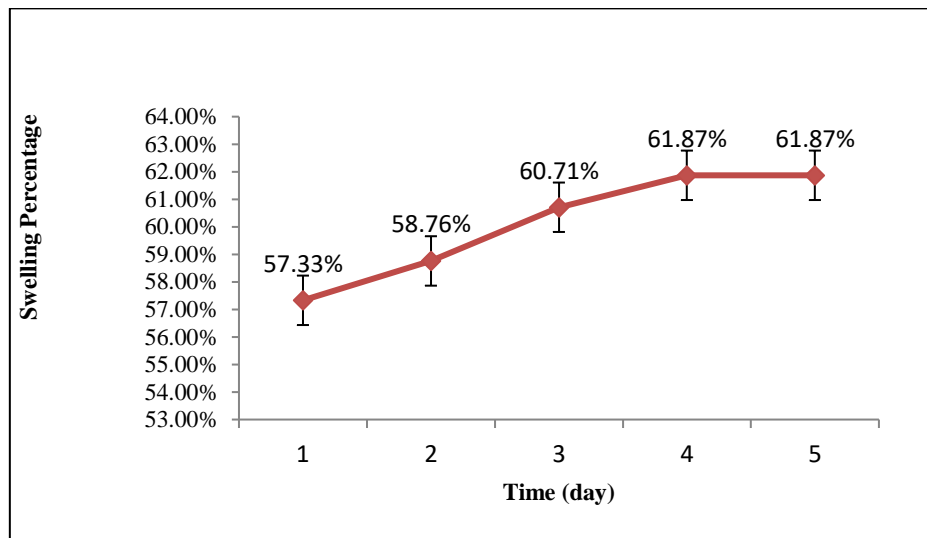


Figure 3.8: Swelling behavior of 3D printed pinna

*Swelling behaviour of the 3D printed ear pinna in aqueous (distilled water) condition.*

### 3.11.4 Surface wettability (Contact angle):

Waterdrop was absorbed by the 3D printed ear pinna surface (Fig.3.9) with zero contact angle.

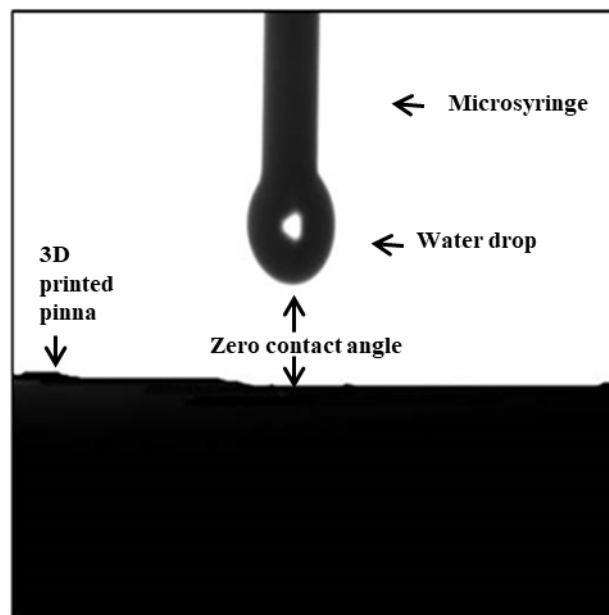


Figure 3.9: Surface wettability of 3D printed pinna

*3D printed ear pinna surface showed zero contact angles*

## 3.11.5 *In vitro* biodegradability:

Table 3.3 illustrates  $52.34\% \pm 01.30\%$  weight loss of the 3D printed pinna after immersion in PBS for 28 days. The initial weight of 3.90 g was reduced to  $1.80 \pm 00.03$  of the pinna.

*Table 3.3: Biodegradability of 3D printed pinna*

3D printed Ear pinna initial weight (g)	Time in PBS (Day)	Temperature (°C)	Biodegradable 3D printed Ear pinna weight (g)	Biodegradable weight (%)
3.9	28	37	$1.80 \pm 0.03$	$53.84 \pm 01.30$
3.9	28	37	$1.80 \pm 0.03$	$53.58 \pm 01.30$
3.9	28	37	$1.90 \pm 0.03$	$49.61 \pm 01.30$
Average:				$52.34 \pm 01.30$

‘ $\pm$ ’ indicated the standard deviation in parameters.

Fig.3.10 a and Fig.3.10 b are showing SEM images of the porous surface morphology before and after *in vitro* biodegradation respectively.

3D printed ear pinna porous architecture which may possibly enhance to its recellularization fate after transplant. The biodegradability of scaffold analysis is as important for whether its biodegradable or not. While most of non-degradable and non-porous scaffold used construct, probable to be extruded after a certain time period.

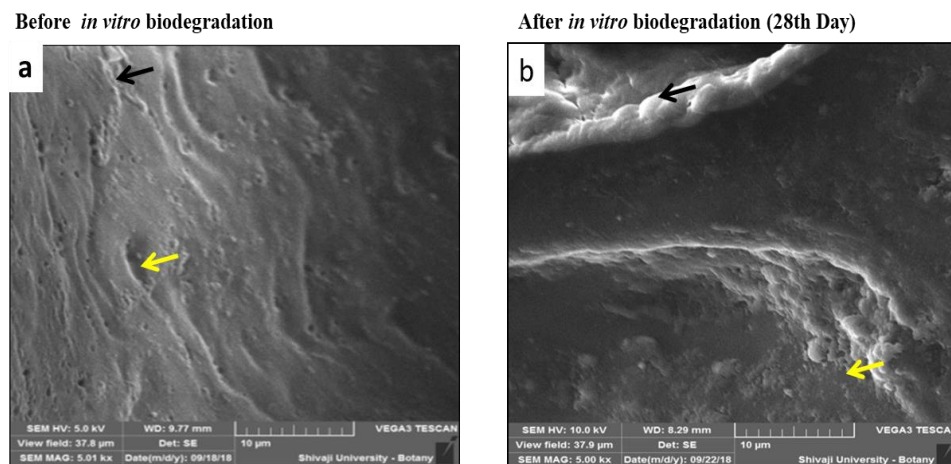


*Figure 3.10 In vitro Biodegradability study of 3D printed ear pinna  
SEM images of [a] before in vitro biodegradation and [b] after in vitro biodegradation (28<sup>th</sup> Day)*

### 3.12 Biocompatibility study *in ovo*:

On day 6[b], 8[d], 10[f] and 12[h], the chick embryos had developed angiogenesis when compared with control (Fig.3.11).

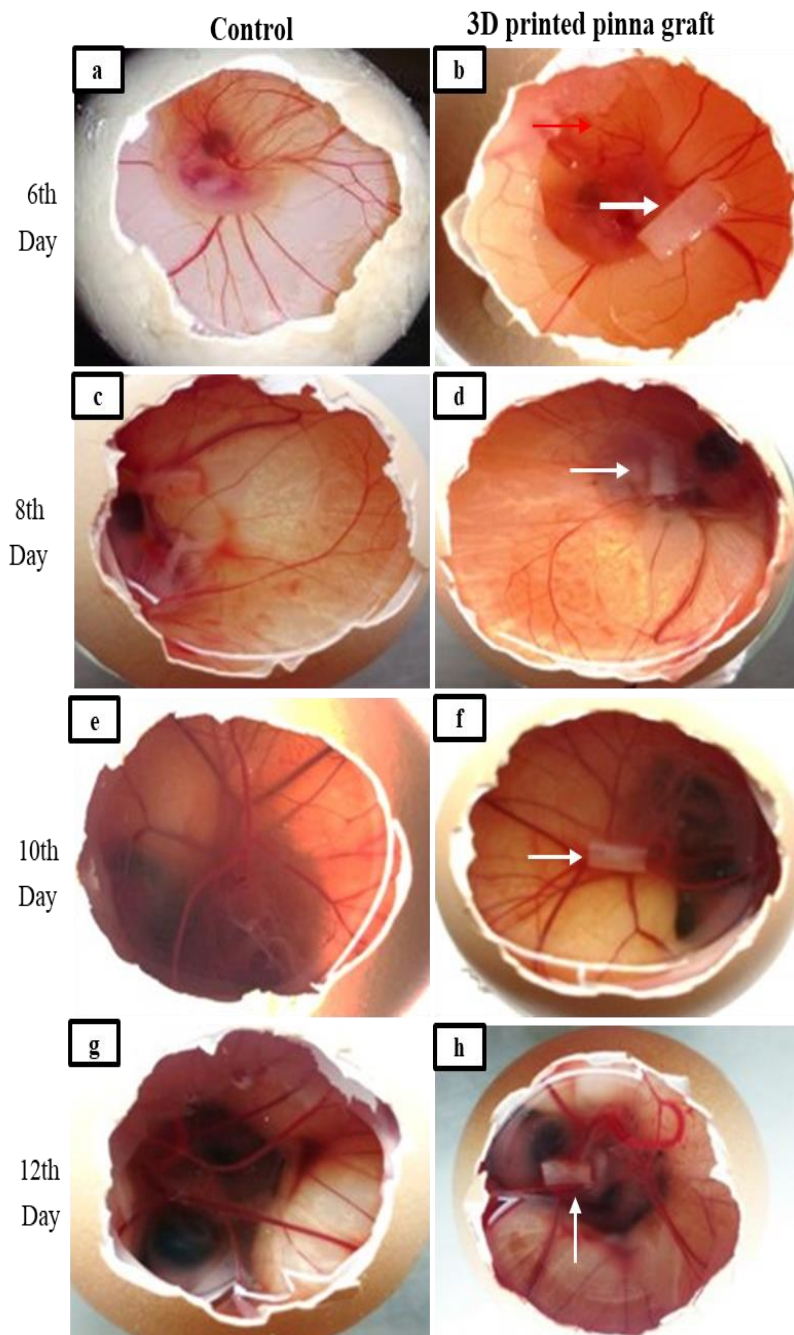
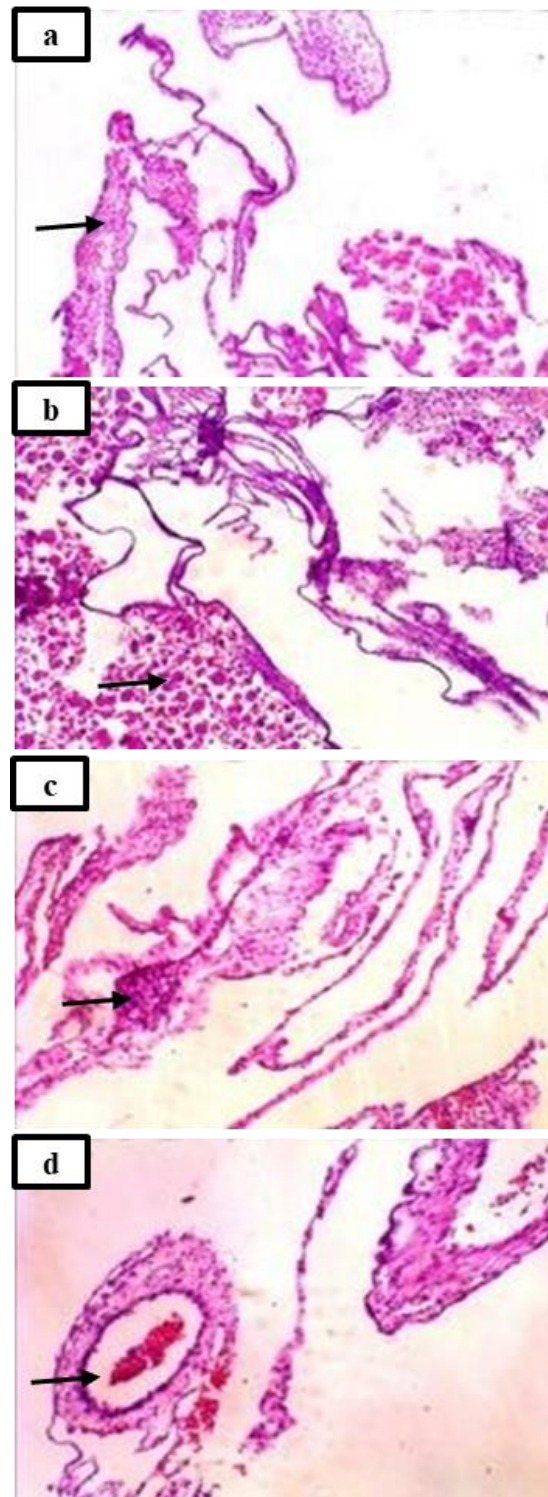


Figure 3.11: 3D printed ear pinna graft biocompatibility and CAM assay

*The CAM assay allows in ovo vascularization of 3D printed pinna graft on the surface. Newly formed vessels are connecting the 3D printed graft on the surface of CAM.*

## Development of 3D Printing for Tissue Engineering of Ear Pinna

HE analysis of CAM on days 6, 8, 10, and 12 showed the proliferation of cells and vascularized network membrane were observed as shown in Fig.3.12.



*Figure 3.12: Histology (HE) of CAM*

*Histology of CAM revealed recellulrization*

SEM study of pinna graft shows fibrous network and recellularization (Fig.3.13).

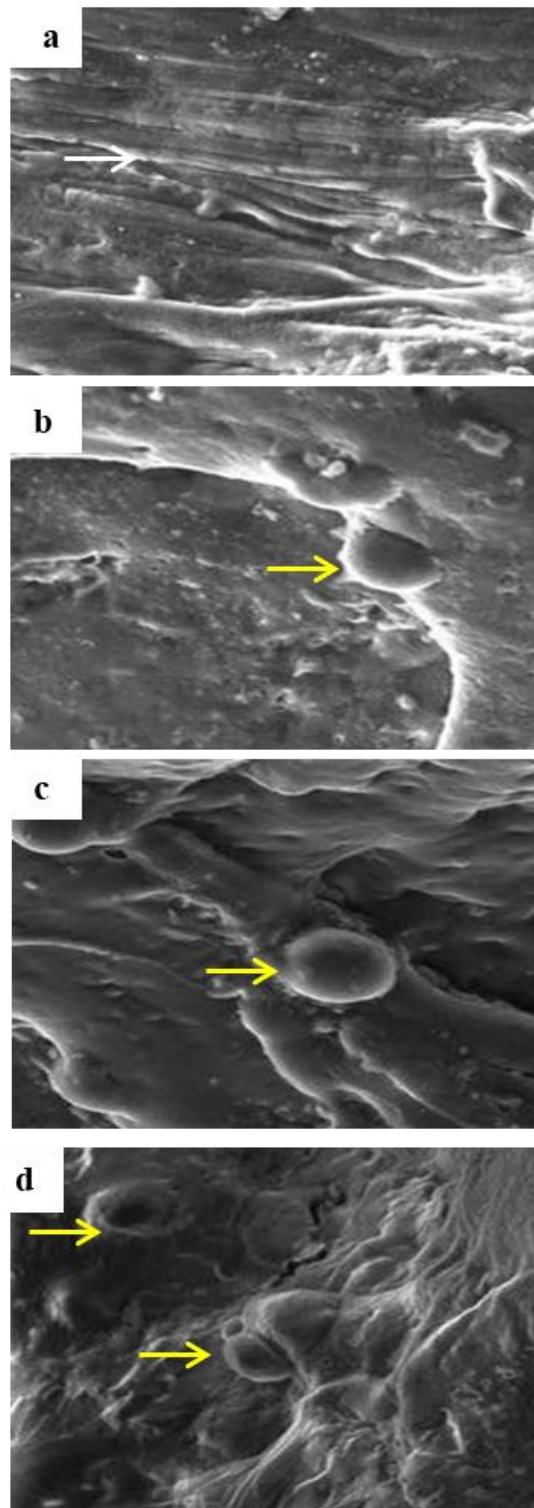


*Figure 3.13: SEM of pinna graft*

*SEM of in ovo 3D printed ear pinna graft: SEM study 3D printed ear graft revealed that fibrous topography and cell migration.*

### 3.13 *In vivo* study of 3D printed ear pinna:

Ultrasound sonography of left side native ear pinna (Fig.3.16a) revealed normal images, while the right ear (Fig.3.16b) with transplanted ear pinna shows an increase in stiffness.

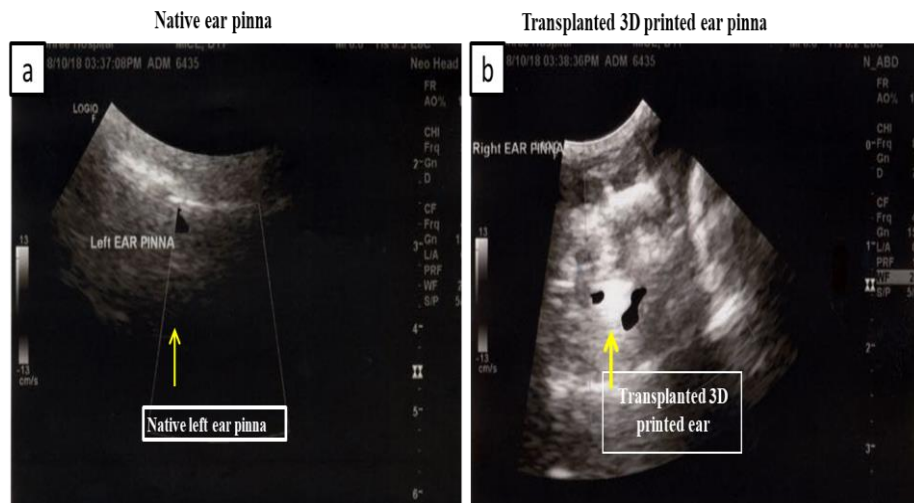


Figure 3.16: Ultrasound sonography (USG) of transplanted 3D printed ear pinna

*Ultrasound Sonography scan of left side nontransplant ear pinna revealed normal images, while the right side of ear pinna post-transplant day 9th revealed an increase in stiffness due to 3D printed pinna transplant*

On day 11, CT scan images of the left side and right side of transplanted 3D printed ear pinna revealed its shape and structural position (Fig.3.17a and b).

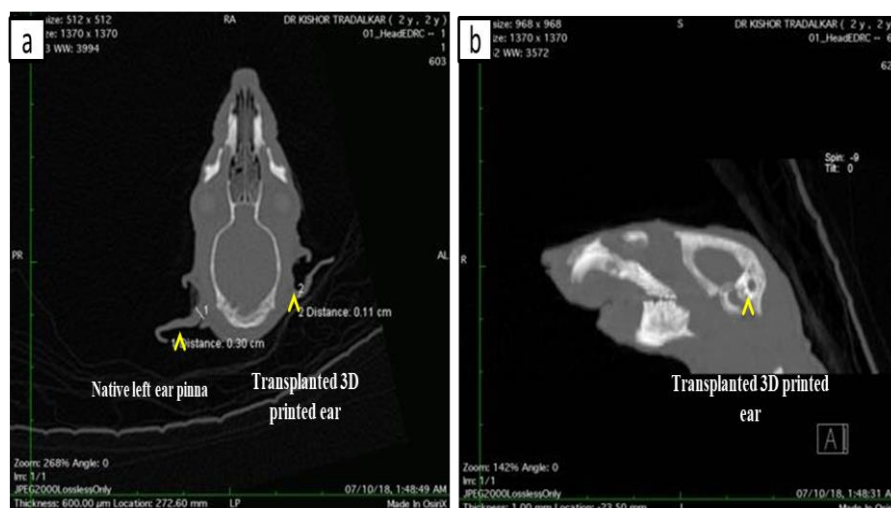
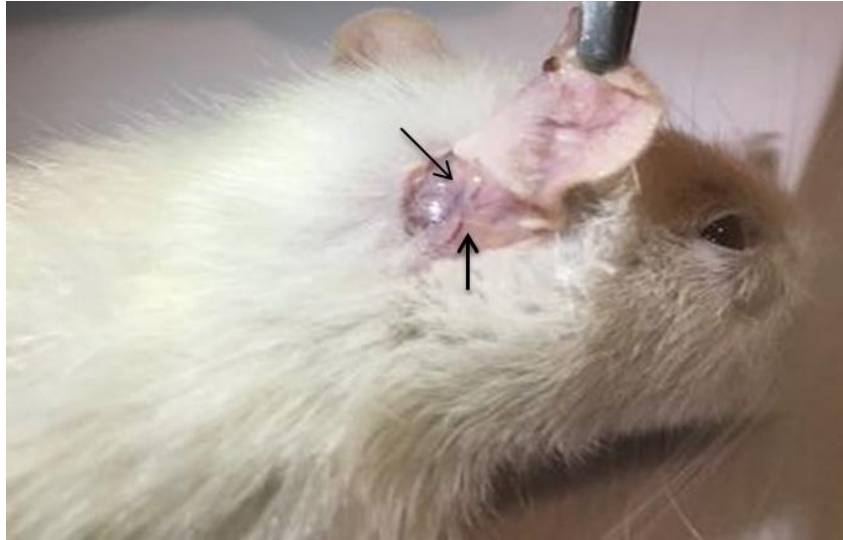


Figure 3.17: Computed Tomography (CT) of transplanted 3D printed ear pinna

*CT scan of left side nontransplant pinna and right sided transplanted 3D printed pinna post-transplant day 11th images revealed its shape fidelity and no internal injuries or bleeding.*

On 30th-day post transplantation, angiogenesis in transplanted 3D printed ear pinna was observed (Fig.3.18).



*Figure 3.18: 3D printed ear transplant angiogenesis.*

### **3.13.1 Biomechanical characterization of 3D printed native rat pinna and transplanted pinna:**

Ultimate tensile load (N) (Fig. 3.20a) of 3D printed, native rat ear pinna and transplanted pinna shows  $66.90 \pm 00.10$ ,  $13.10 \pm 01.51$ ,  $30.10 \pm 05.28$  respectively. Ultimate tensile strength (N/mm<sup>2</sup>) of 3D printed, native rat ear pinna and transplanted pinna (Fig.3.20b) shows  $14.62 \pm 01.00$ ,  $01.36 \pm 00.16$ , and  $4.22 \pm 01.05$  respectively. 3D printed pinna, native rat ear pinna and transplanted pinna elongation at breaking load (%)  $30.80 \pm 11.00$ ,  $20.20 \pm 03.73$ , and  $26.50 \pm 00.71$  respectively (Table 3.4) (Fig.3.20c). There was a small significant difference ( $P > 0.05$ ) in the tensile strength of 3D printed pinna and transplanted pinna. The difference between the elongation of the native pinna and transplanted pinna is small with a significance of  $p < 0.01$ .

## Development of 3D Printing for Tissue Engineering of Ear Pinna

*Table 3.4: Biomechanical characterization (tensile testing) of 3D printed ear pinna, native rat ear pinna and transplanted 3D printed ear pinna*

Biomechanical Testing Parameter	3D printed ear pinna	Rat ear pinna	Transplanted 3D ear pinna
Output Parameter			
Ultimate tensile load (N)	66.90±00.10	13.10±01.51	30.10±05.28
Ultimate tensile strength (N/mm <sup>2</sup> )	14.62±01.00	01.36±00.16	04.22±01.05
Elongation at breaking load (%)	30.80±11.00	20.20±03.73	26.50±00.71

‘±’ indicated the standard deviation in parameters.

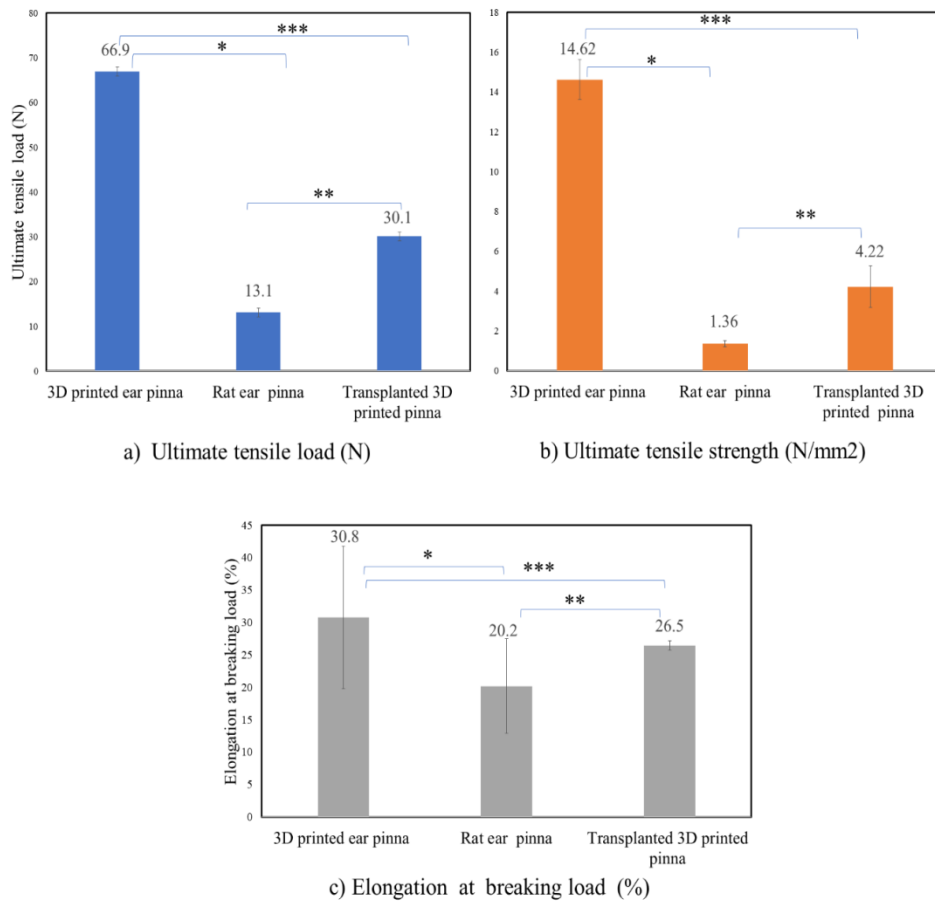


*Figure 3.20: Biomechanical characterization 3D printed ear pinna, native rat ear pinna and transplanted 3D ear pinna.*

*The graphs represent the mean of three individual testing's for tensile load, tensile strength and elongation breaking point ± S.D (n=3). The p-value for all the testing was below statistical significance (\*p<0.05, \*\*p<0.01).*

### 3.13.2 Histological assessment:

HE, TB and SO/FG-stained sections of 3D printed ear pinna were not showing any cellular organization as shown in Fig.3.21. It revealed that the nucleus disappeared and chondrocytes were completely removed while the reduction in undesirable cellular debris. MT staining (collagen network), AB pH 2.5 (no disruption GAG's), and VEG (appearance of elastin) as preserved desirable ECM.

HE stained sections of native rat ear pinna (Fig.3.21g) and transplanted ear pinna (Fig.3.21m) revealed lacunae with chondrocytes nuclei (purple), cytoplasm (pink). TB-stained sections (Fig.3.21h, Fig.3.21n) showed chondrogenic-differentiated tissues and proteoglycans (dark blue). MT-stained sections (Fig.3.21c, Fig.3.21i, and Fig.3.21o) highlighted bundle of collagen (blue). AB-stained sections (Fig.3.21k, Fig.3.21q) revealed that, GAG (blue) is a major structural component of ECM. SO/FG-stained section highlighted recruitment of chondrocyte (orange to red). VEG stained sections (Fig.3.21l, Fig.3.21r) revealed major structural components of elastin fibers (black).

## Development of 3D Printing for Tissue Engineering of Ear Pinna

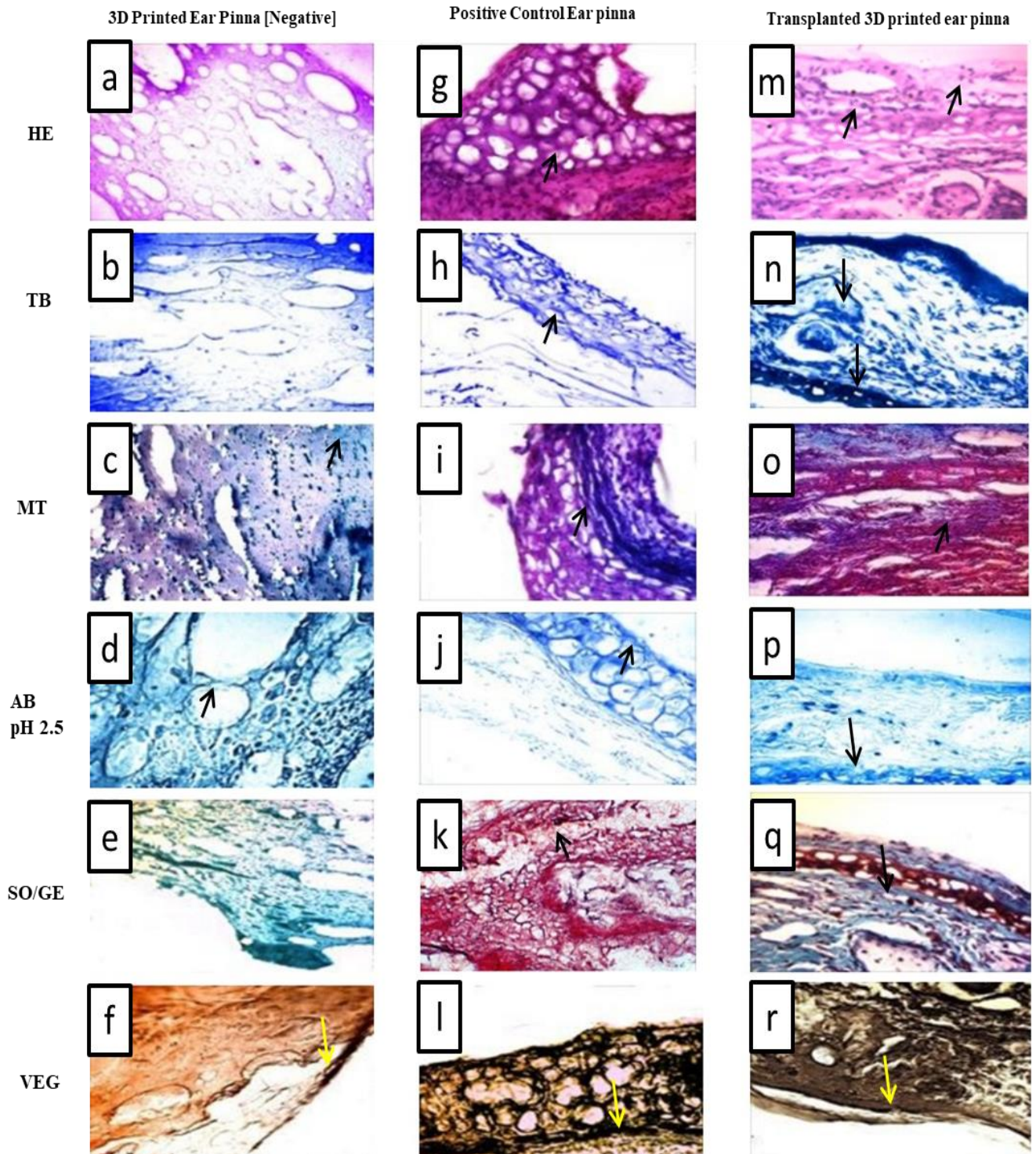


Figure 3.21: Histology of negative, positive control and transplanted 3D printed ear pinna.

The images observed under a microscope for HE, TB, MT, AB, SO/FG, VEG were given for 3D printed pinna [a-f], rat native pinna [g-l], and 3D printed pinna after transplantation [m-r] were shown respectively.

### 3.13.3 SEM analysis:

Scanning electron microscopy of transplanted 3D printed ear pinna (Fig.3.22) shows cell structure, recellularization, and highly organized fibrous network.

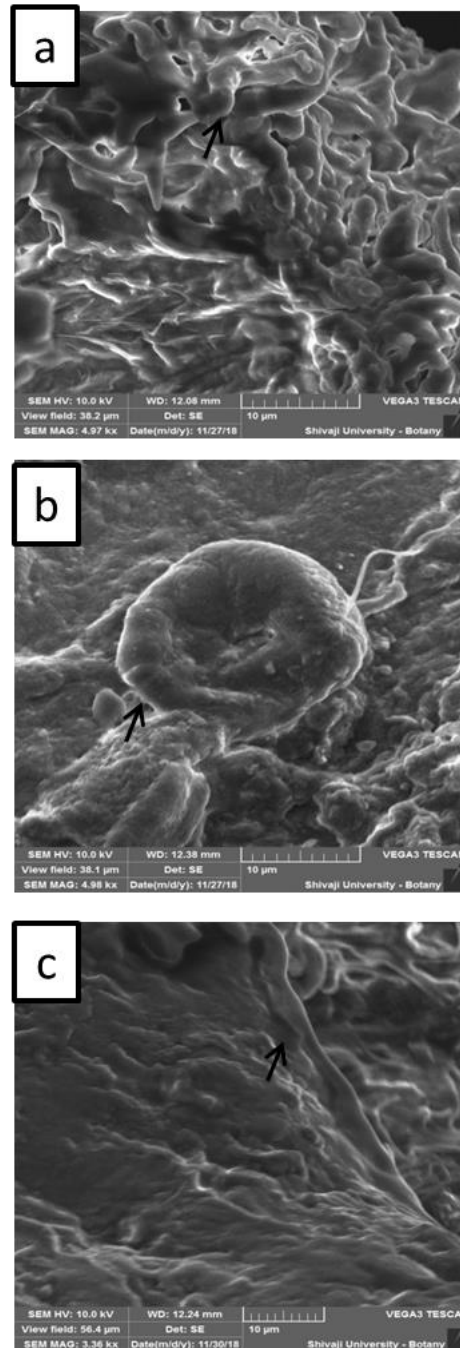
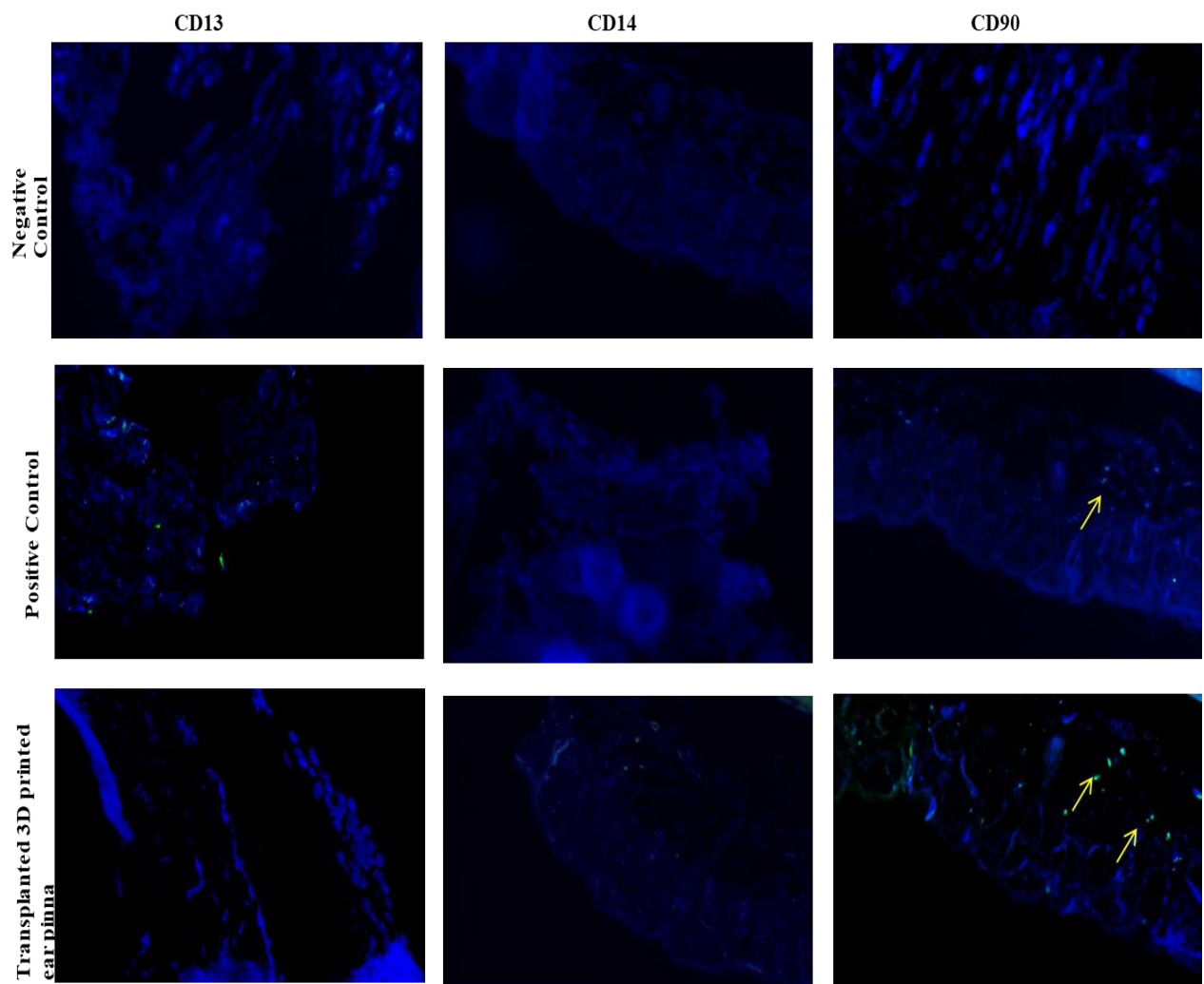


Figure 3.22: SEM images of transplanted 3D printed ear pinna

Scanning electron microscopy of transplanted 3D printed ear pinna cartilage revealed an abundant ECM cell structure with a highly organized elastin and collagen network. The chondrocytes retained a round configuration.

### 3.13.4 IHC:

IHC staining of negative control shows no expression of cell surface markers (Fig.3.23). IHC staining of positive control and transplanted 3D printed ear pinna as shown in (Fig.3.23) revealed that counterstained with DAPI for confirmation of the presence of a nucleus. CD13+, CD90+ markers expressed as fluorescent green in positive control. Similarly, CD14+, CD90+ were expressed in transplanted 3D printed ear pinna.



*Figure 3.23: Immunohistochemical study of negative control, positive control and transplanted 3D printed ear pinna*

*IHC staining with markers  $CD^{13+}$ ,  $CD^{14+}$ , and  $CD^{90+}$  highlighted recellularization in the negative control, positive control, and transplanted pinna respectively.*

### 3.14 Discussion:

There are auricular deformities found worldwide in varying ear shape and size (Mussi et al. 2019). The consequence of microtia or congenital deformities of the external ear reported in individuals are presented as a negative impact on the appearance; meeting fewer people, reduced self-esteem and higher rates of depression, inactive interpersonal skills, and antagonism progress with age (Chung et al. 2013). 3D printing technology may be beneficial for the bioprinting of complex structures of ear pinna as a solution to reduce these psychological, social, and cosmetic impacts.

Preparation of bioink was done according to the patented protocol (Application filing receipt (AFR) for Indian patent application no. 202121004796 Year, 2021) in which xenogenic cartilage was used to obtain dECM slurry after digestion. The polymers added in the dECM slurry provided the viscosity giving an advantage for anatomical structure and mechanical strength. The FTIR peak around  $1094.00\text{ cm}^{-1}$  indicated the stretching of a carboxyl group ( $-\text{C}=\text{O}$ ) and bending of a hydroxyl group ( $-\text{OH}$ ) while  $1406.83\text{ cm}^{-1}$  indicated methyl ( $-\text{CH}_2$ ) group present in PVA. Peak around  $1636.29\text{ cm}^{-1}$  ( $-\text{C}=\text{O}$ ) of gelatine and  $3249.00\text{ cm}^{-1}$  points indicated the presence of ( $-\text{OH}$ ) (Jipa et al. 2012; Tareq et al. 2016). FTIR analysis indicated the esterification, polymerization, and hydrophilic nature of bioink. Optimized dECM bioink viscosity and spreadability exhibited gel-like properties that aided in the extrusion of self-supporting ear pinna structure.

Developed light weighted 3D printer nozzle head can hold the bioink setup. Insulated nozzle setup maintained filamentous viscous bioink providing printing accuracy to print human ear shaped pinna. Degradation of 3D printed ear pinna occurred due to evaporation of bound water, thermo-oxidative decomposition, and finally obtained carbon in the form of ash residues. So, the thermal strength and polymer linkages represented that the 3D printed pinna was thermally stable at room temperature. XRD was showing the crystalline nature (Pal et al.

2007)(Yousefi, Azizeh-Mitra and James, Paul F and Akbarzadeh, Rosa and Subramanian, Aswathi and Flavin, Conor and Oudadesse 2016) of 3D printed ear pinna due to its composite nature. Swelling property revealed the hydrophilic nature of the construct. *In vitro* biodegradability and its SEM analysis proved the degradable and porous nature providing a suitable surface for cell attachment (Dhandayuthapani et al. 2011). The CAM assay represented vascularization (Burgio et al. 2018) after implantation without severe inflammatory response proved non-toxicity of the pinna. The recellularization observed in SEM proved the biocompatible nature of the graft making it suitable for transplantation.

*In vivo* biocompatibility was checked by transplanting the small portion of the 3D printed pinna in a Wistar rat. Their nutritional and physiological status was checked regularly (Lidfors et al. 2014). The rats were having their normal routine of sleeping, eating, drinking, grooming. Scratching with nails near sutures caused the wound in the ear in some rats which were applied further with betadine to restrict infection. We monitored that operated ears did not have any sign of abnormalities like swelling or deformation. USG and CT were performed for analyzing the condition of graft in the live rat. A denser region in ultrasound (Wortsman and Jemec 2008) of the right ear revealed that uniformity in the image shows that the graft was accepted by the host ear and not showing inflammation as well as any other anatomical complication. CT indicating the surface imaging (Lidfors et al. 2014) of the transplanted ear in which shape was maintained and no internal injury or bleeding was seen. Transplanted 3D pinna had developed the blood vessels with host ear which makes graft biocompatible. Vascularisation is responsible for proliferation and differentiation, new cell signalling pathways (Patterson et al. 2010). Angiogenesis plays role in the synthesis of ECM which is a sign of the success of reconstruction of the 3D printed pinna.

Polymers added in the composite bioink had provided an elasticity increase to 3D printed pinna which shows higher ultimate tensile load, ultimate tensile strength, and elongation

breaking load compared to rat ear pinna. 3D printed pinna after transplantation reduces the elongation breaking load but remains higher with respect to native rat ear pinna which can be indicated *in vivo* biodegradation occurred in the scaffold. The current research used 3D printed ear pinna transplanted, which can be biodegradable engineered pinna, may have sufficient time to a new development of ECM (Ragaert 2013) and gain mechanical properties while gradually replacing and degrading.

Chondrocytes and other cells were absent in HE, TB and SO/FG-stained sections of 3D printed ear. Observations convinced the success of the digestion process for removing the antigenic material in the goat cartilage slurry. Similar assays of sections after transplantation represented the development of new cells and chondrocytes. Recellularization in the transplanted graft was similar to the native ear pinna of rat tells the acceptance of graft by the host. MT, AB, and VEG assays were telling that ECM components retained which are required to give the mechanical strength to the 3D pinna. Their presence was providing binding sites for cellular attachment after transplantation which can be seen in stained sections after the transplantation (Ragaert 2013). SEM images after transplantation revealed the synthesis of matured chondrocytes and representing ECM fibers attachment (Ragaert 2013). In IHC, CD13+ had highlighted perichondral cells in the positive control. CD14+ expressed in transplanted ear pinna showing wound healing property (Zanoni and Granucci 2013). CD90+ marker expressed as recruitment of chondrocyte specific progenitor cells (Schmidt et al. 2017) in native rat ear as well as transplanted ear pinna. Similar results for CD90+ in native and transplanted ear pinna have shown that the reconstructed ear pinna was having normal pinna properties. Hence, the regeneration of chondrocytes, GAG, elastin fibers, collagen with retaining ECM in transplanted 3D printed pinna within 30 days cleared the effectiveness of this patented protocol for the reconstruction of the pinna.

Polymers in bioink cross-linked with dECM-rich cartilage provided required viscosity and spreadability to the 3D printed pinna. 3D printing technology had been proved to be useful to construct the precise shape of the human pinna to reduce the cosmetic impacts of pinna deformities like microtia. Mechanical strength, thermal stability, and the hydrophilic nature of 3D pinna made it capable of replacing natural ear in case of loss. Regeneration of chondrocytes progenitor cells, elastin fibers, and ECM fibers on the grafted portion of 3D printed pinna proved its non-toxicity and biocompatibility in the rat. Hence, the aim of the study of bioink for 3D ear pinna was achieved and a clinical trial of 3D printed ear pinna is required to be performed in the future.

### 3.15 Conclusions:

Bioink prepared for the reconstruction of pinna was proved as optimized for printing. Chondrocytes and goat cartilage antigenic materials were removed by alkaline digestion process reduced the possibility of inflammation after transplantation keeping ECM. Polymers cross-linking with ECM provided efficient viscosity to bioink for printing. 3D bioprinting technology gives the flexibility of printing for customized anatomical shape and effective biomechanical properties of the reconstructed ear pinna. The ear had biodegradable, biomechanical and thermo stable properties despite having polymers. Pinna was biocompatible (*in ovo* and *in vivo*) having newly developed chondrocytes, elastin fibers, progenitor cells of ECM after transplantation. Angiogenesis after grafting illustrated that the 3D printed ear pinna was accepted by the animal model which makes graft biocompatible and non-toxic properties nearer to the native ear pinna. Characterization and statistical analysis showing that reconstructed pinna is having properties like native rat pinna. The reconstructed pinna can be utilized as medical objects.

### References:

- Abdi-Azar H, Maleki SA (2014) Comparison of the anesthesia with thiopental sodium alone and their combination with Citrus aurantium L . (Rutaseae) essential oil in male rat. Bull Environ Pharmacol Life Sci 3:37–44
- Al-Suwayeh SA, Taha EI, Al-Qahtani FM, et al (2014) Evaluation of skin permeation and analgesic activity effects of carbopol lornoxicam topical gels containing penetration enhancer. Sci World J 2014:.. <https://doi.org/10.1155/2014/127495>
- Bergholt NL, Lysdahl H, Lind M, Foldager CB (2018) A Standardized Method of Applying Toluidine Blue Metachromatic Staining for Assessment of Chondrogenesis. 1–5. <https://doi.org/10.1177/1947603518764262>
- Borrelli MR, Hu MS, Longaker MT, Lorenz HP (2020) Tissue Engineering and Regenerative Medicine in Craniofacial Reconstruction and Facial Aesthetics. J Craniofac Surg 31:15–27. <https://doi.org/10.1097/SCS.00000000000005840>
- Burgio F, Rimmer N, Pieves U, et al (2018) Characterization and in ovo vascularization of a 3D-printed hydroxyapatite scaffold with different extracellular matrix coatings under perfusion culture. Biol Open 7:.. <https://doi.org/10.1242/bio.034488>
- Cervantes TM, Bassett EK, Tseng A, et al (2013) Design of composite scaffolds and three-dimensional shape analysis for tissue-engineered ear. J R Soc Interface 10:.. <https://doi.org/10.1098/rsif.2013.0413>
- Chen Y, Yan Y, Li X, et al (2014) Application of ultrasound on monitoring the evolution of the collagen fiber reinforced nHAC/CS composites in vivo. Biomed Res Int 2014:.. <https://doi.org/10.1155/2014/418302>

Chung JHY, Naficy S, Yue Z, et al (2013) Bio-ink properties and printability for extrusion printing living cells. *Biomater Sci* 1:763–773. <https://doi.org/10.1039/c3bm00012e>

Copyright T, Co W (1984) *WINSOME*. 59:213–216

Dhandayuthapani B, Yoshida Y, Maekawa T, Kumar DS (2011) Polymeric scaffolds in tissue engineering application: A review. *Int J Polym Sci* 2011:.

<https://doi.org/10.1155/2011/290602>

Fischer AH, Jacobson KA, Rose J, Zeller R (2008) Hematoxylin and eosin staining of tissue and cell sections. *Cold Spring Harb Protoc* 3:3–5.

<https://doi.org/10.1101/pdb.prot4986>

Huhtamäki T, Tian X, Korhonen JT, Ras RHA (2018) Surface-wetting characterization using contact-angle measurements. *Nat Protoc* 13:1521–1538. <https://doi.org/10.1038/s41596-018-0003-z>

Hütten M, Dhanasingh A, Hessler R, et al (2014) In vitro and in vivo evaluation of a hydrogel reservoir as a continuous drug delivery system for inner ear treatment. *PLoS One* 9:.

<https://doi.org/10.1371/journal.pone.0104564>

Jang CH, Koo YW, Kim GH (2020) ASC/chondrocyte-laden alginate hydrogel/PCL hybrid scaffold fabricated using 3D printing for auricle regeneration. *Carbohydr Polym* 248:116776. <https://doi.org/10.1016/j.carbpol.2020.116776>

Jia L, Zhang Y, Yao L, et al (2020) Regeneration of human-ear-shaped cartilage with acellular cartilage matrix-based biomimetic scaffolds. *Appl Mater Today* 20:100639.

<https://doi.org/10.1016/j.apmt.2020.100639>

Jipa IM, Stoica A, Stroescu M, et al (2012) Potassium sorbate release from poly(vinyl

alcohol)-bacterial cellulose films. Chem Pap 66:138–143.

<https://doi.org/10.2478/s11696-011-0068-4>

Kahveci Z, Minday FZ, Cavusoglu I (2000) Safranin O staining using a microwave oven.

Biotech Histochem 75:264–268. <https://doi.org/10.3109/10520290009085130>

Kim JS, Hong S, Hwang C (2016) Bio-ink Materials for 3D Bio-printing. J Int Soc Simul

Surg 3:49–59. <https://doi.org/10.18204/jissis.2016.3.2.049>

Lee JS, Hong JM, Jung JW, et al (2014) 3D printing of composite tissue with complex shape

applied to ear regeneration. Biofabrication 6:. [https://doi.org/10.1088/1758-](https://doi.org/10.1088/1758-5082/6/2/024103)

5082/6/2/024103

Lidfors L, Wichman A, Ewaldsson B, Lindh AS (2014) Enriched cages for groups of

laboratory male rats and their effects on behaviour, weight gain and adrenal glands. Lab

Anim 48:36–49. <https://doi.org/10.1177/0023677213505085>

Maji K, Dasgupta S, Pramanik K, Bissoyi A (2016) Preparation and Evaluation of Gelatin-

Chitosan-Nanobioglass 3D Porous Scaffold for Bone Tissue Engineering. Int J Biomater

2016:. <https://doi.org/10.1155/2016/9825659>

Mangera A, Bullock AJ, Roman S, et al (2013) Comparison of candidate scaffolds for tissue

engineering for stress urinary incontinence and pelvic organ prolapse repair. BJU Int

112:674–685. <https://doi.org/10.1111/bju.12186>

Melo A, Leite-Almeida H, Ferreira C, et al (2016) Exposure to ketamine anesthesia affects

rat impulsive behavior. Front Behav Neurosci 10:1–11.

<https://doi.org/10.3389/fnbeh.2016.00226>

Mota C, Danti S (2019) Ear tissue engineering, Third Edit. Elsevier

- Mussi E, Furferi R, Volpe Y, et al (2019) Ear reconstruction simulation: From handcrafting to 3D printing. *Bioengineering* 6:1–19. <https://doi.org/10.3390/bioengineering6010014>
- Nayyer L, Patel KH, Esmaeili A, et al (2012) Tissue engineering: Revolution and challenge in auricular cartilage reconstruction. *Plast Reconstr Surg* 129:1123–1137. <https://doi.org/10.1097/PRS.0b013e31824a2c1c>
- Noh I, Kim N, Tran HN, et al (2019) 3D printable hyaluronic acid-based hydrogel for its potential application as a bioink in tissue engineering. *Biomater Res* 23:1–9. <https://doi.org/10.1186/s40824-018-0152-8>
- Oseni AO, Crowley C, Boland MZ, et al (2011) Cartilage Tissue Engineering : the Application of Nanomaterials and Stem Cell Technology. *Tissue Eng Tissue Organ Regen* 233–266. <https://doi.org/10.5772/22453>
- Pal K, Banthia AK, Majumdar DK (2007) Preparation and characterization of polyvinyl alcohol-gelatin hydrogel membranes for biomedical applications. *AAPS PharmSciTech* 8:. <https://doi.org/10.1208/pt080121>
- Patterson J, Martino MM, Hubbell JA (2010) Biomimetic materials in tissue engineering. *Mater Today* 13:14–22. [https://doi.org/10.1016/S1369-7021\(10\)70013-4](https://doi.org/10.1016/S1369-7021(10)70013-4)
- Pereira RF, Sousa A, Barrias CC, et al (2018) A single-component hydrogel bioink for bioprinting of bioengineered 3D constructs for dermal tissue engineering. *Mater Horizons* 5:1100–1111. <https://doi.org/10.1039/c8mh00525g>
- Ragaert K (2013) Methods for Improved Flexural Mechanical Properties of 3D-Plotted PCL-Based Scaffolds for Heart Valve Tissue Engineering. *59:669–676*. <https://doi.org/10.5545/sv-jme.2013.1003>

- Rotter N, Steiner A, Scheithauer M (2008) Reconstruction of auricular cartilage using tissue-engineering techniques. *Oper Tech Otolaryngol - Head Neck Surg* 19:278–284.  
<https://doi.org/10.1016/j.otot.2008.10.004>
- Sabale V, Kunjwani H, Sabale P (2011) Formulation and in vitro evaluation of the topical antiageing preparation of the fruit of *Benincasa hispida*. *J Ayurveda Integr Med* 2:124–128. <https://doi.org/10.4103/0975-9476.85550>
- Schmidt LH, Brand C, Stucke-Ring J, et al (2017) Potential therapeutic impact of CD13 expression in non-small cell lung cancer. *PLoS One* 12:1–16.  
<https://doi.org/10.1371/journal.pone.0177146>
- Shieh SJ, Terada S, Vacanti JP (2004) Tissue engineering auricular reconstruction: In vitro and in vivo studies. *Biomaterials* 25:1545–1557. [https://doi.org/10.1016/S0142-9612\(03\)00501-5](https://doi.org/10.1016/S0142-9612(03)00501-5)
- Storck K, Staudenmaier R, Buchberger M, et al (2014) Total reconstruction of the auricle: Our experiences on indications and recent techniques. *Biomed Res Int* 2014:.  
<https://doi.org/10.1155/2014/373286>
- Tareq A, Hussein M, Mustafa A (2016) Synthesis and Characterization of PVA-Gelatin Hydrogel Membranes for Controlled Delivery of Captopril. *Int Res J Pure Appl Chem* 12:1–10. <https://doi.org/10.9734/irjpac/2016/28989>
- Wortsman X, Jemec GBE (2008) Sonography of the ear pinna. *J Ultrasound Med* 27:761–770. <https://doi.org/10.7863/jum.2008.27.5.761>
- Wu S, Liu X, Yeung KWK, et al (2014) Biomimetic porous scaffolds for bone tissue engineering. *Mater Sci Eng R Reports* 80:1–36.  
<https://doi.org/10.1016/j.mser.2014.04.001>

Yamada K (1970) An acriflavine alcian blue technique for dual staining of cartilage and mast cells in paraffin sections yamada Laboratory of Histology , Department of Anatomy School of Medicine , Nagoya Received for Publication November. 3:1–6

Yousefi, Azizeh-Mitra and James, Paul F and Akbarzadeh, Rosa and Subramanian, Aswati and Flavin, Conor and Oudadesse H (2016) Prospect of Stem Cells in Bone Tissue Engineering: A Review. Stem Cells Int 2016:. <https://doi.org/10.1155/2016/6180487>

Zanoni I, Granucci F (2013) Role of CD14 in host protection against infections and in metabolism regulation. Front Cell Infect Microbiol 4:1–6.  
<https://doi.org/10.3389/fcimb.2013.00032>

## Chapter-4

### General Discussion

### General discussion:

The treatment of ear cartilage injury in patients is complicated and current treatment methods have high morbidity. Real therapeutic progress in constructing ear pinna with customized cosmetic benefit may help patients, which is illustrated in the current thesis.

The consequence of auricular deformities reported in individuals has been associated with deficiencies such as psychological negative impacts on the facial appearance (Johns et al. 2017). The current surgical autologous costal cartilage is a time-consuming process, associated with scarring and post-operative discomfort (Jovic et al. 2020) (Nayyer et al. 2012). Xenogenic/ allogenic/ alloplastic surgical material needed lifelong immunosuppression. Otherwise, it causes graft rejection (Storck et al. 2014; Borrelli et al. 2020), while the prosthetic pinna did not look normal (Chinnasamy et al. 2018). Maintenance of cartilage integrity with time and preserving auricular structure remains the major obstacle to make clinically feasible (Chauhan and Guruprasad 2012). Considering all these gaps, a clear need exists to develop an alternative strategy to reconstruct the auricle.

In the 3D molded ear pinna research, five independent methods of decellularization were used for getting desired results. These methods applied on the available xenogenic resource, technical results, and degree of decellularization achieved. The time required for complete decellularization was about 40-80 days due to its dense connective tissue nature and it ensures the complete removal of its antigenic material. The outcome experience with enzymatic treatment revealed a relatively shorter duration of 40 days cycle process which resulted in desirable decellularization with satisfactory shape and good flexibility of elastic cartilage of molded pinna scaffold. The patentable research shows that scaffolds prepared by physicochemical and enzymatic were ideal scaffolds that retain excellent anatomical ear pinna shape molded in different size and shapes i.e., 55, 65, and 75 mm.

## Development of 3D Printing for Tissue Engineering of Ear Pinna

Authors presented a unique decellularization method to generate biocompatible scaffold which can be recellularized post-transplantation and facilitate chondrocyte specific cell recruitment. This study highlights a novel approach to generate xenogenic three-dimensional Tissue Engineered human ear pinna scaffold which can be translated to clinical applications. The results from the study added to our understanding of some of the aspects of limitations in clinical usage of auricle cartilage grafts such as post-transplant management of ear pinna scaffold, graft biocompatibility, donor limitation, and preservation of ECM, mechanical properties and limitation of cartilage recellularization.

In second study, we have presented 3D printing technology for human size ear pinna. For 3D printing, bioink was prepared using goat ear pinna cartilage. Goat ear cartilage was digested with alkali for generating cartilage specific ECM, which was further conjugated with polymers to produce the printable composite cartilage. Patentable bioink preserved the intrinsic dECM to attain the desired viscosity for bioink optimization. Printing of whole human ear pinna was done with extrusion method using prepared bioink. Polymers added in the bioink had provided increased elasticity to 3D printed pinna which resulted in increase in mechanical strength. Structural, physical, mechanical properties were analyzed to check the biodegradability, biocompatibility and *in vivo* regeneration of cartilage-specific cells in the rat. Biocompatible testing of molding and 3D printable pinna conducted on the animal model found satisfactory result of graft transplants. USG and CT gave the idea about 3D printed ear graft acceptance by the host body and not showing any internal injury. Histology and SEM assessment of biocompatible transplant revealed recellularization and new synthesized ECM (GAGs, elastin, and collagen). IHC staining revealed angiogenesis marker VAP, CD13+ highlighting perichondral cells, while CD90 + marker expression revealed that chondrogenic differentiation.

## **Development of 3D Printing for Tissue Engineering of Ear Pinna**

In the current thesis, authors have presented a unique decellularization method to generate biocompatible scaffold which can be recellularized post-transplantation and facilitate chondrocyte specific cell recruitment. The results from the study added to our understanding of some of the aspects of limitations in clinical usage of auricle cartilage grafts such as post-transplant management of ear pinna scaffold, graft biocompatibility, donor limitation, and preservation of ECM, mechanical properties and limitation of cartilage recellularization.

This patentable 3D pinna technology revealed the development of patient-specific complex shape human ear pinna from xenogenic sources with cost-efficient technology. The latest patentable work on the reconstruction of ear pinna using 3D printing technology overcomes autologous reconstruction surgical issues as well as overcomes biocompatible and cartilage in less time of fabrication.

Thus, this thesis highlights a patentable novel approach to generate xenogenic three-dimensional Tissue Engineered human ear pinna scaffold which can be translated to clinical applications and ear bank.

### References:

- Borrelli MR, Hu MS, Longaker MT, Lorenz HP (2020) Tissue Engineering and Regenerative Medicine in Craniofacial Reconstruction and Facial Aesthetics. *J Craniofac Surg* 31:15–27. <https://doi.org/10.1097/SCS.00000000000005840>
- Chauhan DS, Guruprasad Y (2012) Auricular Reconstruction of Congenital Microtia Using Autogenous Costal Cartilage: Report of 27 Cases. *J Maxillofac Oral Surg* 11:47–52. <https://doi.org/10.1007/s12663-011-0290-1>
- Chinnasamy A, Gopinath V, Jain AR (2018) Ear Prosthesis for Postburn Deformity. *Case Rep Otolaryngol* 2018:1–6. <https://doi.org/10.1155/2018/2689098>
- Johns AL, Lewin SL, Im DD (2017) Teasing in younger and older children with microtia before and after ear reconstruction. *J Plast Surg Hand Surg* 51:205–209. <https://doi.org/10.1080/2000656X.2016.1222294>
- Jovic TH, Stewart K, Kon M, Whitaker IS (2020) “Auricular reconstruction: A sociocultural, surgical and scientific perspective.” *J Plast Reconstr Aesthetic Surg* 73:1424–1433. <https://doi.org/10.1016/j.bjps.2020.03.025>
- Nayyer L, Patel KH, Esmaili A, et al (2012) Tissue Engineering. *Plast Reconstr Surg* 129:1123–1137. <https://doi.org/10.1097/PRS.0b013e31824a2c1c>
- Storck K, Staudenmaier R, Buchberger M, et al (2014) Total reconstruction of the auricle: Our experiences on indications and recent techniques. *Biomed Res Int* 2014:1. <https://doi.org/10.1155/2014/373286>

# Chapter-5

## Conclusions

### Conclusions:

In conclusions, novel TE pinna (Molding and 3D printing technique) were characterized and assessed for their suitability for *in vivo* cartilage formation. Based on these results, it was concluded that both TE scaffolds show promise for engineering bio-degradable auricular implants with patient-specific properties and shapes.

In the molded ear pinna study, the xenogenic (Goat ear pinna) decellularized scaffold was obtained. Five independent different methods of decellularization have been used though the duration of 40-80 days for the decellularization process. This could be considered as a long process but considering dense nature of cartilage tissue, it ensures the complete removal of cellular components and minimum destruction of the ECM. The pinna was constructed by a moulding technique using a highly efficient enzymatic decellularization method. The outcomes experienced for this process yielding desirable shape, flexibility, and strength in a short time.

In 3D printing of human ear pinna, xenogenic antigenic materials were removed by alkaline digestion process reduced the possibility of graft rejection after transplantation and keeping tissue-specific dECM. Optimized bioink made with dECM adding polymers gives the viscosity for ideal printing of human ear shape. The time required to print the whole human pinna is respectively less and the dimensions of resulted pinna are precise with required elasticity and mechanical strength.

The present molding and 3D printing technology was designed to yield an ideal decellularized biocompatible human ear pinna shape. The cartilage network-like porous surface and cartilage-specific ECM allowed recruiting new chondrocyte progenitor cells after transplantation. Molding technology suitable for embedding decellularized scaffold to transform into the desired ear shape and cartilage 3D bioink provides the flexibility of

## **Development of 3D Printing for Tissue Engineering of Ear Pinna**

printing for the customized anatomical shape of ear pinna with the help of a custom-made lightweight nozzle head in a very short time.

Especially, 3D bioprinting technology will be the most important tool for complex tissue engineering and organ printing will be a clinical object in hospitals. In these two patented technologies, the authors proposed the generation of tissue-engineered ear pinna as an alternative to overcome the present limitations in clinical usage of auricular cartilage. These two molding and 3D printing technology ear pinna reconstruction research can replace the available techniques as advancement in clinical research and cartilage tissue and ear pinna banks will become prevalent.

## Chapter-6

### Future Scope of work

### Future Scope of work:

The currently available technique to reconstruct the entire ear pinna by surgery remains one of the biggest challenges for plastic surgeons. Through this patented molding technology and optimized 3D printable bioink, the authors proposed the generation of tissue-engineered ear pinna as an alternative to overcome the present surgical or clinical reconstructive ear pinna limitations.

The future scope of patented molding and 3D printing technology is to overcome donor (autologous or allogeneic) limitations. So, it can significantly avoid multiple surgeries in costal cartilage technique and its related side effects like pneumothorax or chest pain or scars or associated scarring and postoperative discomfort. Also, it can solve the age-dependent surgical issues of this technique as pinna can be customized (molded or 3D printed pinna) for every patient with an outer ear deformity. The author suggested that 3D molding or 3D printing of pinna can be helpful for ear pinna reconstruction by plastic surgeons in such a way to skip processes like carving patient-specific auricular shape (3D model -visual aid).

Molded or printed ear pinna can reduce continuous post-transplant monitoring. Hence, it reduces the economic burden on the patient. 3D printed ear can give patient-specific ear so, it can avoid variable cosmetic results and could not be a necessity to replace every few years as the old one wears off just like prosthetic pinna.

Xenogenic dECM in the form of cartilage or bioink can be molded or 3D printed to generate patient-specific pinna which removes the possibility of giving immunosuppressants after transplantation. The author suggested that the pinna was preserving elastic cartilage, tissue-specific ECM (scaffold), porosity, biodegradability. Hence, it has the capacity of *in vivo* or *in vitro* recellularization of chondrocytes.

The molded or 3D printed pinnae maintained its cartilage integrity with time and thus preserving a particular and delicate tissue-specific ECM auricular architecture so it can be

clinically feasible. *In vitro* culture for chondrocytes, expansion does not require as the future perspective that means in this research invented 3D printed cartilage with or without human cells, comprising entire cartilage-specific ECM. In this research, patentable fabrication molding, 3D printable bioink technologies are allowed by TE to develop a simplified process to obtain patient-specific auricular shape from cartilage.

Another future perspective of this invention is to use the 3D printed cartilage for basic or research applications such as clinical application, in vitro toxicology, and 3D ear pinna model. Another future perspective of the invention of 3D printed cartilage, applied to subjects afflicted for acid burn or accidentally loss of ear pinna cartilage or medical object. Patentable ear pinna invention another future perspective in congenital disorders (Microtia and Anotia) or cosmetic pinna substitute and applied to defective pinna region. Another future perspective of the invention is to use regions in need of elastic cartilage tissue augmentation or cartilage repair and said 3D printed ear graft implanted into the said region in need of cartilage tissue augmentation or repair. The author has planned for synthesizing molded and 3D printed ear pinna scaffold as developed ear bank or cartilage bank.